Review | Open Access

Energy Materials

Li *et al. Energy Mater.* **2026**, *6*, 600128 **DOI:**10.20517/energymater.2026.230

Dynamic electrical double layers at solid-liquid interfaces for energy-information flow

Xiang Li[1,#], Zunkang Zhou[1,2,#], Di Wei[1,3,*]

Keywords:
Dynamic electrical double layers, solid-liquid triboelectricity, triboiontronics, iontrovoltaic effect, ionic-electronic coupling, iontronic embodied intelligence

Citation: Li, X.; Zhou, Z.; Wei, D. Dynamic electrical double layers at solid-liquid interfaces for energy-information flow. *Energy Mater.* **2026**, *6*, 600128. https://dx.doi.org/10.20517/energymater.2026.230

Received: 20 Jul 2026
First Decision: 11 Aug 2026
Revised: 18 Aug 2026
Accepted: 4 Sep 2026
Published: 24 Sep 2026

Academic Editor:
Yuhui Chen
Copy Editor:
Fangling Lan
Production Editor:
Fangling Lan

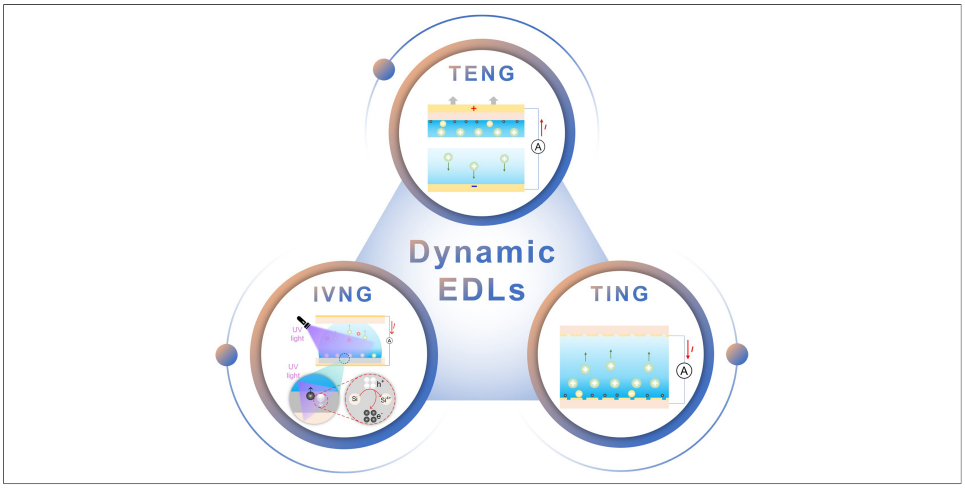

Abstract

Electrical double layers (EDLs) constitute fundamental electrochemical interfaces that, when dynamically regulated, enable tight coupling between energy transduction and information processing. Recent advances have progressively shifted the role of EDLs from passive, equilibrium charge-screening structures to actively reconfigurable ionic-electronic interfaces, thereby establishing a unified physicochemical framework for solid-liquid triboelectricity, triboiontronics, and the emerging iontrovoltaic effect. Here, we synthesize a dynamic EDL-centered perspective that connects the evolution of EDL theory with recent developments in iontronic systems. This framework outlines a continuous conceptual progression from classical conductive-interface descriptions and the two-step model of non-conductive interfaces to triboiontronic regimes in which mechanically induced charge separation drives dynamic ion polarization and further to semiconductor-liquid interfaces where EDL modulation couples with space charge regions to give rise to the iontrovoltaic effect. In parallel, device architectures evolve from solid-liquid triboelectric nanogenerators to triboiontronic nanogenerators and ultimately to iontrovoltaic nanogenerators, reflecting increasing integration of ionic dynamics with electronic transport. Across these regimes,

[1]Beijing Institute of Nanoenergy and Nanosystems, Chinese Academy of Sciences, Beijing 101400, China.
[2]School of Nanoscience and Engineering, University of Chinese Academy of Sciences, Beijing 100049, China.
[3]Centre for Photonic Devices and Sensors, University of Cambridge, Cambridge CB3 0FA, UK.
[#]Authors contributed equally.

[*]**Correspondence to:** Dr. Di Wei, Beijing Institute of Nanoenergy and Nanosystems, Chinese Academy of Sciences, Beijing 101400, China; Centre for Photonic Devices and Sensors, University of Cambridge, 9 JJ Thomson Avenue, Cambridge CB3 0FA, UK. E-mail: weidi@binn.cas.cn

the functional role of EDLs expands from static charge screening to dynamic electrostatic induction, directional ionic transport, and coupled ionic-electronic modulation. This evolution establishes dynamic EDLs as a general platform for co-regulating energy flow and information flow across solid-liquid interfaces. More broadly, dynamic EDLs provide a unifying ionic framework that links interfacial energy conversion with information processing, offering a physical basis for the development of bioinspired iontronic systems and embodied intelligence.

INTRODUCTION

Large-scale brain-inspired simulation initiatives, such as the Blue Brain Project and the Human Brain Project, have substantially advanced digital neural reconstruction and accelerated progress in artificial intelligence (AI)[1-8]. Nevertheless, a fundamental disparity persists between conventional electronic systems and biological intelligence[9-16]. State-of-the-art AI relies on energy-intensive electronic hardware, whereas the human brain achieves perception, learning, memory, and decision-making with a power consumption of only ~20 W[17-21]. This exceptional efficiency arises not solely from neural network architecture, but more fundamentally from the tight coupling between energy utilization and information processing mediated by ionic transport processes[22-27]. In contrast to conventional electronic systems, where energy supply, signal transmission, and computation are largely decoupled, biological nervous systems integrate these functions through ions that simultaneously serve as energy carriers and information carriers[28-37]. Within this framework, electrical double layers (EDLs) emerge as dynamic interfacial structures that regulate ionic transport, interfacial electrochemical signaling, and ionic-electronic coupling, thereby intrinsically unifying energy flow and information flow at the interface[38-45]. Accordingly, understanding the dynamic regulation of EDLs provides a physicochemical basis for elucidating the operating principles of biological intelligence and for designing next-generation bioinspired iontronic systems. Recent advances in bioinspired iontronic architectures further suggest a tangible physical realization of synthetic neural substrates[46,47]. In particular, emerging iontronic systems have been shown to emulate ion-gated neurotransmission, encode memory through asymmetric and history-dependent EDLs, and exhibit learning-like behavior via memristive ionic networks[48,49]. This perspective reframes embodied intelligence as a process in which information processing is intrinsically coupled to local electrochemical state evolution, offering a unified lens linking physical dynamics, interfacial chemistry, and adaptive computation in matter.

Over more than a century, the understanding of EDLs has undergone a profound evolution. Classical EDL theories established the fundamental concepts of charge screening and ionic compensation at conductive interfaces[50-53]. These concepts were subsequently extended to non-conductive solid-liquid interfaces through the two-step EDL model involving interfacial electron transfer and ionic redistribution[54-56]. More recently, triboelectrically induced ion polarization gave rise to triboiontronic dynamic EDLs, demonstrating that interfacial ionic distributions can be actively reconstructed beyond electrochemical equilibrium[57-60]. This concept was further extended through semiconductor-liquid space charge region (SCR) coupling, which establishes ionic-electronic coupling as the physicochemical basis of the iontrovoltaic effect. Consequently, the role of EDLs has evolved from passive electrochemical structures to adaptive iontronic interfaces with continuously expanding regulation capabilities, establishing a common physicochemical foundation for integrating energy transduction with information processing at solid-liquid interfaces[61-68]. Building upon this evolving understanding, dynamic EDLs have driven the rapid evolution of iontronic systems, progressively expanding their functionalities from energy transduction and self-powered sensing to iontronic communication, logic control, and logic computing, thereby enabling the convergence of energy flow and information flow[69-77]. Despite these remarkable advances, current studies have primarily focused on individual EDL models, representative technologies, or specific applications[78-85]. Consequently, the continuous evolution of dynamic EDLs has not yet been recognized as the unifying physicochemical basis underlying the co-evolution of iontronic technologies and energy-information transduction. This missing

perspective has hindered the establishment of a unified framework for understanding the evolution of dynamic EDL-enabled iontronics.

To address this challenge, we establish a unified, dynamic EDL-centered evolutionary framework that systematically links the progression of EDL theories with the expanding capabilities of interfacial regulation, the emergence of representative iontronic technologies, and the progressive convergence of energy conversion and information processing functionalities. Here, dynamic EDL refers to an interfacial ionic structure whose concentration distribution, spatial asymmetry, and electrostatic state can be actively and reversibly reconstructed through external stimuli or interfacial driving forces, rather than simply representing a transient deviation from equilibrium. Unlike conventional transient or non-equilibrium EDLs, which primarily describe time-dependent relaxation processes following perturbations, dynamic EDLs emphasize the controllable and functional evolution of interfacial ionic states, enabling regulation of charge transfer, directional ion transport, ionic-electronic coupling, and ultimately energy and information transduction. Based on this definition, the evolution of EDL theories is first traced by systematically discussing four representative EDL models, namely classical conductive-interface EDLs, the two-step non-conductive EDL framework, triboiontronic dynamic EDLs, and semiconductor-liquid EDL-SCR coupling underlying the iontrovoltaic effect. Building upon this theoretical foundation, the corresponding evolution of three representative dynamic EDL-enabled technologies, solid-liquid triboelectric nanogenerators (S-L TENGs) [Figure 1A and B], triboiontronic nanogenerators (TINGs) [Figure 1C and D], and iontrovoltaic nanogenerators (IVNGs) [Figure 1E and F], is discussed from the perspective of progressively enhanced dynamic EDL regulation[86-94]. Their operating mechanisms and representative applications are then comprehensively reviewed to reveal how dynamic EDLs progressively evolve from enabling efficient energy harvesting to self-powered interface probing and sensing, bionic logic control, iontronic communication, and logic computing, thereby driving the convergence of energy transduction and information processing through dynamic ionic processes. Finally, future opportunities and key challenges toward iontronic embodied intelligence are discussed, highlighting dynamic EDLs as adaptive iontronic interfaces that provide the physicochemical foundation for intrinsically integrating energy flow, information flow, and intelligent regulation in next-generation self-powered iontronic systems.

EVOLUTION OF EDL MODELS AT SOLID-LIQUID INTERFACES

EDLs constitute the fundamental electrochemical framework of solid-liquid interfaces, governing charge organization, ionic transport, and interfacial electrostatic interactions that couple energy transduction with information processing across diverse physicochemical and biological systems[95-100]. Over more than a century, the understanding of EDLs has evolved from classical equilibrium descriptions to dynamically regulated interfacial frameworks. This evolution can be unified as a continuous progression in interfacial regulation capability, spanning from ionic screening to charge generation-redistribution coupling, dynamic ionic regulation, and ultimately ionic-electronic coupling.

Classical EDL models at conductive solid-liquid interfaces

Early studies focused on conductive solid-liquid interfaces, where interfacial charges originate from electrochemical reactions and are compensated by counterions in the adjacent electrolyte. The resulting charge distribution is governed by a balance between electrostatic attraction, thermal motion, and ion diffusion. To describe this behavior, classical models including Helmholtz, Gouy-Chapman, and Gouy-Chapman-Stern (GCS) frameworks were developed [Figure 2]. These models progressively refined the understanding of interfacial screening by incorporating increasingly realistic physical effects. The Helmholtz model treats the interface as a rigid capacitor composed of a charged surface and a compact counterion layer, resulting in a linear potential drop and a strictly localized screening region [Figure 2A][50]. While conceptually simple, it neglects thermal motion and ionic redistribution. The Gouy-Chapman model

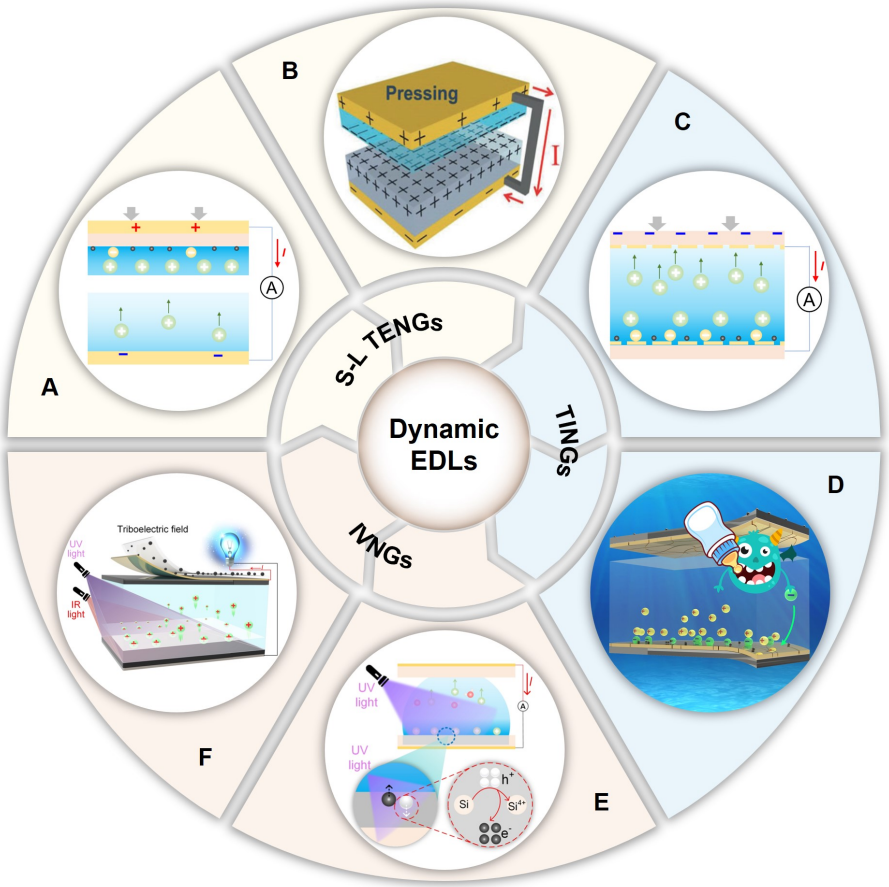

Figure 1. Three representative dynamic EDL-enabled nanogenerators and their operating mechanisms. (A and B) Dynamic EDL-mediated operating mechanism and a representative device architecture of S-L TENGs. Reprinted with permission from[92] Copyright © 2013 WILEY-VCH Verlag GmbH & Co. KGaA, Weinheim; (C and D) Asymmetric EDL-driven ionic migration mechanism and a representative device architecture of TINGs. Adapted with permission from[93] Copyright © 2025 Elsevier Inc.; (E and F) EDL-SCR coupling-enabled ionic-electronic transduction mechanism and a representative device architecture of IVNGs. Adapted with permission from[94] Copyright © 2026 Springer Nature.

introduces thermal fluctuations and ionic diffusion, leading to a spatially extended diffuse layer where ions are distributed according to Boltzmann statistics [Figure 2B][51,52]. This framework captures the exponential decay of potential into the bulk electrolyte but assumes point-like ions, which becomes invalid under high surface charge density. To resolve these limitations, the GCS model integrates a compact Stern layer with a diffuse layer [Figure 2C], explicitly accounting for finite ion size, specific adsorption, and spatial charge separation[53]. This hybrid structure provides a more accurate description of real electrochemical interfaces, especially under moderate-to-high ionic strength conditions[101-104]. This regime establishes a passive ionic screening framework governed by electrostatic equilibrium, forming the first stage of EDL evolution.

Two-step EDL model at non-conductive solid-liquid interfaces

Unlike conductive interfaces, non-conductive solid-liquid interfaces generate surface charges dynamically through interfacial processes. Consequently, EDL formation is no longer governed solely by ionic screening of fixed surface charges but by the coupled evolution of interfacial charge generation and ionic redistribution. The two-step EDL model [Figure 3], introduced by Wang *et al.*, extended classical EDL theory by identifying interfacial electron transfer and surface ionization as the initiating processes of surface charge generation, followed by ionic redistribution to establish the EDL[54-56]. Electron-cloud overlap between liquid molecules and non-conductive surfaces enables partial electron transfer, while simultaneous ion adsorption

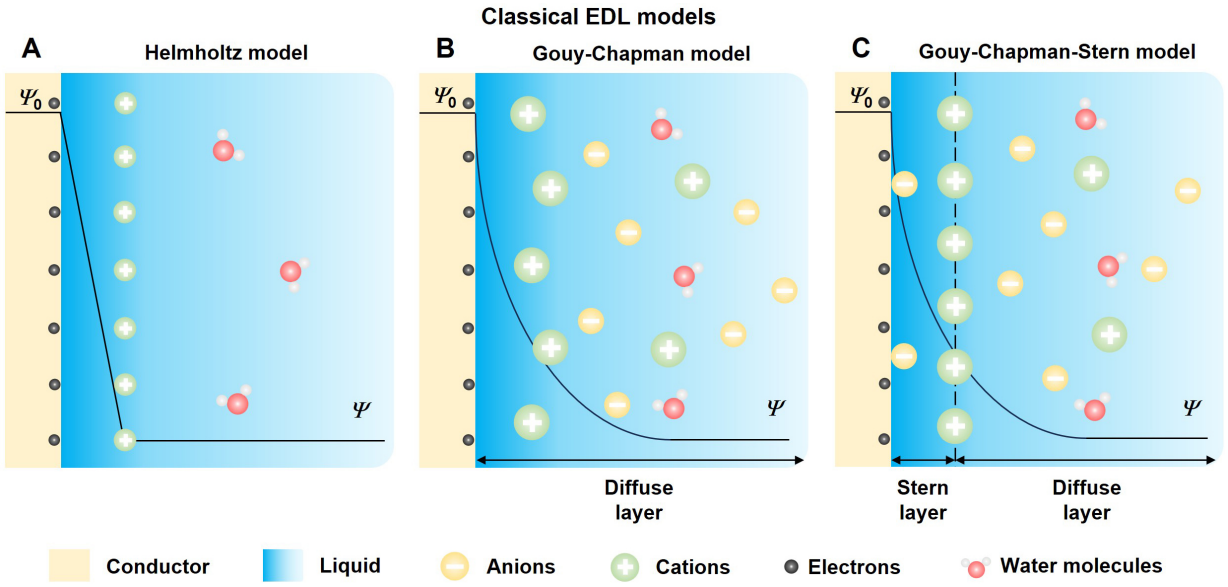

Figure 2. Evolution of classical EDL models at conductive solid-liquid interfaces. (A) Helmholtz model; (B) Gouy-Chapman model; (C) Gouy-Chapman-Stern model.

and dissociation further contribute to net surface charge accumulation. These charges define the inner Helmholtz plane (IHP), which acts as the driving source for subsequent ionic rearrangement. In the second step, the electrostatic field generated by these interfacial charges induces ion migration in the electrolyte, leading to the formation of the outer Helmholtz plane (OHP) and an extended diffuse layer governed by thermal motion and electrostatic interactions.

From a physical perspective, contact electrification at solid-liquid interfaces involves multiple characteristic scales spanning molecular charge transfer, interfacial electrostatic interactions, and ionic redistribution. The initial charge generation process originates from molecular-level interactions at the interface, including electron transfer and ion-related surface reactions, typically occurring within sub-nanometer to nanometer-scale interfacial regions. The associated energy landscape is governed by differences in interfacial electronic states, chemical potentials, hydration energies, and electrostatic interactions. Following charge generation, the compensating ionic rearrangement extends beyond the immediate contact region to establish Stern layers and diffuse layers, with characteristic dimensions determined by surface charge density and electrolyte properties, such as ionic strength and Debye length. The corresponding timescales span from rapid interfacial charge redistribution to slower ionic diffusion and relaxation processes, which regulate the transient and dynamic evolution of EDL structures. Understanding these coupled spatial, energetic, and temporal scales is essential for revealing how microscopic contact electrification events evolve into macroscopic energy conversion and information transduction phenomena. Unlike classical models, this framework explicitly couples charge formation and ionic redistribution as a unified process, revealing that non-conductive interfaces actively participate in EDL construction rather than serving as passive boundaries. This regime marks the transition from equilibrium screening to coupled interfacial charge generation and ionic reorganization.

Triboiontronics driven by triboelectrically induced ion polarization

The two-step EDL model resolved the formation mechanism of EDLs at non-conductive solid-liquid interfaces, yet it remained fundamentally a quasi-equilibrium description. A subsequent conceptual advance emerged with triboiontronics, in which triboelectrically induced ion polarization transforms EDLs from passively formed interfacial structures into dynamically reconfigurable ionic-electronic interfaces. In

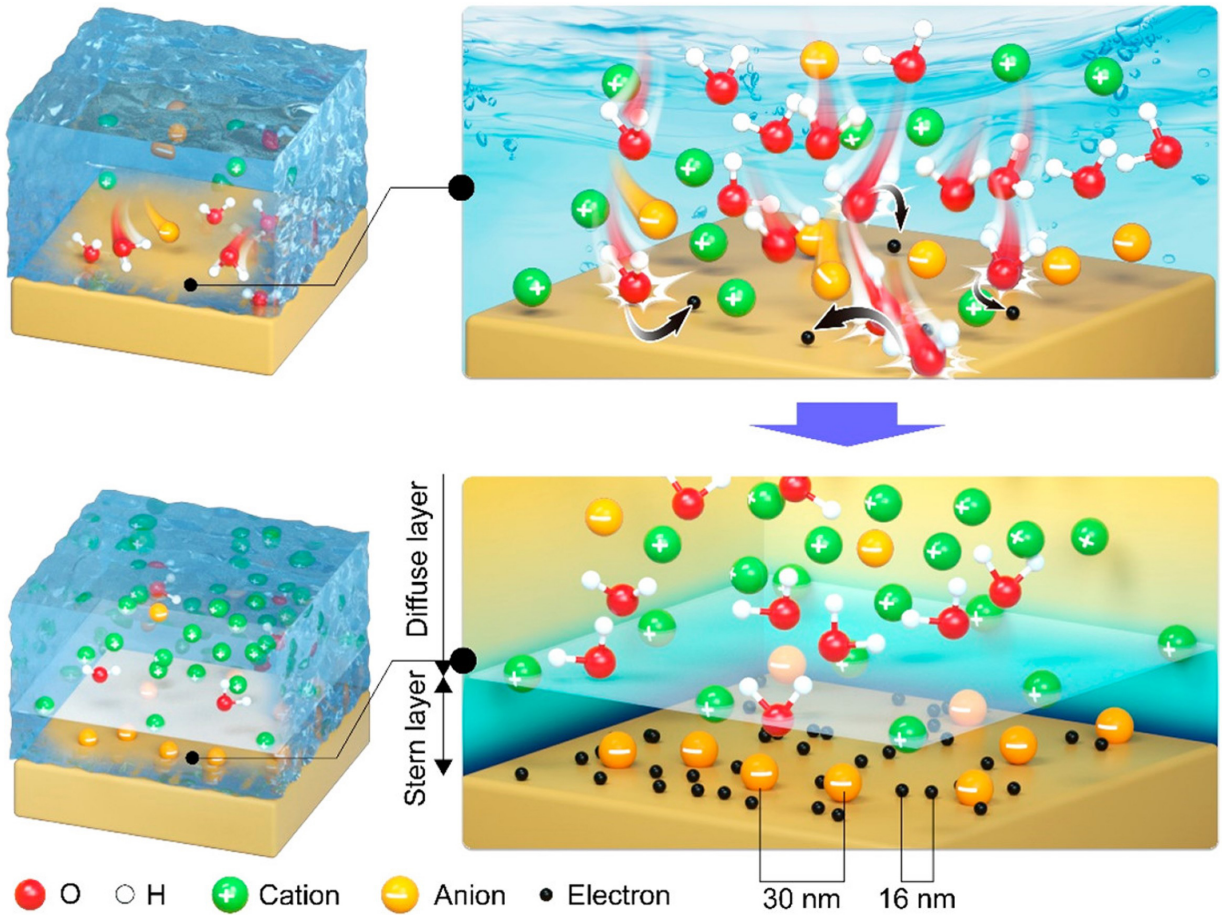

Figure 3. Schematic illustration of the two-step EDL model at non-conductive solid-liquid interfaces. Reprinted with permission from[56] Copyright © 2022 American Chemical Society.

triboiontronic systems, triboelectrically generated surface charges create a long-range electrostatic field that penetrates the dielectric substrate and dynamically modulates interfacial ionic distributions. Recognizing this fundamentally nonequilibrium process, Li *et al.* established the triboiontronic dynamic EDL model [Figure 4], which extends the two-step EDL framework from describing interfacial charge formation to quantitatively capturing the spatiotemporal evolution of dynamic EDLs driven by triboelectrically induced ion polarization[57]. This external field simultaneously influences both the Stern layer and diffuse layer, enabling dynamic tuning of ionic concentration, spatial asymmetry, and charge polarity. As a result, the EDL no longer behaves as a static equilibrium structure but evolves into a reconfigurable ionic system. Under forward triboelectric polarization [Figure 4A], the induced electric field drives anion accumulation at the interface while repelling cations, strengthening interfacial charge density and enhancing local potential gradients[57]. In contrast, reverse polarization reverses the field direction [Figure 4B], triggering ion redistribution in the opposite direction and leading to complete reconstruction of the EDL configuration, including polarity inversion[57]. Through this mechanism, ionic distributions become continuously programmable via mechanical stimuli, establishing a dynamic ionic regulation regime that bridges mechanical energy and interfacial ionic transport. This regime represents a transition from static formation-controlled interfaces to actively programmable ionic systems.

Iontrovoltaic effect enabled by semiconductor–liquid EDL-SCR coupling

The evolution of dynamic EDLs extends interfacial physicochemistry beyond dielectric solid-liquid systems toward semiconductor-liquid interfaces, where electrolyte ion redistribution becomes intrinsically coupled with electronic carrier modulation in the semiconductor. This transition represents a further advancement of

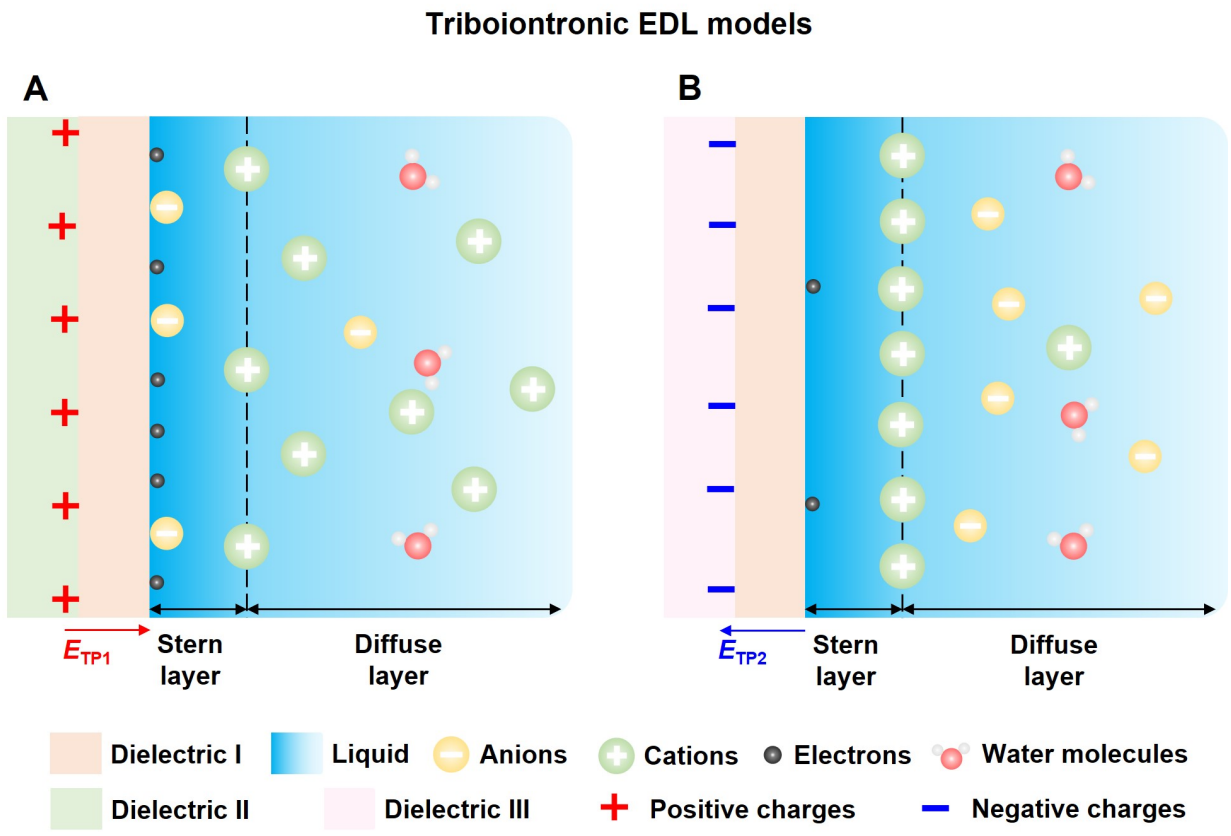

Figure 4. Triboelectrically induced ion polarization enables dynamic reconstruction of EDLs at non-conductive solid-liquid interfaces. (A) Forward polarization-induced EDL reconstruction; (B) Reverse polarization-induced EDL reconstruction.

EDL theory, from purely ionic interfacial structures to coupled ionic-electronic interfaces governed by the mutual interaction between the EDL and the semiconductor SCR through a shared interfacial electric field. Within this framework, Li *et al.* recently introduced the iontrovoltaic effect [Figure 5], which describes interfacial energy conversion arising from dynamic EDL-SCR coupling[94]. Unlike conventional electrochemical or photovoltaic processes, the iontrovoltaic effect originates from actively reconfigurable ionic-electronic interfacial fields, in which ionic redistribution and electronic carrier separation are simultaneously regulated by interfacial electrostatics without the need for external bias[94].

When a liquid droplet contacts a semiconductor surface [Figure 5A], contact electrification and electrochemical potential equilibration drive interfacial charge redistribution, simultaneously generating an SCR in the semiconductor and a compensating EDL at the contact interface[94]. This process establishes an EDL-SCR structure with a built-in electric field that governs carrier separation in the semiconductor. Importantly, this field is not static but dynamically evolves with interfacial conditions, making the system highly sensitive to external perturbations. To further regulate this coupled system, triboelectric polarization can be introduced [Figure 5B]. The externally generated electrostatic field extends across the interface, coupling the electronic response of the semiconductor with the ionic response of the electrolyte. In the semiconductor, it intensifies band bending and SCR formation, while in the electrolyte, it drives ion redistribution and dynamic EDL polarization. This reciprocal ionic-electronic modulation amplifies the interfacial electric field, giving rise to a highly coupled EDL-SCR state that underpins iontrovoltaic signal generation. Quantitatively, the strength of EDL-SCR coupling is governed by the charge densities and capacitances of the liquid-side EDL and semiconductor SCR, together with the corresponding interfacial potential drops. Variations in EDL charge density regulate ionic screening and local interfacial potential,

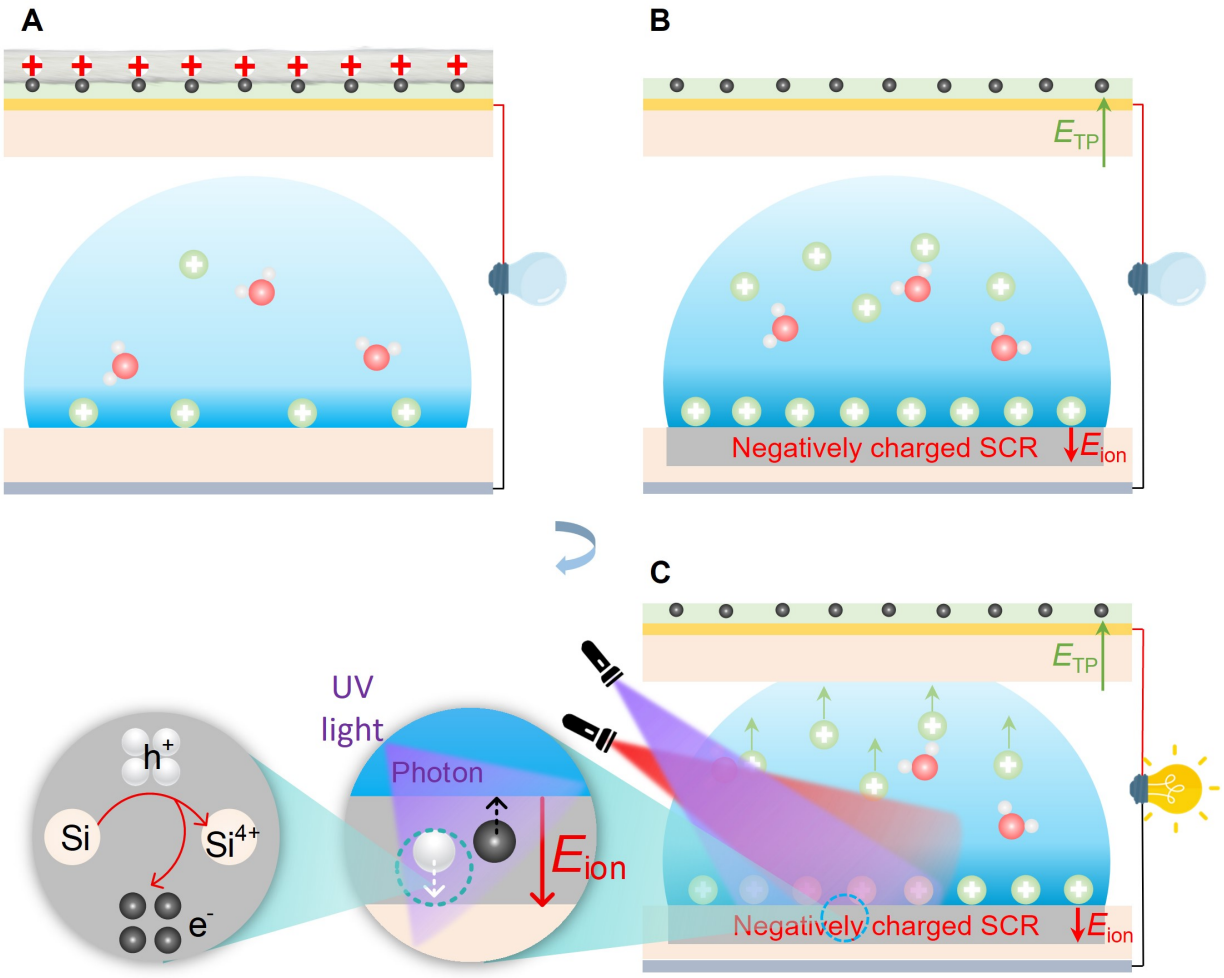

Figure 5. Dynamic EDL-SCR coupling underlying iontrovoltaic effects. Reprinted with permission from[94] Copyright © 2026, Springer Nature. (A) Formation of coupled SCR-EDL structures at semiconductor-liquid interfaces; (B) Triboelectric polarization enhances interfacial field strength and modulates EDL-SCR coupling; (C) Asymmetric EDLs induce ionic chemical potential gradients, enabling directional ion and carrier transport.

whereas changes in SCR charge density modify band bending and carrier separation. Because the EDL and SCR are electrostatically coupled across the same interface, redistribution of charge on either side alters the overall interfacial electric field. The temporal response of this coupled state is further determined by the characteristic timescales of ionic redistribution in the electrolyte and carrier relaxation in the semiconductor, which together control how rapidly the interfacial energy landscape can be reconstructed under external stimulation. When a second semiconductor-liquid interface with a different interfacial state is introduced [Figure 5C], asymmetric EDL-SCR coupling is established across the electrolyte. This asymmetry generates an ionic chemical potential gradient that drives directional ion migration, while the coupled SCRs in the semiconductor electrodes regulate carrier transport. The coordinated evolution of ionic and electronic processes enables synchronized ionic-electronic responses across the entire system. Beyond triboelectric regulation, optical excitation provides an additional modulation pathway. Photoexcited carriers are separated by the interfacial electric field, while interfacial redox reactions continuously reshape local ionic distributions and reinforce EDL asymmetry. In parallel, photothermal effects enhance ionic mobility, accelerating interfacial charge redistribution dynamics. Through the synergistic coupling of triboelectric polarization, optical excitation, thermal modulation, EDL reconstruction, SCR regulation, and carrier separation, a dynamically reconfigurable ionic-electronic energy landscape is established. The iontrovoltaic effect

therefore represents a new paradigm of interfacial energy conversion, in which ionic transport in electrolytes and electronic carrier dynamics in semiconductors are no longer independent processes, but are intrinsically coupled through a unified and dynamically evolving interfacial electric field. Within this EDL-SCR framework, semiconductor-liquid interfaces are transformed from passive charge-transfer boundaries into adaptive ionic-electronic systems governed by coupled electrostatic, ionic, and electronic degrees of freedom. This concept provides a unified physical foundation for iontrovoltaic energy conversion and the development of emerging iontronic technologies.

Collectively, the four EDL frameworks represent a progressive expansion in both interfacial scope and regulatory capability. Classical EDL models, including the Helmholtz, Gouy-Chapman, and GCS frameworks, mainly describe equilibrium or near-equilibrium ionic screening at conductive solid-liquid interfaces, providing the fundamental electrostatic basis for understanding interfacial charge compensation, but without explicitly considering the generation of surface charge or externally driven nonequilibrium reconstruction. The two-step EDL model extends this description to non-conductive interfaces by coupling interfacial charge generation, including electron transfer and surface ionization, with subsequent ionic redistribution, thereby explaining how EDLs are established at dielectric interfaces, although the model is still primarily concerned with EDL formation and relaxation toward quasi-equilibrium states. The triboiontronic dynamic EDL model further introduces triboelectrically induced ion polarization as an external driving mechanism, enabling active, reversible, and programmable reconstruction of ionic concentration distributions and interfacial charge states beyond spontaneous equilibration, but it mainly focuses on ionic redistribution and electrostatic regulation without explicitly incorporating semiconductor carrier energetics. The semiconductor-liquid EDL-SCR framework further expands this picture by coupling liquid-side ionic redistribution with semiconductor SCR formation, band bending, and carrier transport through a shared interfacial electric field, thereby extending EDL regulation from purely ionic processes to coupled ionic-electronic interfaces. Therefore, these four models should not be regarded as mutually exclusive replacements, but rather as progressively expanded descriptions of solid-liquid interfacial physics, evolving from passive ionic screening, to charge-generation and ion-redistribution coupling, to actively programmable ionic regulation, and ultimately to dynamic ionic-electronic coupling.

DYNAMIC EDLs ENABLING INTERFACIAL ENERGY HARVESTING

Building on the progressive expansion of EDL regulation capabilities, dynamic EDLs have enabled a new generation of iontronic systems in which interfacial ionic and electronic processes are directly harnessed for energy transduction and information processing[105-107]. In these systems, energy conversion and signal generation arise from a common physicochemical origin: the dynamic reconfiguration of interfacial ionic distributions governed by time-dependent EDL evolution. Beyond their conventional role as passive charge-screening structures, dynamic EDLs act as active interfacial regulators that integrate ionic transport, electrostatic modulation, and electronic responses. According to the dominant interfacial coupling mechanisms, dynamic EDL-enabled systems can be classified into three representative categories: S-L TENGs, TINGs, and IVNGs. These systems represent a continuous evolution of interfacial regulation, progressing from electrostatic induction-dominated energy conversion, through ionic transport-mediated information transduction, to fully coupled ionic-electronic energy landscapes.

S-L TENGs

Energy conversion at solid-liquid interfaces is fundamentally governed by interfacial charge generation, separation, and transport. For conventional S-L TENGs, the basic operating mechanism is based on the coupling between contact electrification and electrostatic induction. At dielectric solid-liquid interfaces, contact electrification generates interfacial surface charges, corresponding to the initial charge-generation step of the two-step EDL model, while subsequent redistribution of mobile ions establishes the compensating

EDL. Dynamic EDLs therefore provide a liquid-side ionic framework in which charge redistribution, ionic migration, and electrostatic field modulation are intrinsically coupled. Other factors, including wetting behavior, charge trapping, surface properties, and liquid composition, can further regulate charge generation, retention, ionic screening, and consequently the output performance. S-L TENGs are among the earliest and most representative systems in which contact electrification, dynamic EDL evolution, and electrostatic induction are coupled at dielectric solid-liquid interfaces[108-112]. Since the first demonstration of S-L TENG by Wang *et al.*, they have enabled efficient conversion of low-frequency mechanical energy from droplets, waves, and fluid flows into electricity[92,113-118]. In contrast to solid-solid systems, the presence of a liquid introduces mobile ions, making EDL formation and evolution an inherent part of the energy conversion process[119,120]. Quantitatively, the ionic contribution to S-L TENG operation is governed by several interfacial parameters, including surface charge density, Debye length, and EDL capacitance. The surface charge density generated by contact electrification determines the electrostatic driving strength for ionic redistribution, while the Debye length defines the characteristic spatial scale of ionic screening in the liquid and decreases with increasing ionic strength. Correspondingly, the EDL capacitance reflects the ability of the interface to accommodate compensating ionic charge and determines the relationship between interfacial charge accumulation and potential variation. These parameters collectively regulate the degree of ionic screening and the magnitude of interfacial potential modulation, thereby influencing the electrostatic-induction output of S-L TENGs.

S-L TENG operation can be interpreted as a cyclic evolution of dynamic EDLs, where interfacial contact induces charge generation and EDL formation, while separation triggers EDL disruption and ionic redistribution, generating transient interfacial electric fields that drive electron flow in external circuits [Figure 6]. Upon contact between a dielectric surface and a liquid, interfacial charge transfer associated with contact electrification induces ionic redistribution in the electrolyte, leading to the formation of an EDL at the interface [Figure 6A]. During separation, the disruption of this equilibrium state drives diffuse ions away from the interface, weakens electrostatic screening, and generates a transient interfacial electric field that drives electron flow in the external circuit [Figure 6B]. When complete separation is achieved, ionic redistribution approaches a quasi-equilibrium state and the output gradually diminishes [Figure 6C]. Upon re-approach, the interfacial electric field is re-established in the opposite direction, triggering EDL reconstruction and restoring ionic screening, thereby producing alternating current output [Figure 6D]. From this perspective, the operation of S-L TENGs is not solely governed by triboelectric charge induction but is fundamentally dictated by the cyclic reconstruction of dynamic EDLs. This process continuously modulates interfacial electrostatics and governs the coupling between ionic transport in the electrolyte and electron flow in the external circuit. Accordingly, the cyclic evolution of EDLs represents the intrinsic physicochemical origin of energy conversion in S-L TENG systems.

The evolution of S-L TENGs reflects the expanding understanding of interfacial ionic processes and dynamic EDLs at dielectric solid-liquid interfaces[121-127]. Although the concept of dynamic EDLs was not explicitly formulated during the early stage of research, accumulating experimental evidence gradually revealed that interfacial ions and their redistribution play a decisive role in liquid-solid energy conversion, providing the experimental basis for later dynamic EDL theory. The first breakthrough was achieved in 2013, when Lin *et al.* demonstrated a water-based S-L TENG that converts mechanical energy from liquid waves into electricity through contact electrification between water and dielectric polymer surfaces [Figure 7A(i)][92]. At this stage, interfacial charge generation was interpreted primarily within the framework of triboelectric charge transfer; however, the presence of water inherently introduces an ionic environment, implying the formation of an interfacial ionic screening layer adjacent to the charged dielectric surface. From a modern perspective, this process corresponds to the establishment of an EDL, in which interfacial charges on the dielectric induce counterion accumulation and ionic rearrangement in the electrolyte. The device achieved

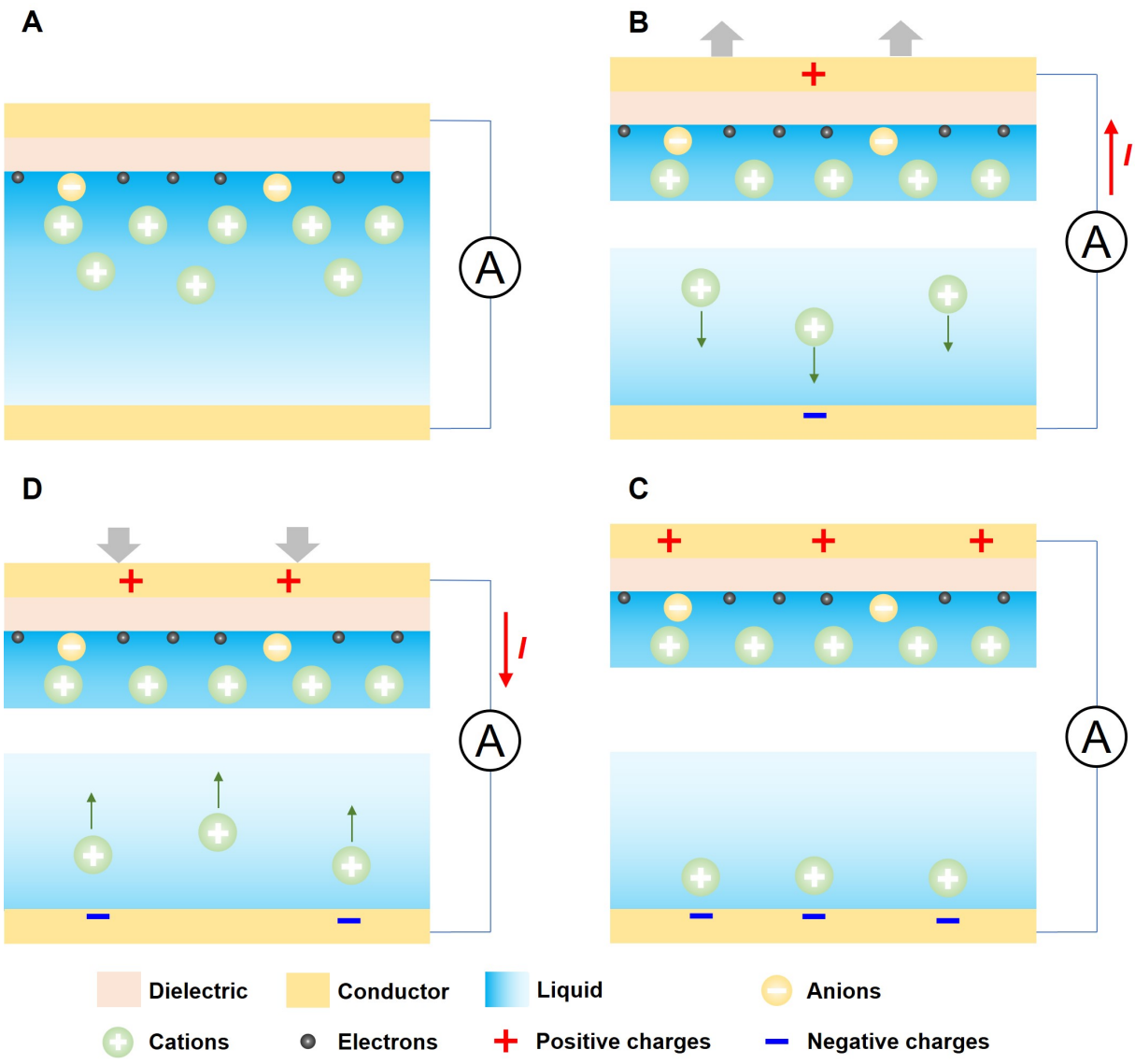

Figure 6. Dynamic EDL-mediated energy-conversion mechanism of S-L TENGs. (A) Contact between a dielectric surface and a liquid induces interfacial charge transfer and ionic redistribution, leading to EDL formation at the interface; (B) Subsequent separation disrupts the EDL, driving ionic migration and generating a transient interfacial electric field that induces electron flow in the external circuit; (C) At complete separation, ionic redistribution approaches a quasi-equilibrium state, corresponding to a maximum charge-separated condition with negligible current output; (D) Re-approach of the dielectric surface reconstructs the EDL, reverses ionic migration, and restores the interfacial electric field, resulting in alternating current output.

an open-circuit voltage (V_{OC}) of ~80 V, a short-circuit current (I_{SC}) in the microampere range, and a peak power (P_R) density of ~50 mW m^{-2} [Figure 7A(ii and iii)], confirming the feasibility of liquid-mediated triboelectric energy harvesting.

Subsequently, the system was extended to droplet-based S-L TENGs proposed by Lin *et al*. in 2014 [Figure 7B(i)], in which discrete droplet dynamics introduced a strongly time-dependent interfacial boundary condition[128]. The droplet impact process, including approach, wetting, spreading, retraction, and detachment, induces continuous reconfiguration of the solid-liquid contact area and associated interfacial charge distribution. This dynamic evolution drives repeated formation, perturbation, and relaxation of ionic screening layers at the interface, which can now be interpreted as spatiotemporally evolving EDL structures.

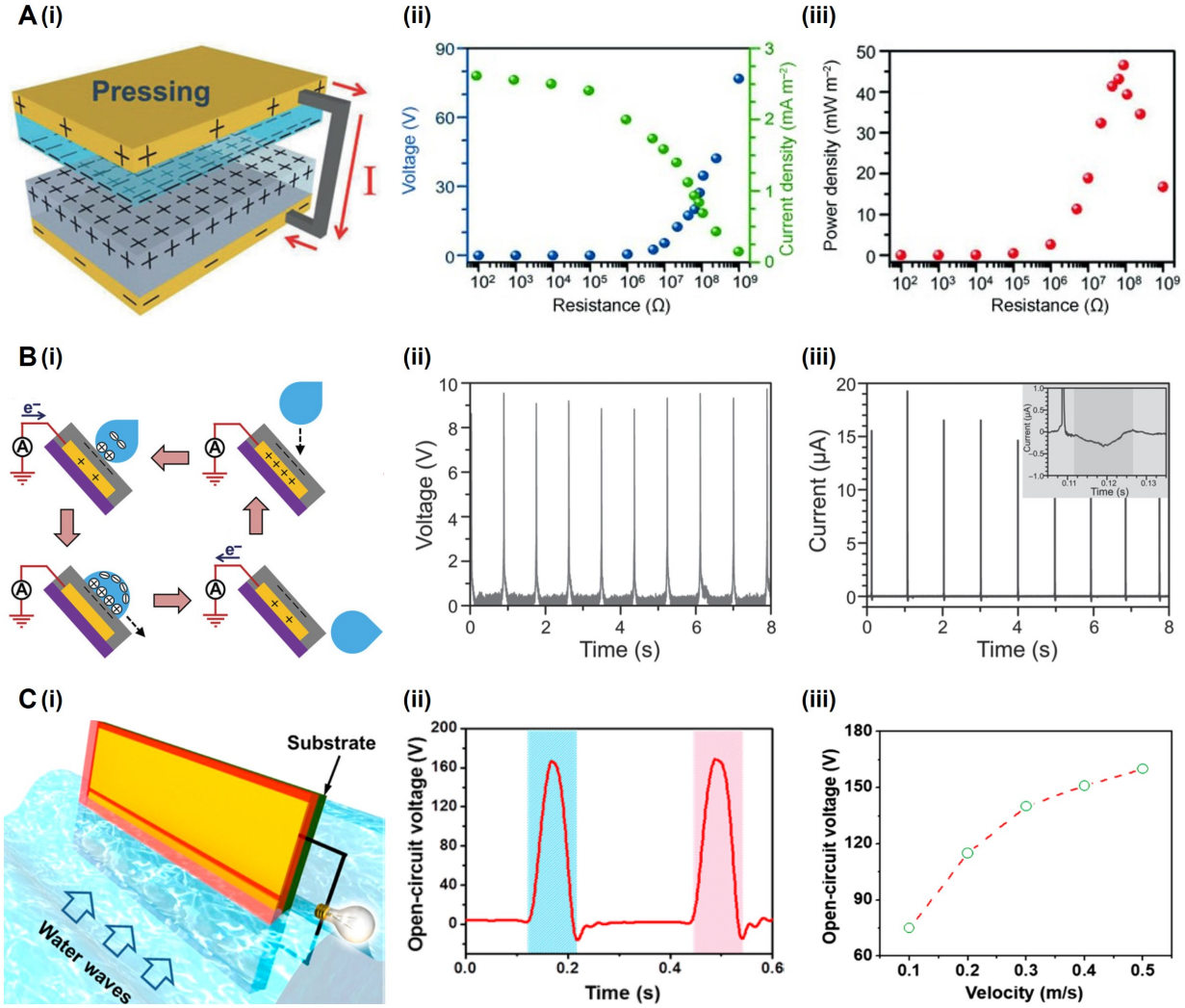

Figure 7. Pioneering developments of dynamic EDL-enabled S-L TENGs. (A) The first water-based S-L TENG (2013) provided early evidence that ionic structures at the liquid side participate in solid-liquid triboelectric energy conversion. Reprinted with permission from[92] Copyright © 2013 WILEY-VCH Verlag GmbH & Co. KGaA, Weinheim; (B) The droplet-driven S-L TENG (2014) revealed that droplet dynamics induce spatiotemporal evolution of interfacial charge distribution and dynamic EDL modulation. Reprinted with permission from[128] Copyright © 2014 WILEY-VCH Verlag GmbH & Co. KGaA, Weinheim; (C) The wave-driven S-L TENG (2014) demonstrated that continuous interfacial perturbations lead to dynamic EDL evolution and ionic redistribution, which directly govern macroscopic energy conversion behavior. Reprinted with permission from[129] Copyright © 2014 American Chemical Society.

Importantly, this system provided clearer evidence that interfacial charge transfer and ionic redistribution are not independent processes but are intrinsically coupled through interfacial electrostatics. The device delivered a V_{OC} of up to ~9.3 V and an I_{SC} of ~17 μA [Figure 7B(ii and iii)], highlighting the sensitivity of interfacial energy conversion to dynamic wetting and ionic redistribution processes. A further conceptual advance was achieved in wave-driven S-L TENGs proposed by Zhu *et al.* in 2014 [Figure 7C(i)], where continuous water-level oscillations introduce a quasi-periodic modulation of the solid-liquid contact interface[129]. In this configuration, interfacial charge accumulation on the dielectric surface and ionic rearrangement in the electrolyte occur simultaneously but continuously evolve with the instantaneous contact area. The resulting spatially distributed EDLs exhibit time-dependent restructuring along the interface, generating dynamic interfacial potential gradients that drive electron transport in the external circuit. This represents one of the earliest demonstrations that spatially and temporally evolving EDLs can directly govern macroscopic energy conversion behavior. The device achieved a V_{OC} of ~160 V, transferred

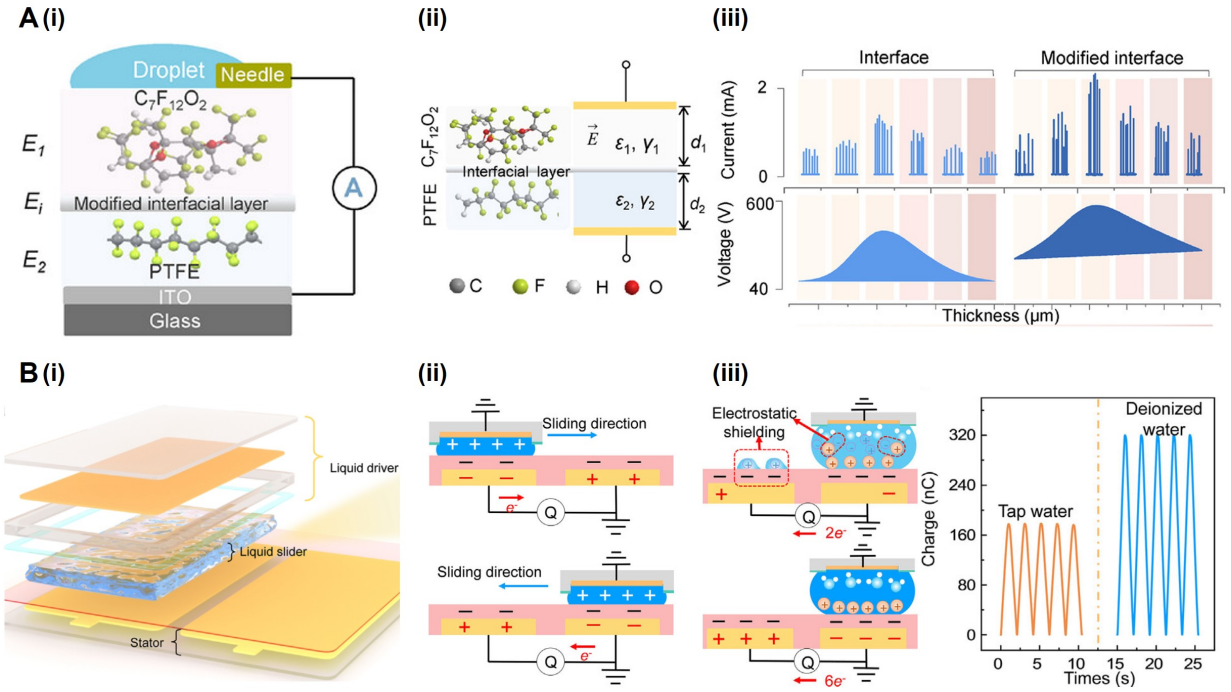

Figure 8. Representative strategies for enhancing energy conversion of S-L TENG through interfacial ionic regulation and engineering. (A) An interfacial polarization-enhanced liquid-droplet triboelectric nanogenerator based on dielectric-constant mismatch and Maxwell-Wagner polarization was developed by Chen *et al.* in 2025. Reprinted with permission from[133] Copyright © 2025 WILEY-VCH GmbH; (B) A three-phase interfacial force-regulated solid-like liquid-slider triboelectric nanogenerator for highly efficient and robust energy harvesting was developed by Gong *et al.* in 2026. Reprinted with permission from[136] Copyright © 2025 WILEY-VCH GmbH.

charge (Q_{SC}) of ~75 nC, and P_R of ~0.12 mW, with performance positively correlated with wave velocity, indicating enhanced interfacial ion dynamics under stronger hydrodynamic perturbations [Figure 7C(ii and iii)].

The recognition of dynamic EDLs as active interfacial regulators has shifted the development of solid-liquid triboelectric systems from empirical optimization toward rational engineering of interfacial ionic processes for enhanced energy conversion[130-135]. Rather than relying solely on conventional surface morphology design or material selection, recent studies have increasingly targeted the manipulation of ionic redistribution, interfacial polarization, and EDL evolution as key parameters governing charge-transfer efficiency and energy-conversion behavior. A representative example was reported by Chen *et al.* (2025), who demonstrated active enhancement of dynamic EDLs through interfacial polarization engineering [Figure 8A(i)][133]. By introducing a dielectric mismatch in a bilayer structure [Figure 8A(ii)], Maxwell-Wagner polarization generated a localized electric field enhancement at the solid-liquid interface. This intensified interfacial field strengthens charge trapping and promotes EDL formation, thereby enhancing charge separation during droplet impact. As a result, significantly improved electrical outputs were achieved, including a V_{OC} of ~540 V, an I_{SC} approaching 2 mA, highlighting the effectiveness of polarization-engineered EDL regulation [Figure 8A(iii)]. More recently, Gong *et al.* (2026) further extended interfacial engineering strategies to three-phase force-regulated solid-liquid systems [Figure 8B(i)][136]. By tuning surface tension, Laplace pressure, viscous resistance, and contact-line dynamics, stable liquid-slider operation was achieved while maintaining conformal solid-liquid contact [Figure 8B(ii)]. This configuration effectively optimizes interfacial charge transfer by simultaneously enhancing contact area, reducing mechanical losses, and stabilizing dynamic EDL evolution. The device delivered a Q_{SC} of ~580 nC, an I_{SC} of 5 μA, and a P_R of 3.14 mW, while maintaining long-term stability and achieving an energy conversion efficiency of 63.47%. Moreover, ionic content in the liquid was identified as a critical factor, where deionized water enabled higher outputs due to reduced electrostatic screening compared with ionic-rich tap water, further confirming the dominant role of EDL screening in interfacial energy conversion [Figure 8B(iii)].

Collectively, advances in S-L TENGs demonstrate a continuous evolution from simple triboelectric charge transfer to interfacial energy conversion governed by dynamic EDL regulation. Across different engineering strategies, including physicochemical environment tuning, interfacial polarization enhancement, and three-phase force modulation, the interfacial ionic environment emerges as a central parameter that governs charge separation, electrostatic field formation, and energy-conversion efficiency. In this framework, the EDL evolves from a passive ionic screening structure into a dynamically reconfigurable interfacial entity that mediates the coupling between ionic transport in the electrolyte and electrostatic induction in the external circuit. The performance of S-L TENGs is therefore fundamentally determined by the interplay between interfacial charge generation, ionic redistribution, and EDL screening dynamics, rather than solely by surface morphology or material properties. This unified perspective establishes dynamic EDL regulation as a general design principle for solid-liquid energy harvesting systems, providing a mechanistic foundation for optimizing interfacial electrostatics, enhancing charge-transfer efficiency, and enabling scalable energy conversion from complex fluid environments.

TINGs enabled by ionic migration between asymmetric EDLs

While dynamic EDLs in S-L TENGs primarily facilitate electron-mediated energy conversion through electrostatic induction, recent advances in interfacial physicochemistry have revealed a broader functionality of dynamic EDLs: their capacity to actively regulate ionic transport. In biological systems, dynamically regulated physicochemical interfaces establish and maintain ionic concentration gradients that drive directional ion migration, enabling efficient energy transfer and information signaling. Inspired by these principles, Li *et al.* developed TING in 2024 based on asymmetric dynamic EDLs at coupled solid-liquid interfaces[137]. This work established dynamic EDLs as programmable ionic regulators capable of mediating not only charge accumulation but also directional ionic transport and information encoding [Figure 9]. In this system, sequential contact between a water droplet and two metal/dielectric hybrid interfaces with different contact histories leads to spatially asymmetric charge distributions. According to the two-step EDL framework, each contact event induces the formation of an EDL through interfacial charge transfer and ionic redistribution. Because the two interfaces are generated under different interfacial states, asymmetric EDL configurations are established across the liquid phase. This asymmetry gives rise to a sustained ionic concentration gradient, which drives directional ionic migration through the electrolyte. Quantitatively, the driving force for this directional ionic transport is governed by the electrochemical-potential difference established between the asymmetric EDLs, which contains contributions from both the ionic concentration gradient and the interfacial electric-potential gradient. A larger concentration difference between the two interfaces generally produces a stronger chemical-potential imbalance and enhances directional ionic flux, while the resulting transport rate is further influenced by ion mobility, diffusivity, valence, and the effective transport distance. In the temporal domain, the persistence of the asymmetric EDL state relative to ionic diffusion and relaxation timescales determines how long the concentration gradient can be maintained and therefore directly affects the duration and stability. Concurrently, ionic-electronic coupling at the interfaces enables charge extraction in the external circuit, resulting in a stable direct-current (DC) output. From the perspective of dynamic EDL evolution, the key advance of TINGs lies in transitioning from transient electrostatic modulation to the deliberate construction of spatially asymmetric EDL architectures that sustain ionic chemical potential gradients. In this regime, triboelectrically induced interfacial polarization is converted into a persistent driving force for ionic transport, fundamentally distinguishing TINGs from S-L TENGs. This establishes dynamic EDLs not only as regulators of interfacial electrostatics but also as active mediators of ionic flux, providing the physicochemical basis for triboiontronic energy transfer and ionic signal transport systems[137].

Based on the asymmetric EDL-driven ionic migration mechanism, a TING was developed using Au/FEP (fluorinated ethylene propylene) hybrid films in 2024 [Figure 10A][137]. In this architecture, the Au layer serves as an efficient charge-collecting electrode, while the exposed FEP regions enable robust EDL

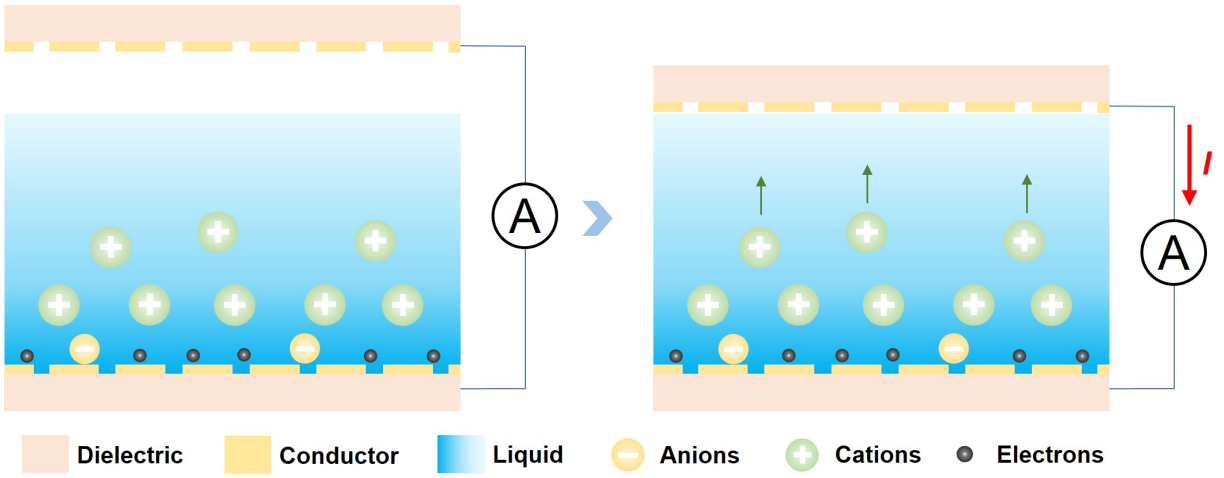

Figure 9. Schematic illustration of the operating mechanism of TINGs, where asymmetric dynamic EDLs at coupled solid-liquid interfaces establish ionic concentration gradients that drive directional ionic migration and enable DC energy conversion.

formation through contact electrification with water, providing a well-defined platform for investigating asymmetric interfacial ionic transport. To validate the governing mechanism, controlled wetting-sequence experiments were performed [Figure 10B]. The device output exhibited a clear dependence on the temporal order of interfacial EDL formation: wetting of the lower interface prior to the upper interface produced a positive output, whereas reversing the sequence led to polarity inversion. Nearly synchronous wetting resulted in negligible signals. Moreover, increasing the temporal asymmetry between the two interfaces significantly enhanced the output intensity, confirming that the electrical response originates from asymmetric EDL-induced ionic concentration gradients rather than conventional electrostatic induction. These results establish a direct correlation between EDL asymmetry and directional ionic transport. The role of the hybrid architecture was further clarified by tuning Au sputtering time [Figure 10C]. Increasing Au coverage enhances electrical conductivity and facilitates ionic-electronic coupling, whereas excessive deposition reduces exposed FEP area, thereby weakening interfacial charge generation and EDL formation. This competition leads to an optimal structural balance, highlighting the necessity of simultaneously optimizing charge collection efficiency and interfacial electrostatic activity. To further elucidate the origin of asymmetric EDL formation, interfacial charge behaviors on dielectric, metallic, and hybrid surfaces were systematically compared [Figure 10D]. Dielectric interfaces favor strong contact electrification and pronounced EDL formation but suffer from limited charge extraction. Metallic interfaces provide efficient electron transport pathways, but exhibit weakened EDL formation due to rapid charge dissipation. In contrast, Au/FEP hybrid interfaces integrate both advantages: the dielectric component sustains robust EDL formation, while the metallic layer ensures efficient charge collection and external circuit coupling. This synergistic configuration enables the coexistence of asymmetric EDL construction, sustained ionic concentration gradients, and effective ionic-electronic coupling, thereby forming the physical basis of triboiontronic energy conversion.

Following the identification of asymmetric EDL-driven ionic transport as the dominant mechanism, the electrical characteristics of TINGs arising exclusively from EDL asymmetry were systematically investigated. Owing to sustained directional ion migration induced by coupled asymmetric EDLs, the device generates stable DC outputs. Under optimized conditions, the TING achieves an I_{SC} of 2.60 mA and a V_{OC} of 0.25 V. More importantly, the Q_{SC} density and P_R density reach 412.54 mC m^{-2} [Figure 10E] and 8.45 W m^{-2}, respectively, confirming that asymmetric EDLs alone can continuously convert interfacial ionic concentration gradients into electrical energy without requiring external bias, mechanical pumping, or

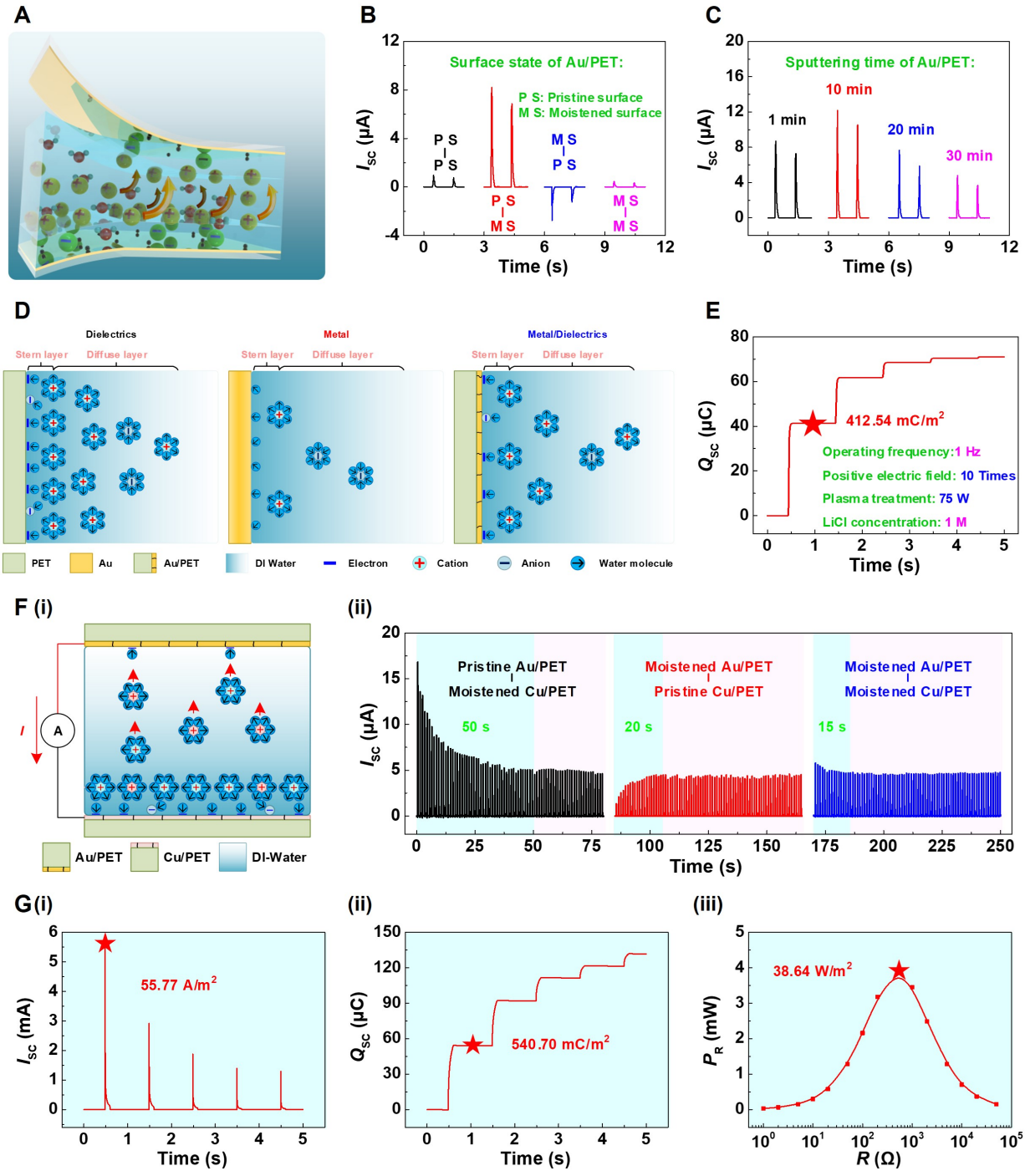

Figure 10. Asymmetric EDL-driven ionic transport and ionic-electronic coupled energy conversion in TINGs. Reprinted with permission from[137] Copyright © 2024 Springer Nature. (A) Construction of a TING based on Au/FEP hybrid interfaces enabling asymmetric EDL formation and ionic transport; (B) Experimental verification of directional ion migration induced by asymmetric EDLs through controlled wetting-sequence measurements; (C) Regulation of triboiontronic output via structural optimization of metal/dielectric hybrid interfaces, balancing charge collection and EDL formation; (D) Comparative EDL configurations at dielectric, metallic, and hybrid interfaces, highlighting their distinct roles in charge generation and transport; (E) DC output arising solely from asymmetric EDL-driven ionic migration; (F) Enhancement of ionic transport through synergistic coupling between asymmetric EDL-induced concentration gradients and interfacial redox reactions; (G) Overall performance enhancement of triboiontronic energy conversion enabled by asymmetric EDL-redox coupling.

electrochemical driving forces. This establishes asymmetric EDLs as an intrinsic ionic transport medium for triboiontronic energy conversion. To further enhance ionic transport, metallic current-collecting layers with

tunable electrochemical activity were introduced to couple asymmetric EDL-driven ion migration with interfacial redox reactions [Figure 10F(i)]. In addition to the ionic concentration gradients generated by asymmetric EDLs, spontaneous oxidation-reduction processes at the metal-liquid interface continuously produce additional ionic species and reinforce interfacial chemical potential differences. The coupling effect was validated through controlled wetting-sequence experiments [Figure 10F(ii)]. Ionic flux driven by EDL asymmetry could either synergize with or oppose redox-induced ionic transport. When both contributions aligned, ionic transport and electrical outputs were significantly enhanced; when they opposed each other, partial cancellation occurred, leading to reduced performance. Benefiting from this synergistic EDL-redox coupling, substantially enhanced triboiontronic outputs were achieved. Compared with the asymmetric EDL-only configuration, the coupled system exhibits markedly improved current, charge transfer, and power generation capabilities, reaching an I_{SC} of 5.58 mA, a Q_{SC} density of 540.70 mC m^{-2}, and a P_R density of 38.64 W m^{-2} [Figure 10G(i-iii)][137]. These enhancements originate from the cooperative interaction between EDL-induced ionic concentration gradients and redox-generated ionic flux, which together amplify both ion migration and ionic-electronic coupling efficiency. Collectively, this work establishes asymmetric EDL formation as the fundamental driving force for triboiontronic energy conversion and demonstrates that ionic transport can be further amplified through coupling with interfacial redox chemistry. More importantly, it redefines dynamic EDLs from passive charge-screening structures into active ionic transport and energy conversion interfaces, providing a systematic experimental foundation for asymmetric EDL-driven triboiontronics.

A further advance in triboiontronics was achieved through triboelectrically induced ion polarization, which enables active reconstruction of ionic concentration distributions within EDLs at solid-liquid interfaces. Unlike conventional TINGs, where ionic transport is governed by spontaneously formed asymmetric EDLs, this polarization strategy introduces an externally generated triboelectric field that actively modulates existing EDL structures, providing an additional degree of freedom for regulating ionic distribution and ionic-electronic coupling[93]. This concept establishes a route toward programmable control of ionic flux and lays the physicochemical foundation for neuromimetic iontronic systems. The operating mechanism is illustrated in Figure 11. Upon contact between the water droplet and the bottom Au/FEP hybrid film, interfacial contact electrification occurs at the exposed dielectric regions, leading to the formation of an EDL at the solid-liquid interface [Figure 11A]. Subsequently, the top Au/FEP electrode undergoes solid-solid contact electrification with an electropositive fur layer, generating triboelectric charges on the FEP surface [Figure 11B]. After separation, the retained surface charges establish a localized electric field that penetrates the liquid phase and modulates ion distribution within the pre-existing bottom EDL [Figure 11C]. Under this field, ionic concentration within the EDL becomes strongly polarized, with enhanced accumulation of anions near the interface and redistribution of cations toward the diffuse layer, leading to a pronounced nonequilibrium ionic asymmetry. When the top electrode recontacts the droplet, a second EDL is formed at the upper interface [Figure 11D]. Because the bottom EDL has already been externally polarized, a significant ionic concentration difference is established between the two interfaces, which drives rapid directional ion migration through the liquid phase. The resulting ionic flux induces charge redistribution at the electrodes via ionic-electronic coupling, enabling efficient electrical signal generation. More importantly, triboelectrically induced ion polarization fundamentally extends the regulatory capability of dynamic EDLs from spontaneous formation processes to active, field-programmable reconstruction of interfacial ionic states. In this regime, EDLs are no longer passive screening layers but reconfigurable electrochemical interfaces capable of encoding, amplifying, and directing ionic fluxes. This mechanism not only enhances triboiontronic energy conversion but also provides a general strategy for coupling ionic transport with signal modulation, offering a key step toward dynamic EDL-enabled energy-information integration.

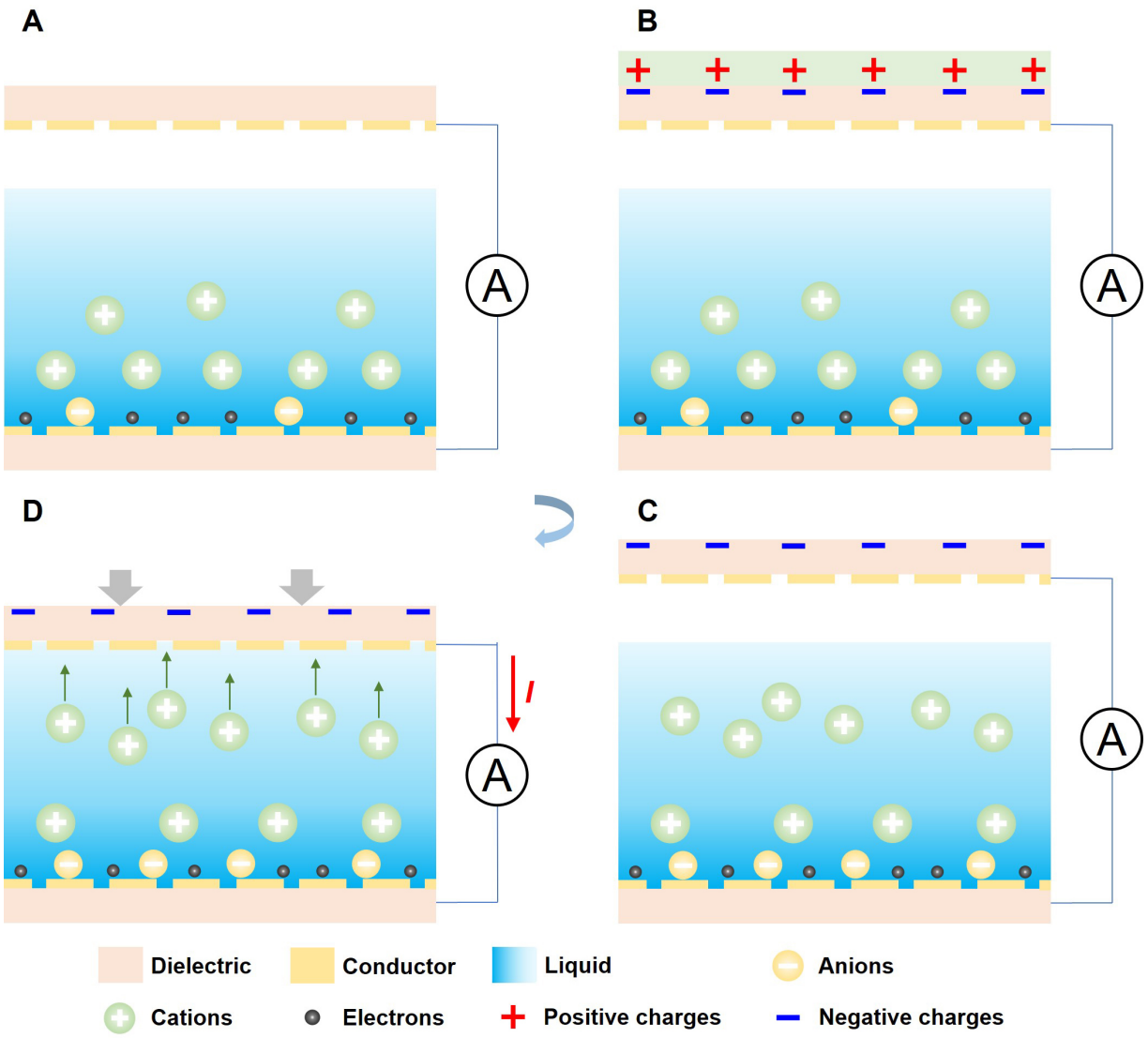

Figure 11. Dynamic regulation of EDLs via triboelectrically induced ion polarization for enhanced triboiontronic energy conversion in TINGs. (A) Formation of the initial EDL at the bottom Au/FEP-water interface through solid-liquid contact electrification; (B) Generation of triboelectric charges on the top FEP surface via solid-solid contact electrification with an electropositive fur layer; (C) Triboelectrically induced polarization field modulates the pre-formed EDL, driving active redistribution of ionic concentration and enhancing interfacial ionic asymmetry; (D) Formation of coupled asymmetric EDLs and amplified ionic concentration gradients, enabling directional ion migration and ionic-electronic coupled energy conversion.

Li *et al.* further developed a TING enhanced by triboelectrically induced ion polarization in 2025, enabling active regulation of interfacial ionic distributions for enhanced ionic energy conversion and programmable ionic transport [Figure 12A][93]. Inspired by Maxwell's demon and biological ion pumps [Figure 12A(i and ii)], this concept establishes a unified framework in which triboelectric energy is converted into an external electrostatic driving field that actively reconstructs ionic configurations within EDLs [Figure 12A(iii)]. Analogous to adenosine triphosphate (ATP)-driven ion pumps that maintain nonequilibrium ionic gradients across neuronal membranes, triboelectrically induced polarization injects mechanical energy into the interfacial system, enabling ions to be driven against equilibrium distributions and forming highly polarized asymmetric EDL states. The resulting amplified ionic concentration gradients provide an enhanced driving force for directional ion migration and ionic-electronic coupled energy conversion. To verify this mechanism, remote ionic regulation experiments were conducted using a water droplet-polyethylene terephthalate (PET) interface [Figure 12B]. A triboelectrically charged FEP film or

electropositive fur layer was positioned above the interface without physical contact, generating a remote polarization field. Experimental results show that a negatively charged FEP layer increases the droplet charge from 0.54 to 0.94 nC and shifts the substrate potential negatively, whereas a positively charged layer reduces the droplet charge to 0.25 nC. These observations confirm that externally applied triboelectric fields can non-contactly modulate ionic distributions within EDLs. Within the two-step EDL framework, the negative electrostatic field enhances anion accumulation at the interface and increases EDL charge density, whereas the positive electrostatic field weakens interfacial ionic asymmetry by promoting ion redistribution toward equilibrium. This establishes triboelectrically induced ion polarization as a Maxwell's demon-like interfacial regulator that actively reconstructs EDL charge states through externally supplied mechanical energy. Having established active EDL regulation, the influence of interface architecture on triboiontronic output was further investigated [Figure 12C]. Pure dielectric interfaces enable strong EDL formation and large ionic concentration gradients but suffer from poor charge extraction due to limited conductivity. In contrast, metallic interfaces provide efficient electron transport, but exhibit weakened EDL formation. Hybrid metal/dielectric interfaces integrate these advantages: the dielectric component sustains asymmetric EDL formation, while the metallic layer enables efficient ionic-electronic coupling and charge collection. As a result, conventional TINGs based on Au/FEP hybrid interfaces generate an I_{SC} of 23.6 μA. More importantly, introducing triboelectrically induced ion polarization further amplifies EDL asymmetry, increasing the I_{SC} to 31.1 μA, thereby demonstrating that active field-driven reconstruction of EDLs provides an effective route to enhance ionic transport and triboiontronic energy conversion.

After optimizing the solid-phase interface, the role of ionic charge carriers in triboiontronic energy conversion was systematically investigated [Figure 12D]. Increasing the LiCl concentration from 10^{-4} M to saturation continuously enhanced the I_{SC} from 0.14 to 2.22 mA. This improvement arises from the synergistic effects of increased ionic density within the EDL and enhanced electrolyte conductivity, both of which strengthen ionic transport and ionic-electronic coupling across the interface. Further enhancement was observed by tuning ion valence. Replacing Li^+ with divalent Mg^{2+} ions increased the charge-carrying capacity of the electrolyte, leading to a maximum I_{SC} of 4.22 mA in saturated $MgCl_2$ solutions. This result highlights the critical role of ionic valence in governing interfacial charge density and EDL-mediated transport efficiency. Interestingly, $AlCl_3$ exhibits distinct transport behavior compared with monovalent and divalent electrolytes. Although lower-concentration $AlCl_3$ solutions produce higher outputs, the performance decreases at higher concentrations and eventually reverses polarity under saturated conditions. Molecular dynamics simulations reveal a nontrivial hierarchy of ion mobility ($H^+ > Cl^- > Al^{3+}$ In concentrated $AlCl_3$ solutions, strong hydrolysis leads to the dominance of highly mobile H^+ species, which reshapes the effective EDL structure and alters the primary charge-transfer pathway, ultimately resulting in output polarity inversion. These results reveal that ionic transport in triboiontronic systems is dictated by a complex interplay among ionic concentration, valence, hydration structure, and diffusion kinetics, rather than by concentration and charge state alone. Rational co-engineering of interfacial architectures and ionic species therefore provides an effective strategy for enhancing triboiontronic outputs. Under optimized conditions, the TING delivered a P_R of 6.89 mW [Figure 12E]. More importantly, the system demonstrates that ionic transport directionality can be fundamentally regulated through electrolyte-dependent EDL reconstruction, enabling controllable modulation of output magnitude and polarity, with stable negative output reaching -1.79 mW. To further enhance both output magnitude and operational stability, interfacial redox reactions were integrated into the triboelectrically polarized system, forming a synergistically enhanced TING configuration. In this hybrid system, redox processes continuously generate additional ionic species and reinforce interfacial concentration gradients, thereby sustaining directional ion migration and strengthening ionic-electronic coupling. As a result, the ES-TING achieved a P_R of 34.67 mW [Figure 12F]. Correspondingly, the Q_{SC} density and P_R density reached 5,237.51 mC m^{-2} and 346.7 W m^{-2}, respectively. These findings demonstrate that coupling triboelectrically induced ion polarization with interfacial redox

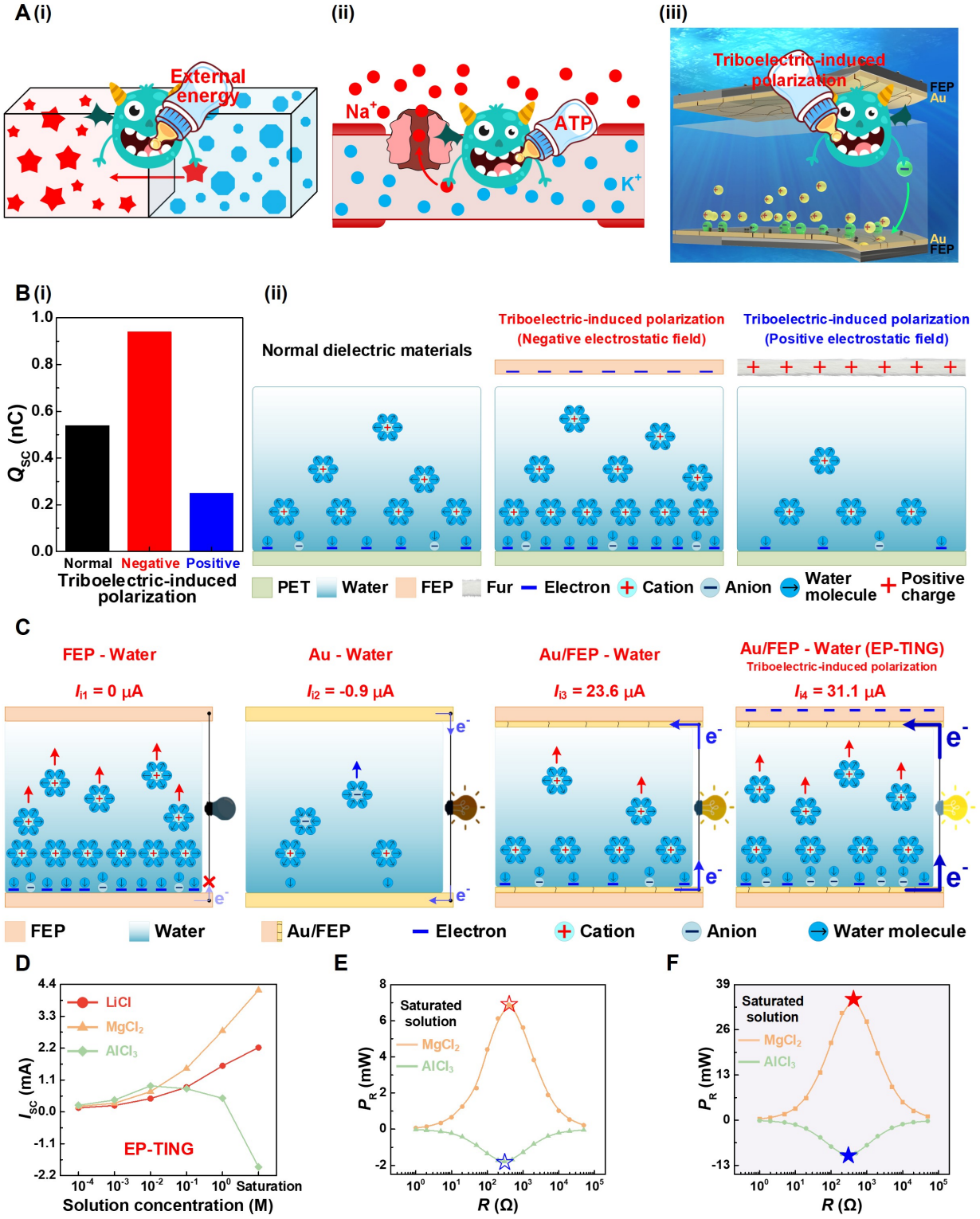

Figure 12. Triboelectrically induced ion polarization enabling active regulation of EDLs and higher-performance triboiontronic energy conversion. Reprinted with permission from[93] Copyright © 2025 Elsevier Inc. (A) Conceptual framework of a triboiontronic Maxwell's demon inspired by classical Maxwell's demon and biological ion pumps, where triboelectric energy is converted into an external electrostatic field to actively generate nonequilibrium ionic concentration gradients within coupled EDLs; (B) Experimental demonstration of triboelectrically induced ion polarization via remote modulation of EDL charge distributions and interfacial electrostatic potentials; (C) Comparison of triboiontronic energy conversion performance across dielectric, metallic, and metal/dielectric hybrid interfaces, highlighting the synergistic roles of robust EDL formation and efficient ionic-electronic coupling; (D) Effects of electrolyte properties, including ionic concentration, valence state, and diffusion kinetics, on triboiontronic energy conversion behavior; (E) Demonstration of enhanced and programmable triboiontronic outputs enabled by triboelectrically induced ion polarization; (F) Synergistic enhancement of ionic transport and energy conversion through coupling triboelectrically induced ion polarization with interfacial redox reactions.

chemistry provides a robust strategy to simultaneously amplify EDL asymmetry, sustain ionic transport, and enhance ionic-electronic energy conversion efficiency.

Taken together, TINGs represent a transition of dynamic EDLs from electrostatic induction-mediated interfaces to ion-transport-dominated energy conversion systems. In contrast to S-L TENGs, which rely on transient charge screening, TINGs exploit asymmetric EDLs to establish sustained ionic concentration gradients that drive directional ion migration and enable DC output. With triboelectrically induced ion polarization, EDLs are further transformed into actively tunable interfacial systems, where ionic distributions can be dynamically reconstructed to regulate ion flux direction, transport intensity, and output polarity. This introduces a programmable ionic transport mode beyond spontaneous interfacial equilibration. Furthermore, coupling interfacial redox reactions with polarized EDLs enhances both ionic generation and transport continuity, leading to improved ionic-electronic coupling and energy conversion efficiency. Collectively, TINGs establish a hierarchical evolution from asymmetric ionic transport to actively programmable ionic regulation.

IVNGs enabled by EDL-SCR coupling

Triboiontronic systems are fundamentally governed by asymmetric EDL-mediated ionic transport within electrolytes. Extending dynamic EDL regulation to semiconductor-liquid interfaces enables the coupling of ionic migration with electronic carrier modulation, representing a transition from purely ionic regulation toward integrated ionic-electronic functionality. Building upon the dynamic coupling between EDLs and semiconductor SCRs, the semiconductor-liquid iontrovoltaic effect introduces a new paradigm of interfacial energy conversion in which ionic and electronic processes are simultaneously regulated by a shared interfacial electric field [Figure 5]. Introduced by Li *et al.* in 2026, IVNGs represent a further evolution of dynamic EDL systems, extending their regulatory capability from charge generation and ionic transport at interfaces to coupled modulation of semiconductor carrier dynamics [Figure 13A][94]. In contrast to TINGs, where energy conversion is governed primarily by asymmetric EDL-driven ionic migration, IVNGs introduce semiconductor SCRs as an additional regulatory degree of freedom, enabling coordinated control of ionic redistribution in the electrolyte and carrier energetics in the semiconductor. To validate this concept, a series of experiments was performed to determine whether triboelectrically induced ion polarization can simultaneously modulate ionic distributions within EDLs and electronic states within SCRs. Local pH measurements showed reversible changes in H^+ concentration under opposite polarization states [Figure 13B(i and ii)], providing direct evidence that external electrostatic fields can dynamically reconstruct interfacial ionic distributions and regulate the local electrochemical environment. At the same time, the effect of triboelectrically induced ion polarization on semiconductor energetics was investigated using Kelvin probe force microscopy (KPFM) and operando electrochemical characterization based on Mott-Schottky analysis. KPFM measurements revealed reversible shifts in the surface potential and work function of p-type silicon under opposite polarization states, demonstrating that the external electrostatic field can effectively modulate the electronic energy levels of the semiconductor [Figure 13C]. To further determine whether this regulation persists under realistic semiconductor-liquid operating conditions, *in situ* Mott-Schottky measurements were performed to probe the SCR properties at the semiconductor-electrolyte interface. Consistent shifts in flat-band potential were observed under different polarization conditions, confirming that triboelectric polarization can dynamically regulate semiconductor band bending and the interfacial electric field [Figure 13D]. Taken together, these results provide compelling evidence that triboelectrically induced ion polarization simultaneously modulates ionic distributions within EDLs and carrier energetics within SCRs. Such dynamic EDL-SCR coupling substantially strengthens the interfacial electric field and enhances the cooperative regulation of ionic and electronic charge distributions. As a consequence, IVNGs exhibit stronger ionic concentration gradients in the electrolyte, greater charge accumulation in the semiconductor, and more efficient directional ionic migration, ultimately leading to significantly enhanced

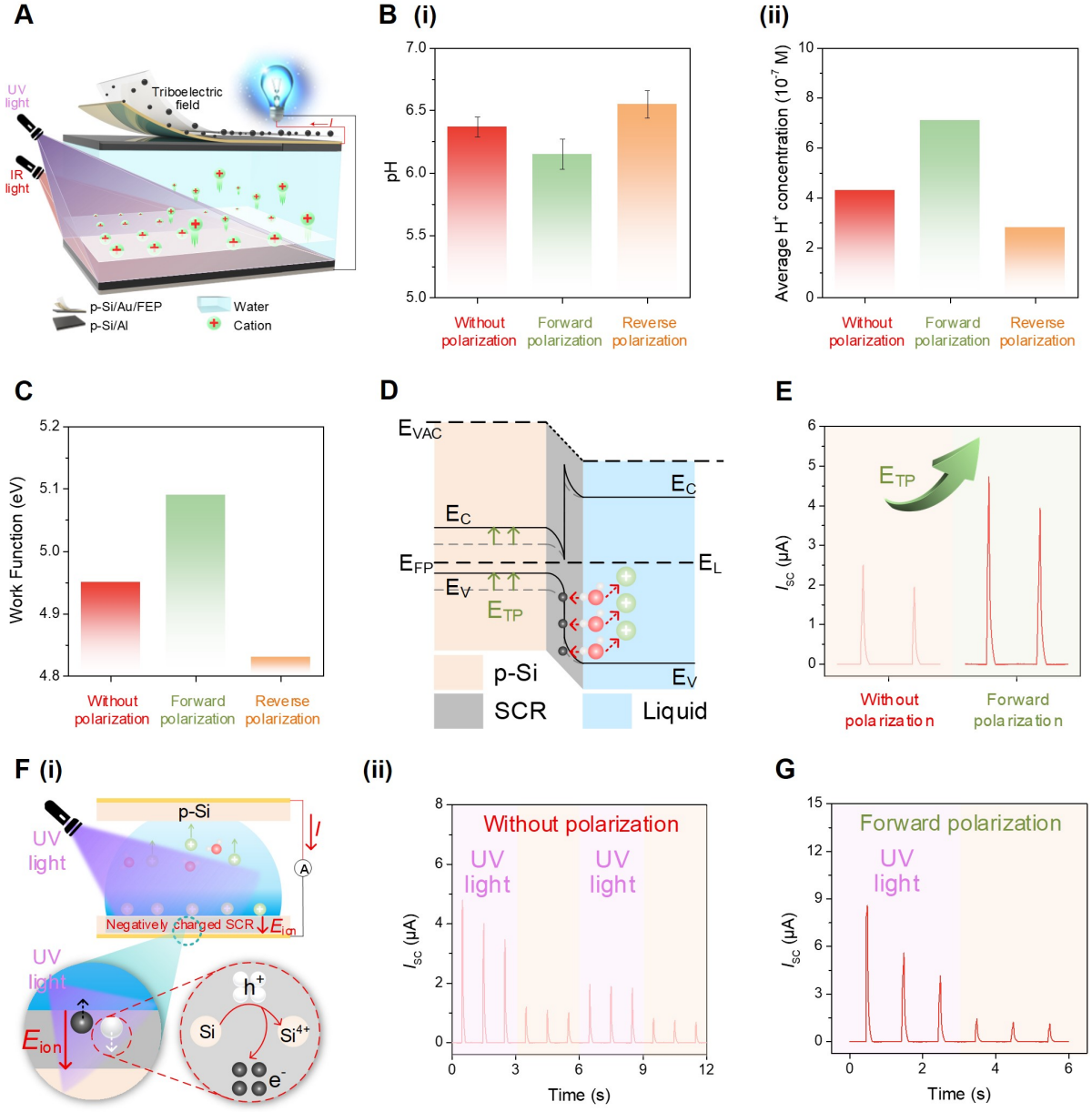

Figure 13. IVNG was developed by Li *et al.*, and the dynamic EDL-SCR coupling and photo-enhanced iontrovoltaic energy conversion were experimentally verified. Reprinted with permission from[94] Copyright © 2026, Springer Nature. (A) Device structure of the IVNG; (B) Experimental verification of triboelectric-polarization-induced ionic redistribution within EDLs through reversible variations in local pH and proton concentration under opposite polarization states; (C) Surface-potential characterization showing semiconductor work function modulation by triboelectrically induced ion polarization; (D) Semiconductor band bending and SCR charge density could be regulated by triboelectrically induced ion polarization; (E) Enhanced electrical output enabled by triboelectric-polarization-strengthened EDL-SCR interactions. (F) Photoexcitation introduces a further level of coupling between ionic transport and semiconductor carrier dynamics; (G) Synergistic enhancement of iontrovoltaic energy conversion through the cooperative effects of triboelectric polarization and photoexcitation.

electrical output [Figure 13E]. These findings demonstrate that dynamic EDL-SCR coupling establishes a new mechanism for iontronic energy conversion, in which ionic transport and semiconductor carrier dynamics are intrinsically integrated within a unified interfacial framework.

Photoexcitation provides an additional pathway for coupling ionic transport with semiconductor carrier dynamics, further expanding the regulatory dimensions of dynamic EDL-SCR interfaces [Figure 13F(i)]. Under illumination, photogenerated electron-hole pairs are efficiently separated by the enhanced interfacial

electric field within the coupled EDL-SCR system. Concurrently, photogenerated holes migrate toward the semiconductor-liquid interface, where they participate in interfacial oxidation reactions that generate additional ionic species, thereby further amplifying EDL asymmetry. As a result, photoinduced carrier separation and ionic transport become intrinsically interdependent rather than independent processes. The rapid disappearance of the enhanced output upon removal of illumination confirms that the observed response originates from reversible interfacial electrostatic modulation and electrochemical reactions, rather than irreversible chemical changes [Figure 13F(ii)]. When photoexcitation is coupled with triboelectric polarization, a pronounced synergistic enhancement is observed [Figure 13G]. The strengthened EDL-SCR electric field simultaneously promotes carrier separation in the semiconductor and accelerates interfacial redox kinetics, while photoinduced ionic generation continuously reinforces interfacial charge asymmetry. This positive-feedback loop establishes a dynamically reinforced EDL-SCR coupling state, leading to significantly enhanced ionic transport and energy conversion efficiency. Notably, the efficiency of this iontrovoltaic process critically depends on the directionality of the built-in interfacial electric field within the coupled EDL-SCR region. Only when the interfacial field simultaneously favors carrier separation and interfacial redox activation can photoexcitation effectively amplify ionic asymmetry and directional ion migration. These results highlight the central role of SCR energetics in governing ionic-electronic coupling and establish dynamic EDL-SCR interactions as the fundamental mechanism underpinning iontrovoltaic energy conversion.

Following the establishment of dynamic EDL-SCR coupling as the basis of the iontrovoltaic effect, research has shifted towards the rational design of ionic-electronic interfaces with controllable energy landscapes. As iontrovoltaic conversion is governed by the coupled evolution of ionic redistribution, semiconductor carrier dynamics and interfacial electrochemical processes, its performance can be optimized through simultaneous manipulation of band alignment, interfacial asymmetry, electrolyte chemistry and external-field interactions. Among these strategies, semiconductor work-function engineering provides the first demonstration that electronic energy landscapes can be tailored to regulate EDL-SCR coupling and iontrovoltaic output [Figure 14A]. By coupling p-type silicon with metal current collectors of different work functions, the iontrovoltaic output was found to be strongly dependent on metal-semiconductor band alignment. Low-work-function metals facilitate carrier extraction and interfacial charge transfer, whereas high-work-function metals induce interfacial field opposition that suppresses carrier collection. These results highlight band engineering as an effective route to regulate carrier dynamics and strengthen ionic-electronic coupling at semiconductor-liquid interfaces. Building on this principle, interfacial energetic asymmetry was further introduced to enhance dynamic EDL-SCR coupling. By replacing the top Au/p-Si electrode with a metal/FEP hybrid interface, a highly asymmetric dual-EDL configuration was constructed [Figure 14B(i)], which simultaneously enhances directional ionic migration and promotes hole-driven interfacial oxidation reactions. The generated ionic products further reinforce interfacial charge asymmetry, establishing a self-amplifying ionic environment that strengthens both EDL formation and ionic transport. As a result, a redox-coupled iontrovoltaic nanogenerator (RC-IVNG) was realized, in which ionic migration and interfacial electrochemical reactions jointly contribute to energy conversion. Finally, the integration of triboelectric polarization and photoexcitation further amplifies this coupled system. Triboelectrically induced ion polarization enhances both EDL asymmetry and SCR band bending, while photoexcited carriers participate in interfacial redox reactions that continuously generate additional ionic species. These processes collectively establish a positive-feedback loop among carrier separation, ionic generation, and directional ion transport. The RC-IVNG achieves significantly enhanced ionic transport and energy conversion performance, demonstrating a unified strategy for engineering higher-efficiency iontrovoltaic systems [Figure 14B(ii)].

Beyond semiconductor band structures and interfacial asymmetry, electrolyte composition provides a critical handle for manipulating ionic transport, EDL evolution, and the resulting ionic-electronic coupling in iontrovoltaic systems [Figure 14C]. Increasing ionic strength compresses the EDL, reduces the Debye length,

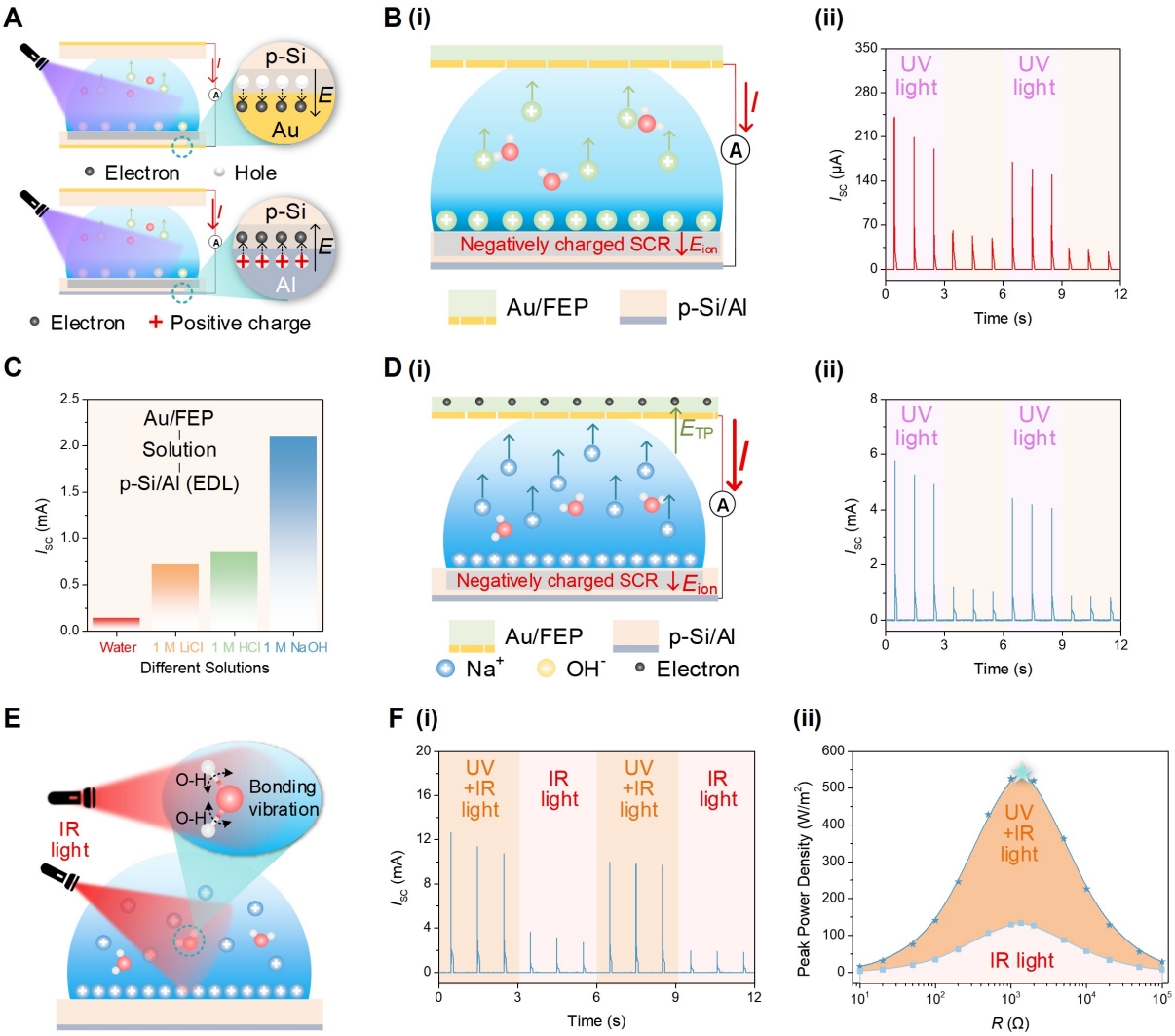

Figure 14. Multidimensional engineering of dynamic EDL-SCR coupling toward higher-performance iontrovoltaic energy conversion. Reprinted with permission from[94] Copyright © 2026, Springer Nature. (A) Solid-state band engineering via work-function modulation to regulate carrier energetics in semiconductor-liquid interfaces; (B) Enhancement of dynamic EDL-SCR coupling through redox-assisted ionic enrichment, strengthening interfacial electric fields and ionic-electronic interactions; (C) Electrolyte engineering for modulating EDL structure, ionic concentration, and transport kinetics; (D) Alkaline electrolyte-enabled ionic generation and enhanced photoactivated iontrovoltaic transduction via improved wettability and continuous interfacial redox processes; (E) Photothermal regulation of ionic mobility and transport kinetics within asymmetric EDLs under infrared irradiation. (F) Under optimized conditions, the RC-IVNG delivers an I_{SC} of ~12.6 mA and a P_R density of 541 W m^{-2}.

and accelerates ion migration within coupled EDL structures[94]. In addition, electrolyte chemistry simultaneously modulates interfacial wettability and redox kinetics, thereby jointly influencing EDL formation density and ion-generation efficiency. Among various electrolytes, alkaline media exhibit particularly pronounced enhancement effects. In concentrated NaOH solutions, improved wettability promotes the formation of dense and stable EDLs, while non-passivating silicon oxidation continuously generates soluble ionic species, sustaining long-term interfacial charge replenishment and directional ion transport [Figure 14D(i)]. Under UV illumination, the resulting photoactivated RC-IVNG achieves milliampere-level current output, demonstrating the capability of dynamic EDL-SCR systems for high-flux ionic energy conversion [Figure 14D(ii)]. To further accelerate ionic transport, photothermal regulation was introduced via infrared irradiation [Figure 14E]. Owing to the strong absorption of water in the infrared regime, localized heating increases ionic mobility, decreases viscosity, and reduces internal resistance,

thereby significantly enhancing ion diffusivity and transport kinetics within asymmetric EDLs. When photothermal activation is combined with triboelectric polarization, photoexcitation, and redox-driven ionic generation, a pronounced multiphysical-field synergistic effect emerges. Under optimized conditions, the RC-IVNG delivers an I_{SC} of ~12.6 mA [Figure 14F(i)], corresponding to a P_R density of 541 W m^{-2} [Figure 14F(ii)]. This performance represents one of the highest reported outputs for dynamic EDL-enabled ionic energy conversion systems. Overall, IVNGs demonstrate that dynamic EDLs can extend beyond conventional ionic transport regulation and directly couple with semiconductor carrier dynamics through SCR modulation. The resulting EDL-SCR hybrid system enables coordinated control of interfacial electric fields, ionic migration, carrier separation, and redox reactions, establishing a unified framework for multiphysical-field iontronic energy conversion. These findings position dynamic EDL-SCR coupling as a general paradigm for next-generation solid-liquid interfacial energy transduction.

Experimentally, the iontrovoltaic contribution should be distinguished from conventional photoelectrochemical, redox/corrosion, and concentration-cell processes by examining the origin, controllability, and reversibility of the interfacial driving force. In a baseline IVNG, directional output can be generated in the absence of illumination and external bias through deliberately established asymmetry between coupled semiconductor-liquid EDL-SCR interfaces, distinguishing it from a purely photoelectrochemical process. The iontrovoltaic output is further correlated with reversible modulation of both liquid-side ionic distributions and semiconductor-side carrier energetics, as evidenced by polarization-dependent local ion-concentration changes, surface-potential/work-function shifts, and flat-band-potential variations. In contrast, conventional concentration cells derive their electromotive force primarily from a pre-existing bulk concentration difference between two electrolytes, whereas iontrovoltaic systems generate the relevant ionic chemical-potential asymmetry through dynamically differentiated interfacial EDL states even when the bulk liquid composition is nominally identical. Redox or corrosion reactions can coexist with and amplify iontrovoltaic conversion, as in RC-IVNGs, but they are treated as additional Faradaic contributions rather than the defining origin of the iontrovoltaic effect. Accordingly, control experiments under dark conditions, identical bulk electrolyte composition, reversed interfacial polarization/asymmetry, and reversible field modulation, together with operando characterization of EDL and SCR states, provide practical criteria for separating iontrovoltaic transduction from conventional electrochemical contributions.

Collectively, the evolution of S-L TENGs, TINGs, and IVNGs establishes a unified framework for dynamic EDL-enabled energy transduction at solid-liquid interfaces. As summarized in Table 1, these three systems exhibit distinct physical boundaries in terms of dominant interface, driving force, output mode, and characteristic electrical performance, while their representative voltage, current, power density, active area, operating conditions, and normalization methods also differ substantially. Therefore, the reported performance values should be interpreted within their respective experimental contexts rather than as directly comparable benchmarks. It should also be recognized that these three device categories are currently at different stages of development. S-L TENGs constitute a comparatively mature field that has been extensively investigated by many independent research groups, with their operation generally understood within the established framework of contact electrification and electrostatic induction, while wetting behavior, charge trapping, surface chemistry, and liquid composition can further modulate the interfacial charge dynamics and electrical output. In contrast, TINGs and IVNGs are more recently introduced concepts, and the literature explicitly adopting these device definitions and corresponding mechanistic frameworks remains comparatively limited. Their present interpretation therefore relies mainly on the initially demonstrated asymmetric-EDL-driven ionic transport and EDL-SCR-coupled ionic-electronic transduction, respectively, while related independent studies on nonequilibrium EDL regulation, concentration-gradient-driven ion migration, semiconductor-liquid charge redistribution, and interfacial ionic-electronic coupling provide important complementary physical context. Further independent

Table 1. Comparison of the physical characteristics, operating boundaries, and representative performance metrics of S-L TENGs, TINGs, and IVNGs

Dimension	S-L TENG	TING	IVNG
Dominant interface	Dielectric-liquid	Metal/dielectric-liquid coupled interfaces	Semiconductor-liquid
Dominant driving force	Contact electrification and electrostatic induction associated with dynamic EDL reconstruction	Ionic concentration gradient induced by asymmetric EDLs	Interfacial electric field arising from EDL-SCR coupling
Typical output	AC	DC	DC
Output characteristics	Higher V_{OC}	Higher Q_{SC} density	Higher P_R density
Power density	~448 W m^{-2}[133]	~346.7 W m^{-2}[93]	~541 W m^{-2}[94]
V_{OC}	~540 V[133]	~0.60 V[93]	~0.9 V[94]
I_{SC}	~2 mA[133]	~18.62 mA[93]	~12.6 mA[94]
Active area	9 cm^2[133]	1 cm^2[93]	1 cm^2[94]
Power-density calculation	Reported active-area normalization	Reported active-area normalization	Reported active-area normalization

S-L TENGs: Solid-liquid triboelectric nanogenerators; TINGs: triboiontronic nanogenerators; IVNGs: iontrovoltaic nanogenerators; EDL: electrical double layer; DC: direct-current; SCR: space charge region.

validation across different materials, electrolytes, device architectures, and operating conditions will be important for establishing the generality and physical boundaries of these emerging mechanisms. Across these systems, interfacial EDLs evolve from passive charge-screening structures in S-L TENGs, to actively reconfigurable ionic transport media governed by asymmetric concentration gradients in TINGs, and ultimately to fully coupled ionic-electronic interfaces integrating semiconductor SCRs in IVNGs. This progression reflects a fundamental shift in the role of EDLs, from static electrostatic screening layers to dynamically programmable interfacial units capable of regulating charge generation, ionic migration, and carrier dynamics in a coordinated manner. Accordingly, the dominant energy-conversion mechanism transitions from electrostatic induction, to ion-driven transport, and finally to coupled ionic-electronic transduction under multiphysical-field regulation. Importantly, this evolution reveals that interfacial energy conversion is not governed by a single charge-carrier type, but emerges from hierarchical coupling among ionic distributions, interfacial electrostatics, and electronic band structures. Within this framework, dynamic EDLs serve as a unifying physicochemical platform linking mechanical stimuli, ionic transport, and electronic responses, thereby enabling the continuous transformation of environmental energy into electrical output.

DYNAMIC EDLs ENABLING INFORMATION TRANSDUCTION

Beyond mediating interfacial energy harvesting, dynamic EDLs also provide a fundamental physicochemical platform for information transduction at solid-liquid interfaces[138-145]. In iontronic systems, energy generation and information processing are inherently intertwined, with spatiotemporal ionic concentration gradients serving as both physicochemical state variables and dynamic carriers of signal propagation[146-153]. Inspired by this coupling, triboelectrified solid-liquid interfaces enable continuous conversion of external stimuli and interfacial perturbations into time-resolved ionic and electrical signals through dynamic reconfiguration of interfacial ion distributions. In this framework, dynamic EDLs function not only as charge-regulating interfaces but also as adaptive information carriers capable of encoding, transmitting, and processing signals in a self-powered manner. Consequently, dynamic EDLs bridge energy flow and information flow within a unified interfacial system, enabling self-powered interface probing and sensing, bionic logic control, iontronic communication, and logic computing.

Interfacial charge probing via S-L TENGs

Among the various information-transduction functions enabled by dynamic EDLs, interfacial charge probing represents one of the most direct routes for extracting physicochemical information from solid-liquid interfaces[154-160]. In contrast to conventional electrochemical techniques that often require conductive substrates, external bias, or equilibrium conditions, triboelectrified interfaces intrinsically generate electrical signals that are directly coupled to interfacial charge transfer, ionic redistribution, and EDL evolution. As a result, triboelectric outputs can serve as sensitive, real-time fingerprints of interfacial processes, enabling operando monitoring of charge dynamics at solid-liquid interfaces. Over recent years, triboelectric probing has evolved from simple charge-transfer quantification to spatiotemporal charge imaging and, more recently, to chemical-information decoding, establishing a new paradigm for self-powered interfacial interrogation. An initial milestone was reported in 2021, when Zhang *et al.* developed a droplet-driven S-L TENG as a self-powered probe for interfacial charge-transfer analysis [Figure 15A(i)][161]. By using spatially separated electrodes beneath a dielectric substrate, the device enabled position-resolved monitoring of charge accumulation during droplet motion. The results revealed a continuous increase in transferred charge along the droplet trajectory, demonstrating that liquid-solid contact electrification is a progressive process rather than an instantaneous event [Figure 15A(ii)]. Systematic comparisons across aqueous, electrolyte, and organic systems further confirmed that electron transfer dominates interfacial charge generation, while dissolved ions primarily modulate the process through EDL formation and electrostatic screening [Figure 15A(iii)]. Beyond mechanistic insights, this platform also exhibited sensitivity to electrolyte concentration, solvent composition, and molecular interactions, highlighting its potential for self-powered interfacial-state sensing.

To further enhance spatial resolution, a pixeled S-L TENG array was subsequently developed for spatiotemporal mapping of interfacial charge evolution [Figure 15B(i)][162]. By integrating 432 independently addressable electrodes with 0.4 mm resolution, two-dimensional charge-transfer distributions during droplet motion could be directly reconstructed [Figure 15B(ii)]. The resulting charge maps revealed pronounced spatial heterogeneity in interfacial charge accumulation, providing experimental support for the coupled nature of electron transfer and ion-driven EDL screening. Importantly, the platform demonstrated the capability to encode both physical parameters (e.g., droplet velocity, light intensity) and chemical properties (e.g., pH), indicating that triboelectric charge patterns inherently contain multidimensional information [Figure 15B(iii)]. This marked a transition from scalar charge measurement to spatially resolved interfacial information imaging. Building on this concept, triboelectric charge mapping was further extended to operando chemical-information extraction [Figure 15C(i)][163]. By correlating dynamic charge-transfer patterns with interfacial chemical processes, the system enabled real-time monitoring of redox reactions, catalytic transformations, and molecular conversions. For example, oxidation of Fe^{2+} to Fe^{3+}, enzymatic hydrolysis, and catalyst evolution processes each produced distinct charge-transfer signatures, allowing direct visualization of reaction kinetics and interfacial state evolution [Figure 15C(ii)]. These results demonstrate that triboelectric signals can serve not only as indicators of charge dynamics but also as encoded representations of underlying chemical processes. Collectively, these advances reveal a continuous evolution of dynamic EDLs from charge-transfer reporters to adaptive information-processing interfaces. By exploiting the coupled dynamics of ionic redistribution and charge transfer, dynamic EDLs provide an intrinsic mechanism for encoding and decoding interfacial physical and chemical states. In this context, S-L TENG-based triboelectric probing represents more than a self-powered sensing strategy; it establishes a general framework for operando interrogation of interfacial processes and the development of future electroionic information systems.

Operando EDL probing via S-L TENGs

Beyond interfacial charge probing, triboelectric outputs from S-L TENGs can be interpreted as real-time signatures of interfacial ionic redistribution and dynamic EDL evolution, enabling operando reconstruction

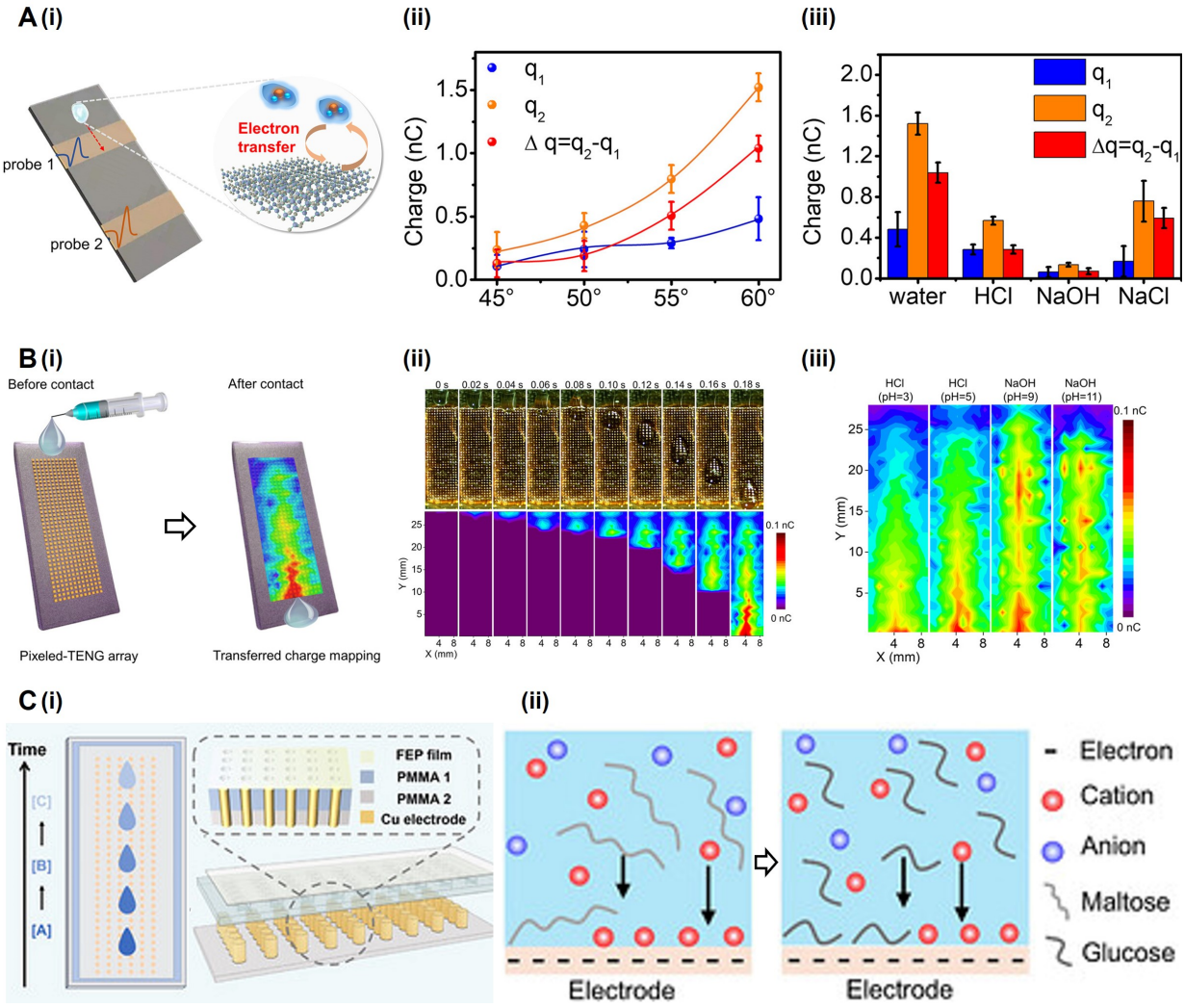

Figure 15. S-L TENGs-enabled interfacial information sensing via triboelectric charge probing. (A) Droplet-driven S-L TENG-based interfacial charge-transfer measurement at solid-liquid interfaces. Reprinted with permission from[161] Copyright © 2021 American Chemical Society; (B) Spatiotemporal charge-transfer imaging using a pixeled S-L TENG array for real-time visualization of interfacial charge evolution. Reprinted with permission from[162] Copyright © 2023 American Chemical Society; (C) Time-resolved charge-transfer mapping for chemical-information extraction, enabling operando monitoring of interfacial reactions and catalyst dynamics. Reprinted with permission from[163] Copyright © 2026 WILEY-VCH GmbH.

of dielectric interfaces. Unlike conductive solid-liquid systems, where EDL structures can be readily characterized using conventional electrochemical techniques under applied bias and well-defined electrode configurations, dielectric solid-liquid interfaces represent a fundamentally more challenging regime for operando investigation. This limitation arises from the absence of intrinsic electronic conduction pathways in the dielectric solid phase, as well as the strongly coupled nature of interfacial charge generation, ionic redistribution, and electrostatic screening. Consequently, the formation and evolution of EDLs at dielectric interfaces cannot be directly accessed using traditional electrochemical or spectroscopic methods, leaving their dynamic behavior largely unresolved. Within this framework, a particularly insightful demonstration was reported in 2024 by Wei *et al.*[69], who developed a single-electrode S-L TENG-based triboelectric probing platform to investigate the interfacial transition from ice-dielectric contact electrification to water-dielectric electrochemical interfaces. This approach enabled direct monitoring of the emergence, transformation, and evolution of interfacial EDLs during the solid-liquid phase transition.

To resolve the evolution pathway, the phase transition was divided into four representative stages: ice, initial melting, partial melting, and complete melting. During early melting, the emergence of microscale water regions increases effective contact area, leading to enhanced charge transfer and a peak output approximately six times higher than that of pure ice. As melting progresses, however, the increasing liquid fraction introduces ion-mediated screening, and the gradually forming EDL begins to attenuate interfacial charge accumulation. Upon complete melting, a stable solid-liquid interface with a fully developed EDL is established, resulting in a reduced but steady triboelectric output. The initial ice state is governed by electron-dominated solid-solid contact electrification. With partial melting, interfacial water introduces ions and initiates EDL formation, including the development of Stern and diffuse layers. Concurrently, the growing EDL progressively screens triboelectrically generated surface charges, leading to a competition between contact-area enhancement and electrostatic screening. At full melting, the system reaches a quasi-equilibrium EDL state, where charge generation and screening are balanced, producing stable triboelectric signals. Collectively, this work demonstrates that triboelectric outputs can serve as sensitive operando fingerprints of dynamic EDL evolution. More importantly, it establishes a unified picture linking phase transition, interfacial charge transfer, and EDL formation, providing a powerful platform for visualizing nonequilibrium interfacial electrochemical processes.

A further advance in dynamic EDL-enabled information sensing was achieved through the development of a triboelectric probing strategy capable of directly resolving electrolyte-dependent EDL structures at dielectric solid-liquid interfaces. Unlike previous studies focused primarily on charge-transfer processes or phase-transition-induced EDL evolution, this approach employs S-L TENGs as operando probes to establish a direct correlation between triboelectric outputs and interfacial ionic configurations, enabling quantitative visualization of EDL reconstruction under different electrolyte conditions. Wei *et al.* demonstrated that triboelectric signals encode electrolyte-dependent EDL configurations, transforming triboelectric measurements into a self-powered strategy for deciphering ion-specific interfacial organization[164]. As illustrated in Figure 16A, a vertical contact-separation S-L TENG was utilized as a triboelectric charge-transfer probe. During repeated contact between a polytetrafluoroethylene (PTFE) dielectric surface and various electrolyte solutions, the transferred triboelectric charge was continuously recorded as a real-time indicator of interfacial charge distribution and EDL evolution. Three representative electrolyte systems were systematically investigated: symmetric electrolyte LiCl, large-anion asymmetric electrolyte Li[TFSI], and large-cation asymmetric electrolyte [EMIM]Cl. Owing to their distinct ionic sizes, mobilities, and interfacial affinities, these systems provide a model platform for elucidating ion-specific effects on EDL regulation at dielectric interfaces.

The concentration-dependent triboelectric responses are summarized in Figure 16B. For LiCl solutions, the Q_{SC} monotonically decreases with increasing concentration while maintaining constant polarity [Figure 16B(i)], indicating progressive EDL compression and enhanced electrostatic screening under increasing ionic strength[164]. In contrast, both Li[TFSI] and [EMIM]Cl exhibit pronounced polarity inversion at high concentrations [Figure 16B(ii and iii)]. While their lower-concentration behavior resembles that of LiCl, a critical concentration (~10^{-1} M) triggers a transition from monotonic attenuation to charge inversion, indicating a fundamental reconstruction of interfacial charge distribution and EDL structure in concentrated asymmetric electrolytes. To rationalize these behaviors, concentration-dependent EDL evolution models were proposed [Figure 16C]. For LiCl [Figure 16C(i and ii)], the EDL follows a classical two-step structure composed of an IHP, OHP, and diffuse layer. Increasing ionic strength compresses the diffuse layer and strengthens charge screening, but the overall charge polarity remains unchanged. For Li[TFSI] [Figure 16D(i and ii)], the large steric size and reduced mobility of $[TFSI]^-$ anions suppress their participation in interfacial screening, while Li^+ ions preferentially accumulate near the interface[164]. At high concentrations, excessive cation accumulation leads to overcompensation of surface charge, resulting in EDL reconstruction

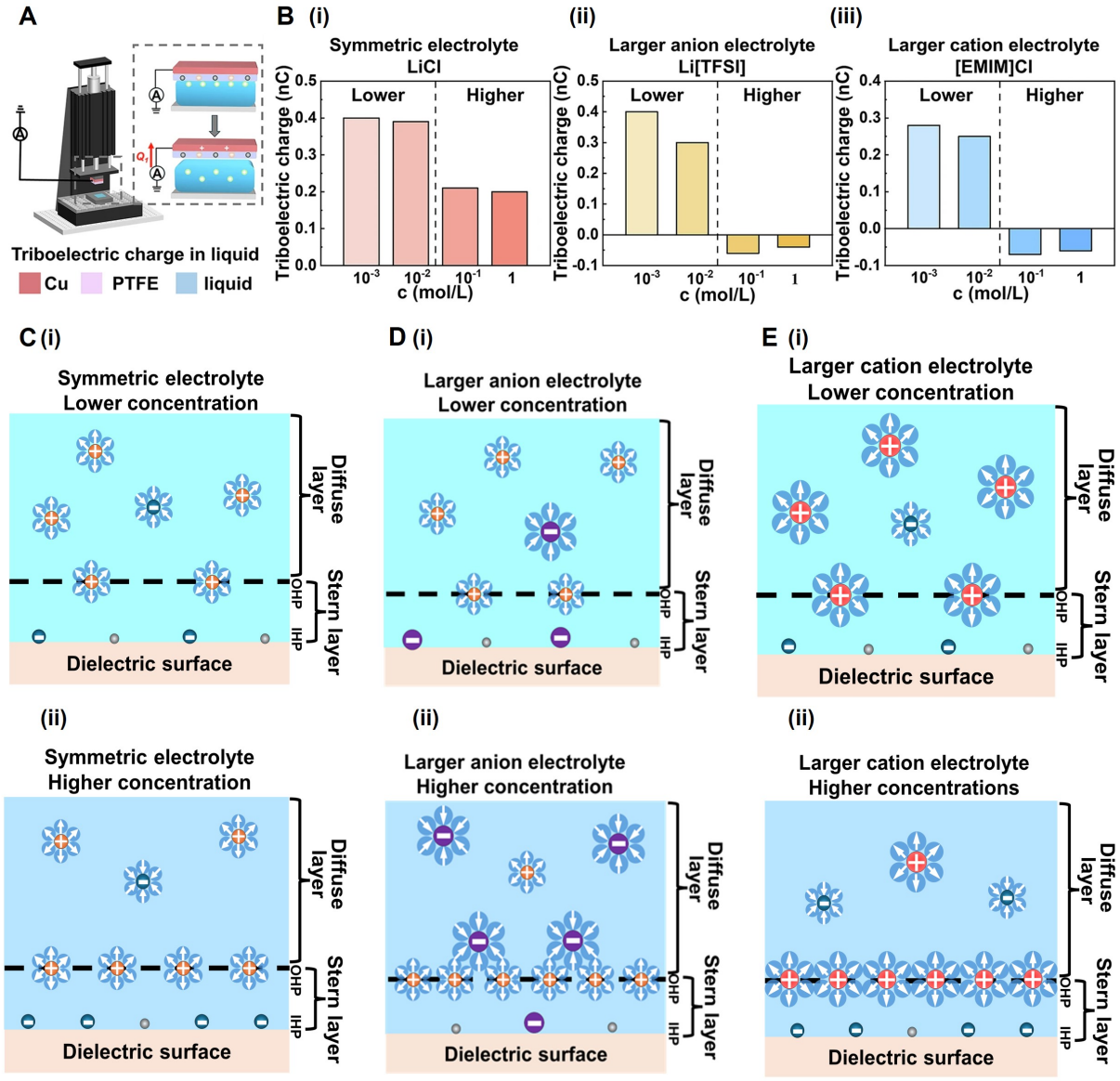

Figure 16. Dynamic EDL probing reveals electrolyte-dependent interfacial ionic structures at dielectric solid-liquid interfaces developed by Wei *et al.* in 2025. Reprinted with permission from[164] Copyright © 2025 Springer Nature. (A) S-L TENG-based triboelectric charge-transfer probing platform for operando characterization of EDLs formed in different electrolyte environments at dielectric solid-liquid interfaces; (B) Evolution of triboelectric signals with increasing electrolyte concentration for LiCl, Li[TFSI], and [EMIM]Cl, revealing distinct pathways of EDL reconstruction and interfacial charge regulation; (C-E) Proposed models of electrolyte-dependent EDL evolution, showing EDL compression in LiCl and charge inversion induced by ion-specific adsorption and mobility asymmetry in concentrated Li[TFSI] and [EMIM]Cl electrolytes.

and charge inversion driven by mobility asymmetry. For [EMIM]Cl [Figure 16E(i and ii)], EDL inversion originates from strong interfacial adsorption of hydrophobic $[EMIM]^+$ cations, which dominate the OHP at elevated concentrations and induce positive charge overcompensation. In this case, charge inversion is governed primarily by ion-specific adsorption rather than transport asymmetry. These results demonstrate that triboelectric outputs can serve as highly sensitive operando fingerprints of electrolyte-dependent EDL reconstruction. More importantly, S-L TENG-based probing provides a direct experimental route to resolve ion-specific effects in dielectric interfacial electrochemistry, revealing how ionic size, mobility, and interfacial affinity collectively govern EDL structure and its dynamic evolution.

Collectively, these two representative studies establish S-L TENGs as a universal operando platform for probing EDLs at dielectric solid-liquid interfaces. By converting interfacial charge-transfer processes into measurable electrical signals, this strategy enables real-time visualization of both phase-transition-induced EDL evolution and electrolyte-dependent EDL reconstruction. Importantly, these results demonstrate that triboelectric outputs are not only sensitive to interfacial charge generation but also encode the structural dynamics of ion distributions within EDLs. Therefore, S-L TENGs provide a unified experimental framework for decoding dielectric interfacial electrostatics under nonequilibrium conditions, bridging charge transfer, ionic organization, and EDL formation within a single operando sensing paradigm.

Interfacial information sensing via S-L TENGs

Dynamic EDLs not only serve as sensitive probes of interfacial physicochemical processes but also function as intrinsic transducers that convert external stimuli into measurable electrical signals. As evidenced by operando studies of phase transitions and electrolyte-dependent EDL reconstruction, variations in temperature, ionic composition, molecular adsorption, and interfacial states continuously regulate EDL structures and modulate interfacial charge-transfer behavior. Consequently, the electrical outputs of S-L TENGs are inherently governed by dynamic EDL evolution, effectively encoding rich information about the surrounding environment. Building upon this principle, dynamic EDLs have emerged as universal interfacial information-encoding media, enabling liquid identification, thermal sensing, chemical monitoring, and physiological signal detection in self-powered environmental and biomedical systems[165-169]. One of the earliest demonstrations of dynamic EDL-enabled environmental recognition was reported in 2023 by Wei *et al.*, who developed a self-powered triboelectric taste-sensing platform based on the S-L TENG[170]. Different liquids exhibit distinct ionic compositions, polarities, viscosities, and interfacial affinities, leading to characteristic EDL configurations and charge-transfer behaviors during solid-liquid contact electrification. These differences generate unique triboelectric signal patterns, which can be decoded as electrical fingerprints for liquid identification. Coupled with machine-learning analysis, the system achieved recognition accuracies exceeding 91%, demonstrating that dynamic EDLs can effectively encode complex physicochemical information into electrical signals. Beyond liquid identification, dynamic EDLs are also highly sensitive to thermal stimuli. In 2022, Feng *et al.* reported a thermoresponsive S-L TENG based on a temperature-responsive copolymer [Figure 17A(i)][171]. The temperature-induced conformational transition near the lower critical solution temperature modulates interfacial hydration structure, wettability, and EDL configuration. These coupled variations significantly alter interfacial charge transfer, resulting in a ~27-fold increase in output current from 20 to 60 °C [Figure 17A(ii)]. This result demonstrates that dynamic EDLs can efficiently transduce thermal signals into electrical outputs through temperature-dependent interfacial ionic reorganization.

Dynamic EDLs can further encode chemical information in aqueous environments. In 2021, Kaswan *et al.* developed a droplet-based triboelectric nanosensor integrated with molecular recognition interfaces for chemical sensing [Figure 17B(i)][172]. Selective adsorption of target ions or molecules continuously reconstructs interfacial charge distributions and EDL structures, producing measurable changes in triboelectric outputs [Figure 17B(ii)]. The platform enabled sensitive detection of heavy-metal ions below regulatory thresholds and extended to biological species monitoring through adsorption-induced interfacial modulation [Figure 17B(iii)]. These findings establish that dynamic EDLs can transduce subtle chemical variations into electrical signals, enabling self-powered water-quality and biochemical sensing. More recently, dynamic EDL-enabled sensing has been extended from environmental monitoring to physiological signal detection in wearable systems. In 2024, Li *et al.* developed a bioinspired heterogeneous-wettability TENG for sweat analysis [Figure 17C(i)][173]. Driven by wettability-gradient-induced transport and capillary pressure, sweat ions are continuously enriched at the interface, dynamically modulating EDL structures and enhancing triboelectric outputs. The device exhibited a V_{OC} increase from 82 to 148 V with rising electrolyte

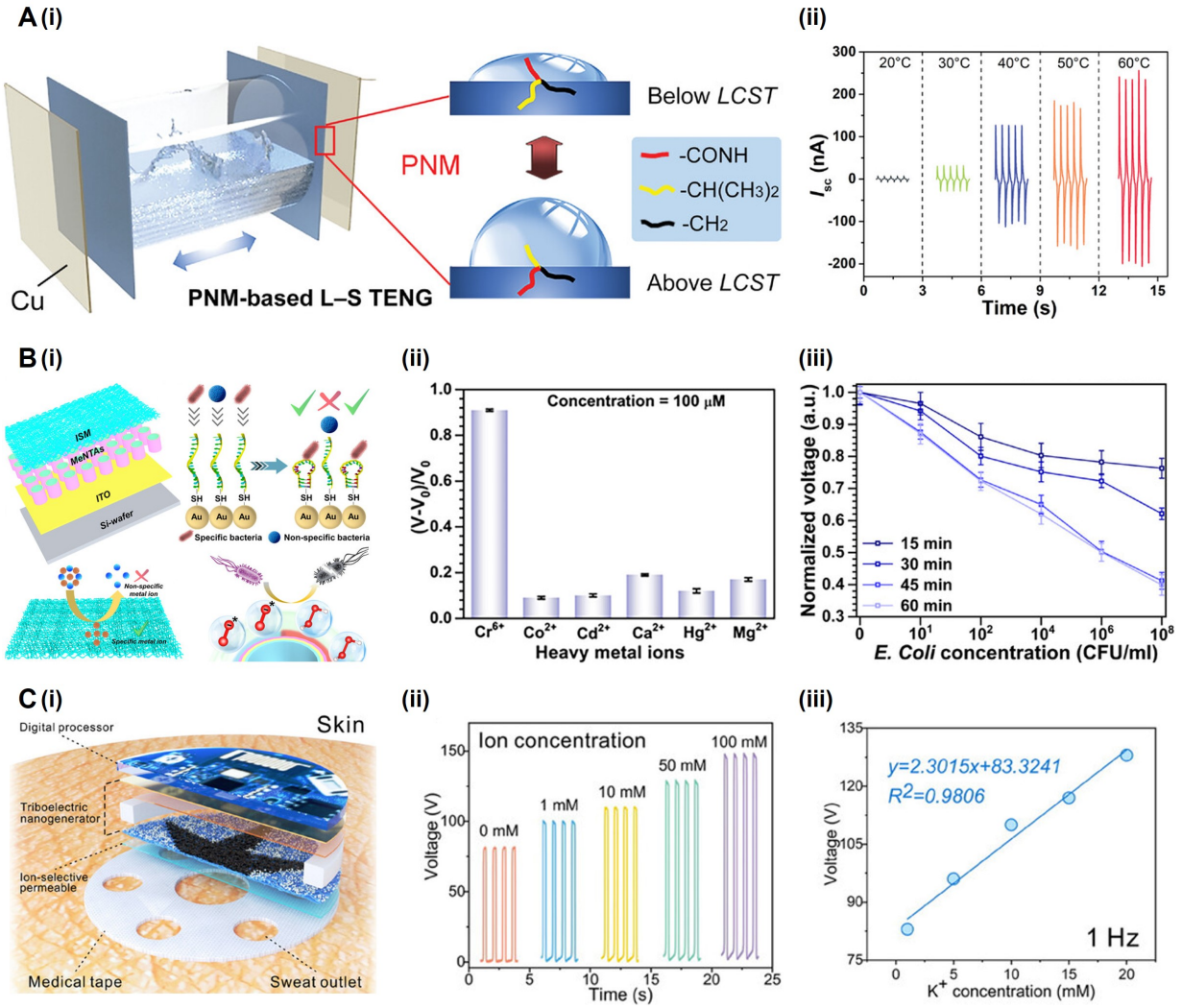

Figure 17. Dynamic EDL-enabled environmental and physiological sensing via S-L TENGs. (A) Temperature sensing enabled by thermally regulated interfacial hydration structures and dynamic EDL evolution, developed by Feng *et al.* in 2022. Reprinted with permission from[171] Copyright © 2022 WILEY-VCH GmbH; (B) Chemical-information sensing through ion- and contaminant-induced EDL reconstruction at solid-liquid interfaces, developed by Kaswan *et al.* in 2025. Reprinted with permission from[172] Copyright © 2025 WILEY-VCH GmbH; (C) Physiological-information sensing through sweat-ion-mediated modulation of interfacial EDLs and triboelectric outputs in wearable systems, developed by Li *et al.* in 2025. Reprinted with permission from[173] Copyright © 2025 WILEY-VCH GmbH.

concentration [Figure 17C(ii)] and achieved a signal-to-noise ratio of 51 dB. By integrating ion-selective membranes, selective detection of Na^+, K^+, and Ca^{2+} ions was further realized, enabling real-time physiological monitoring [Figure 17C(iii)]. This work highlights the potential of dynamic EDLs as a bridge between interfacial electrochemistry and wearable biosensing, opening new opportunities for self-powered health monitoring systems. These studies demonstrate that dynamic EDLs provide a universal interfacial mechanism for encoding environmental and physiological information into electrical signals via S-L TENGs. By coupling interfacial ionic redistribution with charge-transfer processes, diverse external stimuli, including chemical composition, temperature, molecular adsorption, and biological ion flux, can be effectively transduced into distinct triboelectric signatures. This establishes dynamic EDLs as a general information-encoding platform for self-powered sensing systems, bridging interfacial electrochemistry with environmental monitoring and wearable bioelectronics.

Bionic logic control via TINGs

S-L TENGs establish dynamic EDLs as interfacial information-encoding media for sensing external physicochemical stimuli, and further TINGs extend this functionality from signal generation to ionic information transmission and processing. This transition relies on the programmable regulation of ionic distributions, polarity, and transport direction within dynamic EDLs. In biological nervous systems, information is encoded and transmitted through dynamic ionic concentration gradients and membrane-potential variations across cell membranes. Inspired by this principle, triboiontronics explores whether dynamic EDLs at solid-liquid interfaces can function as programmable ionic-information carriers rather than merely as energy-conversion or sensing interfaces. A pioneering advance was reported by Li *et al.* in 2023, who demonstrated dynamic regulation of EDL charge distributions through triboelectrically induced ion polarization[57]. Triboiontronic systems use triboelectrically generated electrostatic fields to actively regulate ionic distributions within both the Stern layer and diffuse layer. Through this process, ionic polarity, ionic concentration, and ionic transport direction can be dynamically programmed, enabling bidirectional ionic-electronic signal conversion and establishing dynamic EDLs as functional units for ionic information transmission and logic regulation.

To demonstrate this concept, a triboiontronic bionic neurologic circuit was constructed for bidirectional ionic-electronic signal conversion. In the initial state, the naturally formed EDL generated only weak ionic signals because of the limited charge density within the diffuse layer. When positively charged fur contacted the PET substrate, triboelectric polarization enhanced the negative charge density within the Stern layer, inducing cation enrichment in the diffuse layer and generating positive ionic signals. These ionic signals were subsequently converted into forward electronic currents through interfacial ionic-electronic coupling. After removal of the fur, residual negative triboelectric charges on the PET surface reversed the interfacial ionic distribution, promoting anion enrichment and producing negative ionic signals, which generated reverse electronic currents in the external circuit. Through reversible switching among these EDL states, physical contact events were encoded into ionic polarity states and further converted into corresponding electronic outputs without an external power supply. As a proof-of-concept demonstration, the triboiontronic neurologic circuit was used to regulate the rhythmic motion of a virtual robot. This work demonstrated that dynamic EDLs can function not only as ionic-information carriers but also as active information-processing interfaces capable of implementing neuromimetic signal transmission, polarity regulation, and logic control.

Beyond ionic signal polarity regulation, dynamic EDLs can also control the transport behavior of charged liquid carriers, enabling programmable logic control. In 2025, Li *et al.* developed a triboelectric-programmed droplet manipulation strategy based on dynamic EDL regulation and triboelectric wetting[70]. In this system, the triboelectric charge polarity carried by droplets was programmed by tailoring ionic distributions within the solid-liquid interfacial EDLs, allowing droplet motion to be controlled by external triboelectric fields. To reveal the role of dynamic EDLs in droplet information regulation, the authors investigated the influence of ionic species and concentration on droplet triboelectric charging. For conventional LiCl solutions, droplets remained positively charged over a broad concentration range after contact electrification with PTFE. In contrast, [EMIM]Cl droplets exhibited a concentration-dependent polarity transition. At low concentrations, they behaved similarly to LiCl droplets and carried positive charges. At higher concentrations, however, the droplet polarity gradually reversed and became negative. This polarity inversion originates from concentration-dependent EDL reconstruction, where asymmetric ionic packing and interfacial adsorption alter the dominant charge-transfer pathway during solid-liquid contact electrification. Based on this mechanism, droplets with different programmed charge polarities exhibited opposite transport behaviors under the same triboelectric field. Positively charged droplets were attracted toward negatively charged field regions, whereas negatively charged droplets were repelled and transported in the opposite direction. Because droplet polarity was determined by the underlying EDL structure, dynamic EDL regulation

effectively translated interfacial ionic information into programmable droplet trajectories. The system achieved ultrafast droplet transport velocities approaching 450 mm s^{-1} on common dielectric surfaces without chemical surface modification, demonstrating efficient EDL-mediated control of ionic carriers. More importantly, this EDL-programmed droplet transport enabled ionic logic functions. By arranging positive and negative triboelectric-field regions along the transport pathway, droplets with different charge polarities could be selectively routed toward distinct output terminals. Through this process, ionic information encoded in EDL structures was converted into droplet-motion pathways and then translated into distinct electrical outputs. The resulting system further demonstrated robotic motion control without external power supplies or complex electronic circuits.

Collectively, these studies establish TINGs as dynamic EDL-enabled platforms for ionic information transmission and bionic logic control. Compared with S-L TENG-based information sensing, where EDL evolution is mainly used to encode external stimuli into electrical fingerprints, TING-based information systems actively manipulate ionic polarity, ionic flux, and ionic carrier transport pathways. This transition extends the role of dynamic EDLs from passive information encoding to programmable information routing and logic execution. Dynamic EDLs therefore evolve into active ionic-information-processing units, providing a promising route toward autonomous iontronic logic systems and embodied ionic intelligence.

Information transmission via TINGs

Dynamic EDLs can regulate ionic polarity and support logic operations at individual solid-liquid interfaces, and further extending such local ionic signaling into efficient long-range information transmission remains a major challenge. In biological nervous systems, ionic concentration gradients across cell membranes not only encode information but also support signal propagation over macroscopic distances through coordinated ionic transport and continuous maintenance of nonequilibrium electrochemical states. Inspired by this principle, Li *et al.* demonstrated in 2025 that dynamically regulated asymmetric EDLs can function not only as local ionic-information-processing interfaces but also as long-range ionic-information transmission channels, thereby enabling wireless underwater communication through coupled triboiontronic interfaces[93]. Building upon the asymmetric EDL-driven ionic migration mechanism of TINGs, a wireless underwater triboiontronic communication platform was developed. In this system, periodic contact-separation motion at the transmitting interface generated time-dependent ionic pulses through the dynamic formation and reconstruction of asymmetric EDLs. These ionic pulses propagated through the aqueous medium and were subsequently converted into electrical signals at the receiving terminal through interfacial ionic-electronic coupling. In this way, mechanical stimuli were encoded into ionic fluxes and transmitted underwater without relying on conventional acoustic, optical, or electromagnetic communication modes.

To evaluate the capability for long-distance ionic-information transmission, the distance between two coupled Au/FEP-liquid interfaces was systematically varied in different aqueous environments. Benefiting from triboelectrically enhanced asymmetric EDLs, stable ionic communication was achieved over distances of up to 30 cm, despite each triboiontronic unit having an active area of only 1 cm^2. Reliable signal transmission was observed in deionized water, tap water, artificial seawater, and saturated $MgCl_2$ solution, with I_{SC} of approximately 20, 40, 110, and 420 μA, respectively. These results indicate that increasing ionic conductivity and carrier concentration substantially promotes directional ionic migration and enhances long-range communication performance. More importantly, the realization of centimeter-scale signal propagation demonstrates that dynamic EDL coupling can effectively overcome the spatial confinement of individual interfacial EDLs. The received electrical pulses were further decoded using an ASCII-based encoding protocol to reconstruct character information. To improve communication reliability and suppress environmental interference, the initial pulses were designed as a judgment region, where the characteristic attenuation behavior of triboiontronic signals was used to identify the information source, while the

subsequent pulses constituted the information region encoding the message. Using this strategy, the character sequence "OK" was successfully transmitted and decoded underwater. Collectively, this work demonstrates that dynamically evolving asymmetric EDLs can serve not only as ionic transport pathways but also as active ionic-information carriers capable of encoding, transmitting, and regenerating signals over macroscopic distances. More fundamentally, it reveals that dynamic EDLs are not restricted to localized interfacial charge regulation; through coupled asymmetric EDL construction and triboelectrically induced ion polarization, they can be extended into long-range iontronic communication channels. This advance marks an important transition from ionic information encoding and local logic regulation toward distributed ionic communication networks, opening new opportunities for underwater communication, large-scale iontronic systems, and future iontronic embodied intelligence[174].

Light-gated iontronic computing via IVNGs

Dynamic EDLs in S-L TENGs and TINGs enable information acquisition and ionic information transmission, respectively, and their functionality can be further extended toward iontronic computing through dynamic EDL-SCR coupling in IVNGs. This transition is critical because iontronic computing enables dynamic EDL systems to move beyond sensing and communication toward active information processing, providing a key step toward energy-information-integrated iontronic intelligence[48,175-181]. By introducing semiconductor carrier dynamics into iontronic systems, IVNGs provide an additional degree of freedom for regulating ionic information states. This enables programmable iontronic computing through cooperative interactions among photocarrier excitation, interfacial electrochemical reactions, SCR modulation, and asymmetric EDL-mediated ionic transport. A representative example was recently demonstrated by Li *et al.*, who developed a light-gated iontronic computing architecture based on RC-IVNGs [Figure 18][94]. Owing to the strong coupling among photocarrier generation, interfacial oxidation, and dynamic EDL-SCR interactions, the RC-IVNG exhibited two stable and distinguishable ionic-current states under different illumination conditions. In the absence of UV irradiation, the device remained in a low-current state. Under UV illumination, photogenerated carriers were separated by the coupled EDL-SCR electric field, while interfacial oxidation reactions generated additional ionic species and reinforced EDL asymmetry, resulting in a significantly enhanced ionic current [Figure 18A]. These reproducible current states provide a robust physical basis for optically encoded iontronic information. As a result, the ionic transport state of the device can be programmably switched between different information states through external optical inputs.

Based on this principle, two RC-IVNG units were employed as independently addressable input nodes, where the illumination-off and illumination-on states were assigned as logical "0" and "1", respectively. Because each RC-IVNG generated distinct ionic-current outputs under different optical conditions, the resulting ionic signals could be combined and processed through specific coupling configurations [Figure 18B]. By defining appropriate output-current thresholds, representative Boolean logic functions, including OR, AND, NOR, and NAND operations, were successfully realized [Figure 18C-F]. Importantly, these operations were achieved directly through optically regulated ionic transport without relying on transistors, external bias voltages, or conventional electronic logic components. More significantly, the logical behavior of RC-IVNGs originates from intrinsic matter-energy-information coupling at semiconductor-liquid interfaces. Ionic species act as physical information carriers, optical excitation serves as a programmable energy input, semiconductor carrier dynamics regulate interfacial electronic states, and dynamic EDL-SCR coupling governs the evolution of ionic information states. Within this framework, information encoding, signal modulation, and logic computation are integrated within a single interfacial iontronic system. IVNG-based light-gated computing demonstrates that dynamic EDLs can evolve beyond sensing interfaces and ionic communication channels into active computational units capable of regulating ionic fluxes and processing information. By integrating photonic stimulation, semiconductor carrier

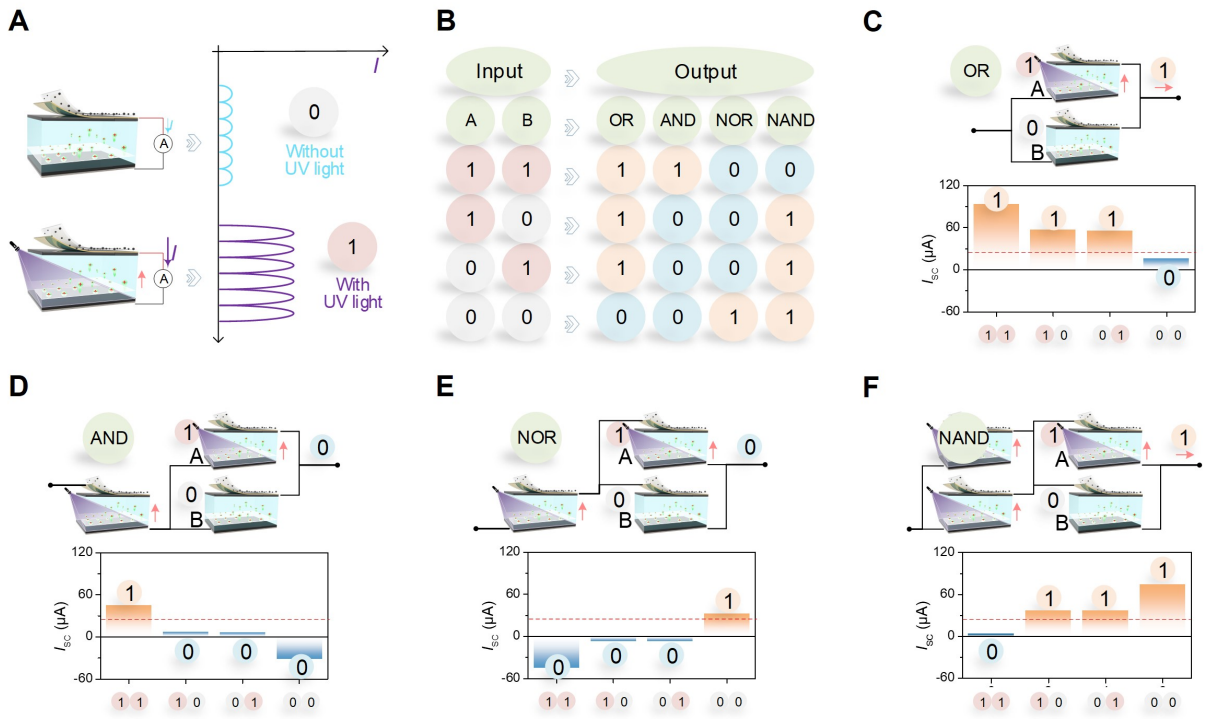

Figure 18. Light-gated iontronic computing enabled by dynamic EDL-SCR coupling in RC-IVNGs, developed by Li *et al.* in 2026. Reprinted with permission from[94] Copyright © 2026 Springer Nature. (A) Optical encoding of binary iontronic information states through illumination-controlled ionic-current outputs in RC-IVNG units; (B) Construction of a light-gated iontronic computing architecture using independently addressable RC-IVNG input nodes; (C-F) Realization of representative Boolean logic functions, including OR, AND, NOR, and NAND operations, through optically regulated ionic transport and dynamic EDL-SCR interactions.

dynamics, ionic transport, and Boolean logic operations, IVNGs establish a new paradigm for light-gated iontronic information processing.

Collectively, S-L TENGs, TINGs, and IVNGs reveal a continuous evolution of dynamic EDLs from interfacial information-encoding media to programmable ionic-information channels and ionic-electronic computational units. In S-L TENGs, dynamic EDLs encode external stimuli into triboelectric fingerprints; in TINGs, asymmetric EDLs enable bionic logic control and long-range iontronic communication; and in IVNGs, EDL-SCR coupling integrates semiconductor carrier dynamics to realize light-gated iontronic computing. This progression establishes dynamic EDLs as a unified physicochemical platform for sensing, communication, and computation at solid-liquid interfaces, providing an essential foundation for self-powered iontronic intelligence and matter-energy-information integrated systems. In terms of experimental evidence, the mechanisms discussed above can be distinguished according to the nature and extent of their validation. For S-L TENGs, contact electrification and electrostatic induction constitute the well-established operating framework, with interfacial ionic screening and EDL evolution extensively supported across diverse solid-liquid systems. For TINGs, asymmetric-EDL-driven directional ionic transport has been experimentally validated through controlled interfacial asymmetry, polarity-dependent responses, wetting-sequence regulation, and corresponding ionic-transport behavior. For IVNGs, dynamic EDL-SCR coupling has been supported by complementary measurements of local ionic redistribution, semiconductor surface potential and work function, flat-band potential, and electrical output under controlled interfacial regulation. These results provide strong experimental support for the proposed TING and IVNG mechanisms, while continued studies across broader material and device systems will further expand their general applicability. In contrast, large-scale adaptive iontronic networks and iontronic embodied intelligence remain prospective directions rather than experimentally established capabilities.

ENERGY-INFORMATION FLOW THROUGH DYNAMIC EDLS

The preceding sections demonstrate that dynamic EDLs provide a unified physicochemical foundation for energy transduction and information processing at solid-liquid interfaces[182-187]. Through the dynamic regulation of ionic distributions, concentration gradients and interfacial electrostatic states, EDL-based systems enable a broad range of functionalities, including environmental energy harvesting, ionic signal generation, interfacial sensing, information transmission, long-range communication and logic computation within a unified iontronic framework. These advances suggest a broader perspective: dynamic EDLs may provide a physical pathway towards iontronic embodied intelligence, in which energy utilization and information processing are intrinsically coupled through ionic transport and interfacial electrochemical dynamics. A compelling analogy can be found in biological neural systems. Unlike conventional electronic architectures, where energy supply, sensing, communication, memory, and computation are typically realized through physically separated functional units, biological intelligence emerges from the seamless integration of these processes through dynamic ionic regulation[188-197]. In the human brain [Figure 19A], large-scale neuronal and synaptic networks achieve extraordinary energy efficiency because ionic concentration gradients simultaneously function as energy reservoirs, information carriers, and computational substrates[198-206]. This operating principle is enabled by the coordinated function of ion pumps and ion channels embedded within neuronal membranes [Figure 19B]. Ion pumps continuously consume metabolic energy to drive Na^+ and K^+ transport against their concentration gradients, thereby establishing nonequilibrium ionic distributions and maintaining membrane polarization. Upon external stimulation, voltage-gated ion channels transiently open, allowing ions to flow along these stored electrochemical gradients and generating dynamic membrane-potential changes that propagate as action potentials. Thus, neural signaling is not simply an information-transfer process, but an intrinsically coupled ionic process in which energy generation, release, and information transmission are governed by the same physicochemical landscape. During polarization, metabolic energy is converted into asymmetric ionic concentration gradients and stored as electrochemical potential energy; during depolarization, this stored energy is released through directional ion migration, simultaneously transmitting information and activating downstream neuronal responses. The continuous polarization-depolarization cycle therefore integrates energy storage, signal propagation, and adaptive regulation within a unified ionic medium, providing a fundamental physicochemical basis for biological neural computation and embodied intelligence.

From the perspective of dynamic EDLs, an artificial analog of this biological operating principle can be realized at triboelectrified solid-liquid interfaces [Figure 19C]. In triboiontronic systems, triboelectrically induced ion polarization drives ions away from equilibrium, establishing highly polarized EDLs with asymmetric ionic distributions. Analogous to ATP-driven ion pumping in biological neurons, this process converts external energy into nonequilibrium electrochemical gradients, thereby generating energy in the form of interfacial electrochemical potential while simultaneously defining ionic information states. Upon the formation of coupled asymmetric EDLs, these stored ionic gradients drive directional ion migration through the electrolyte. Similar to ion-channel-mediated depolarization, this process releases stored electrochemical energy while generating ionic signals and electrical outputs through coupled ionic-electronic interactions. Dynamic EDLs therefore provide a common physicochemical mechanism through which energy storage, information generation, and signal propagation are intrinsically integrated. This unifying principle is manifested across dynamic EDL-enabled iontronic systems. In S-L TENGs, dynamic EDLs transduce mechanical, chemical, thermal, and physiological stimuli into characteristic triboelectric signatures for self-powered sensing. In TINGs, triboelectrically polarized asymmetric EDLs govern ionic polarity, directional ion transport, information routing, and long-range iontronic information transmission. In IVNGs, dynamic coupling between EDLs and semiconductor SCR further integrates ionic transport with semiconductor carrier dynamics, enabling multimodal energy harvesting, light-gated ionic transport, and iontronic Boolean logic. Despite these diverse functionalities, all three systems rely on the same underlying

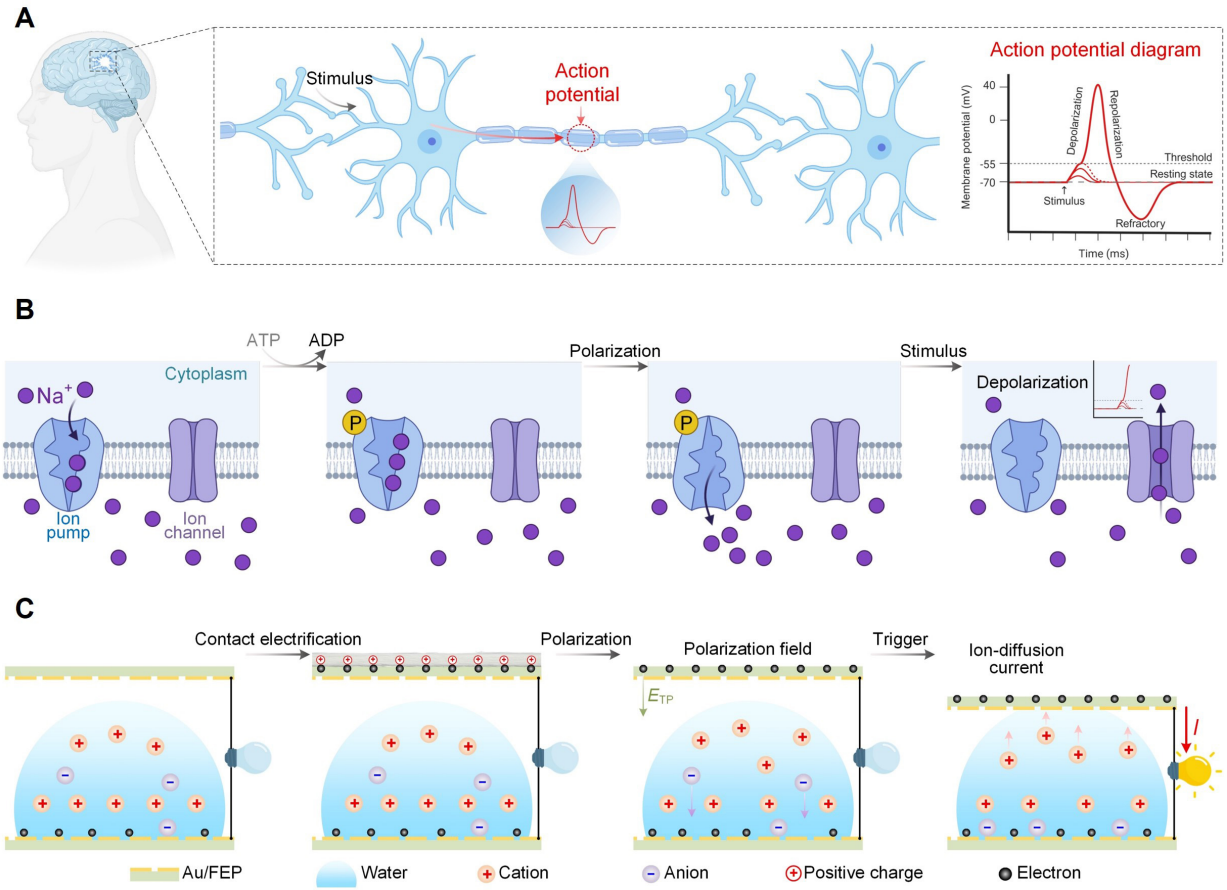

Figure 19. Biological inspiration and dynamic EDL-mediated energy-information integration toward iontronic embodied intelligence. Reprinted with permission from[206] Copyright © 2025 OAE. (A) Biological neural systems integrate energy flow and information flow through large-scale ionic transport networks; (B) Action-potential generation and propagation based on ATP-driven ion polarization and ion-channel-mediated depolarization, illustrating the energy-information coupling mechanism underlying biological intelligence; (C) Dynamic EDL-mediated ion polarization and directional ionic transport in triboiontronic systems, providing an artificial analog for coupling energy conversion, information transmission, and signal regulation at solid-liquid interfaces.

mechanism: the dynamic regulation of ionic distributions, concentration gradients, and interfacial electrochemical potentials. Dynamic EDLs therefore constitute artificial ionic interfaces that integrate energy harvesting, information encoding, signal transmission, and computation within a unified iontronic framework.

Importantly, these functionalities represent distinct levels of information processing and should not be directly equated with adaptive intelligence. In the present context, sensing refers to the transduction of external physical or chemical stimuli into distinguishable ionic or electrical signals, while information transmission involves the propagation or routing of encoded ionic signals between spatially separated interfaces. Logic operation represents a higher level of predefined information processing, in which multiple inputs are mapped to deterministic outputs according to established rules. In contrast, learning requires history-dependent modification of system responses, memory retention, or plasticity, whereas adaptive intelligence further requires autonomous perception, decision-making, actuation, feedback, and environment-dependent self-adjustment. Most dynamic EDL-enabled systems reviewed here currently demonstrate sensing, ionic information transmission, and predefined logic operations, while genuine learning and closed-loop adaptive intelligence remain emerging objectives rather than established capabilities. Accordingly, the term “energy-information flow” used in this review refers specifically to the

physical coupling between energy conversion and information generation, transmission, or processing through shared ionic and interfacial electrochemical processes, rather than implying intelligence itself. From this perspective, the progression from self-powered sensing to ionic communication and logic processing provides a physicochemical pathway toward, rather than a realization of, iontronic embodied intelligence. Such a future architecture would require perception, communication, computation, actuation, and feedback to emerge from continuous interactions with the physical environment while maintaining energetic autonomy. By integrating iontronic energy generation with progressively more advanced information functions, dynamic EDLs therefore provide a promising physicochemical foundation for the future development of iontronic embodied intelligence.

OUTLOOKS AND CHALLENGES

The studies discussed in this Review establish dynamic EDLs as a unifying physicochemical framework that intrinsically couples energy generation with information processing at solid-liquid interfaces. Through the dynamic regulation of ionic distributions, dynamic EDLs have evolved from passive charge-screening structures into adaptive iontronic interfaces capable of energy harvesting, environmental sensing, ionic communication, and information processing. More fundamentally, by integrating ionic transport, energy conversion, and signal propagation within the same electrochemical landscape, dynamic EDLs provide a physical basis for bridging energy flow and information flow. This capability distinguishes iontronic systems from conventional electronic architectures and suggests a promising route towards embodied intelligence based on iontronic rather than purely electronic processes.

A major opportunity lies in the development of self-powered iontronic nervous systems, in which environmental energy harvesting, ion polarization, signal generation, and information processing are seamlessly integrated within a common dynamic EDL framework. By exploiting triboelectrically induced ion polarization, asymmetric EDL coupling and EDL-SCR interactions, future iontronic systems may continuously convert environmental energy into programmable ionic signals while simultaneously supporting sensing, communication and computation without external power sources. Such architectures would represent a transition from energy-autonomous sensors to energy-autonomous information-processing systems. Beyond individual devices, dynamic EDLs also provide a foundation for distributed iontronic networks. Coupled iontronic interfaces could enable coordinated ionic communication across multiple nodes, allowing collective sensing, parallel information processing, and adaptive decision-making over extended spatial scales. Such networked ionic architectures could underpin emerging technologies including autonomous underwater communication, distributed environmental monitoring, soft robotic swarms, and cooperative bioelectronic systems. Ultimately, dynamic EDLs may enable closed-loop iontronic platforms in which sensing, communication, computation, actuation, and feedback are integrated within a unified ionic framework. Through adaptive EDL reconstruction, programmable ionic transport and history-dependent interfacial regulation, these systems may acquire self-optimization, environmental adaptation and increasingly autonomous behaviors, providing a potential physicochemical foundation for iontronic embodied intelligence.

Despite these advances, several fundamental challenges remain before this vision can be realized. First, the fundamental principles governing information propagation, nonlinear ionic interactions, and self-organization in dynamic EDL networks remain poorly understood. A predictive theoretical framework capable of linking interfacial electrochemistry, multiscale ionic transport, and system-level information dynamics has yet to be established. Second, although dynamic EDLs effectively regulate local ionic transport, extending these mechanisms to stable, low-loss, and long-range ionic communication in complex liquid environments remains a major challenge for scalable iontronic networks. Third, most existing systems remain externally programmed and exhibit limited adaptability. Unlike biological nervous systems, they

generally lack intrinsic memory, synaptic plasticity, and autonomous learning, highlighting the need for dynamic EDL architectures capable of history-dependent regulation, self-reconfiguration, and adaptive evolution. Fourth, the practical stability of dynamic EDL-enabled systems remains a major challenge for long-term operation. Electrolyte evaporation and repeated ion migration can alter ionic concentration and interfacial EDL states, leading to output drift. Surface contamination and chemical modification may further change surface charge, wettability, and ion adsorption, reducing reproducibility. In electrochemically active systems, electrode corrosion and irreversible Faradaic reactions can progressively degrade the interface, while slow ionic relaxation may introduce hysteresis and history-dependent responses. Addressing these issues will require improved electrolyte confinement, chemically stable and anti-fouling interfaces, corrosion-resistant materials, and standardized long-term cycling protocols.

More broadly, dynamic EDLs should be viewed not simply as interfacial electrochemical structures, but as adaptive ionic platforms that integrate energy generation, information transduction, and environmental interaction within a common physicochemical framework. Establishing quantitative principles that connect dynamic EDL evolution, ionic transport, information encoding, and adaptive behavior will be essential for transforming iontronics from individual energy-conversion and sensing devices into self-powered, distributed, and intelligent ionic systems. Continued advances in dynamic EDL engineering, triboiontronics, and iontrovoltaics therefore have the potential to establish a new generation of embodied iontronic technologies in which energy flow and information flow are intrinsically unified, opening new directions for intelligent matter inspired by biological ionic systems.

DECLARATIONS

Authors' contributions

Conceived the concept: Wei, D.
Performed the research, analyzed the results and wrote the paper: Wei, D.; Li, X.; Zhou, Z.

Availability of data and materials

Not applicable.

AI and AI-assisted tools statement

Not applicable.

Financial support and sponsorship

This work was supported by the China Postdoctoral Science Foundation (certificate number 2025M781041), Postdoctoral Fellowship Program of China Postdoctoral Science Foundation (Grant Number GZC20260537), and National Natural Science Foundation (Grant number 22479016).

Conflicts of interest

All authors declared that there are no conflicts of interest.

Ethical approval and consent to participate

Not applicable.

Consent for publication

Not applicable.

REFERENCES

1. Markram, H. The blue brain project. *Nat. Rev. Neurosci.* **2006**, *7*, 153-60. DOI PubMed
2. Siva, N. What happened to the human brain project? *Lancet* **2023**, *402*, 1408-9. DOI

3. Salles, A.; Bjaalie, J. G.; Evers, K.; et al. The human brain project: responsible brain research for the benefit of society. *Neuron* **2019**, *101*, 380-4. DOI
4. Agiza, A. A.; Oakley, K.; Rosenstein, J. K.; et al. Digital circuits and neural networks based on acid-base chemistry implemented by robotic fluid handling. *Nat. Commun.* **2023**, *14*, 496. DOI PubMed PMC
5. Larson, C. China's AI imperative. *Science* **2018**, *359*, 628-30. DOI PubMed
6. Daniotti, S.; Wachs, J.; Feng, X.; Neffke, F. Who is using AI to code? *Science* **2026**, *391*, 831-5. DOI PubMed
7. Ji, J.; Pan, Y.; Zhang, Z.; Xia, T.; Zhang, F.; Huang, Y. AI-enabled flexible sensing skin for next-generation aircraft: toward embodied intelligence. *Research* **2026**, *9*, 1305. DOI PubMed PMC
8. Xu, H.; Wang, Z.; Wang, Y.; et al. Intelligent metasurface cloak reaches a new plateau: AI-assisted surface engineering for self-adaptive supportive invisibility. *Research* **2026**, *9*, 1130. DOI PubMed PMC
9. Vaughan, O. Two nanometre CMOS technology. *Nat. Electron.* **2024**, *7*, 1063-1063. DOI
10. Hiramoto, T. Five nanometre CMOS technology. *Nat. Electron.* **2019**, *2*, 557-8. DOI
11. Koch, U.; Uhl, C.; Hettrich, H.; et al. A monolithic bipolar CMOS electronic-plasmonic high-speed transmitter. *Nat. Electron.* **2020**, *3*, 338-45. DOI
12. De Schotten M, Forkel SJ. The emergent properties of the connected brain. *Science* **2022**, *378*, 505-10. DOI PubMed
13. Dorkenwald, S.; Matsliah, A.; Sterling, A. R.; et al. Neuronal wiring diagram of an adult brain. *Nature* **2024**, *634*, 124-38. DOI
14. Dolgin, E. Brain tissues, assemble! *Nature* **2025**, *641*, 809-12. DOI PubMed
15. Jin, B.; Wang, Z.; Wang, T.; Meng, J. Memristor-based artificial neural networks for hardware neuromorphic computing. *Research* **2025**, *8*, 0758. DOI PubMed PMC
16. Xie, J.; Shan, X.; Zou, N.; et al. All-optically controlled memristive device based on Cu_2O/TiO_2 heterostructure toward neuromorphic visual system. *Research* **2025**, *8*, 0580. DOI PubMed PMC
17. Pandey, S. V.; Saurav, K. V.; Ismail, A.; Rahaman, S.; Radha, B. Nanofluidic ionic memory for next-generation computing. *Nat. Rev. Mater.* **2026**, 919. DOI
18. Sarpeshkar, R. Analog versus digital: extrapolating from electronics to neurobiology. *Neural. Comput.* **1998**, *10*, 1601-38. DOI PubMed
19. Debus, C.; Piraud, M.; Streit, A.; Theis, F.; Götz, M. Reporting electricity consumption is essential for sustainable AI. *Nat. Mach. Intell.* **2023**, *5*, 1176-8. DOI
20. D'orgeval, A.; Sheehan, S.; Avenas, Q.; Assoumou, E.; Sessa, V. Generative AI impact assessment through a life cycle analysis of multiple data center typologies. *Appl. Energy.* **2026**, *406*, 127288. DOI
21. Yang, J.; Xiao, W.; Jiang, C.; Hossain, M. S.; Muhammad, G.; Amin, S. U. AI-powered green cloud and data center. *IEEE. Access.* **2019**, *7*, 4195-203. DOI
22. Wang, T.; Tufenkjian, A.; Ajijola, O. A.; Oka, Y. Molecular and functional diversity of the autonomic nervous system. *Nat. Rev. Neurosci.* **2025**, *26*, 607-22. DOI PubMed
23. Gunsch, G.; Paradie, E.; Townsend, K. L. Peripheral nervous system glia in support of metabolic tissue functions. *Trends. Endocrinol. Metab.* **2023**, *34*, 622-39. DOI PubMed
24. Bucci, A.; Büttner, M.; Domdei, N.; et al. Synchronization of visual perception within the human fovea. *Nat. Neurosci.* **2025**, *28*, 1959-67. DOI PubMed PMC
25. Zhang, Y.; Luan, P.; Qiao, Q.; et al. An axonal brake on striatal dopamine output by cholinergic interneurons. *Nat. Neurosci.* **2025**, *28*, 783-94. DOI PubMed PMC
26. Varró, A.; Tomek, J.; Nagy, N.; et al. Cardiac transmembrane ion channels and action potentials: cellular physiology and arrhythmogenic behavior. *Physiol. Rev.* **2021**, *101*, 1083-176. DOI
27. Yang, H.; Wang, K.; Chen, Y.; et al. Excitatory synapses onto axonic spines jump-start action potentials and route information flow. *Nat. Neurosci.* **2026**, *29*, 1303-12. DOI
28. Mariantoni, M.; Wang, H.; Yamamoto, T.; et al. Implementing the quantum von neumann architecture with superconducting circuits. *Science* **2011**, *334*, 61-5. DOI
29. Gonzalez-zalba, M. F.; De, Franceschi. S.; Charbon, E.; Meunier, T.; Vinet, M.; Dzurak, A. S. Scaling silicon-based quantum computing using CMOS technology. *Nat. Electron.* **2021**, *4*, 872-84. DOI
30. Pal, A.; Chavan, T.; Jabbour, J.; Cao, W.; Banerjee, K. Three-dimensional transistors with two-dimensional semiconductors for future CMOS scaling. *Nat. Electron.* **2024**, *7*, 1147-57. DOI
31. Varadarajan, S. G.; Hunyara, J. L.; Hamilton, N. R.; Kolodkin, A. L.; Huberman, A. D. Central nervous system regeneration. *Cell* **2022**, *185*, 77-94. DOI PubMed PMC
32. Yoder, N.; Yoshioka, C.; Gouaux, E. Gating mechanisms of acid-sensing ion channels. *Nature* **2018**, *555*, 397-401. DOI PubMed PMC
33. Luo, Y.; Liu, B.; Qiu, Y.; et al. Divalent metal ions enhance bone regeneration through modulation of nervous systems and metabolic pathways. *Bioact. Mater.* **2025**, *47*, 432-47. DOI PubMed PMC

34. Davila-Velderrain, J.; Van Giesen, L. Voltage-gated ion channel diversity underlies neuronal excitability and nervous system evolution. *Nat. Commun.* **2025**, *16*, 11534. DOI PubMed PMC
35. Zhao, J.; Zhou, H.; Fu, T.; Wang, H.; Zhang, T.; Li, L. High-performance iontronic hydrogel acoustic sensor for low-frequency underwater sound detection and intelligent recognition. *Research* **2026**, *9*, 1292. DOI PubMed PMC
36. Zhang, L.; Xie, Y.; Shi, S.; et al. Bioderived cellulose aerogel fibers with hierarchical porosity for millisecond hydrovoltaic sensing. *Research* **2026**, *9*, 1324. DOI PubMed PMC
37. Zhang, D.; Liu, W.; Feng, L.; et al. Innovative advances in droplet microfluidics. *Research* **2025**, *8*, 0856. DOI PubMed PMC
38. Su, K.; Bian, Z.; Mu, Y.; et al. Pyrrolidine ionic liquid enables dynamic EDL regulation for highly stable aqueous Zn Ion capacitors. *Energy. Storage. Mater.* **2025**, *81*, 104480. DOI
39. Wu, Q.; Qi, Y. Revealing heterogeneous electric double layer (EDL) structures of localized high-concentration electrolytes (LHCEs) and their impact on solid-electrolyte interphase (SEI) formation in lithium batteries. *Energy. Environ. Sci.* **2025**, *18*, 3036-46. DOI
40. Lim, Y.; Kim, Y.; Kim, N.; Choi, J. Ion pairing dynamics leading to a non-linear electrochemical structure of an electric double layer on a carbon electrode. *Nano. Energy.* **2025**, *146*, 111506. DOI
41. Lee, D.; Jeon, Y. U.; An, M.; et al. Tailored zwitterion electrolyte-driven electric double layer dynamics for enhanced ion retention in artificial synapses. *Adv. Funct. Mater.* **2025**, *36*, e13684. DOI
42. Zhang, Y.; Huang, H.; Tian, J.; et al. Modelling electrified microporous carbon/electrolyte electrochemical interface and unraveling charge storage mechanism by machine learning accelerated molecular dynamics. *Energy. Storage. Mater.* **2023**, *63*, 103069. DOI
43. Shin, S.; Kim, D. H.; Bae, G.; et al. On the importance of the electric double layer structure in aqueous electrocatalysis. *Nat. Commun.* **2022**, *13*, 174. DOI PubMed PMC
44. Chen, B.; Zhai, Z.; Huang, N.; et al. Highly localized charges of confined electrical double-layers inside 0.7-nm layered channels. *Adv. Energy. Mater.* **2023**, *13*, 2300716. DOI
45. Unalan, H. E.; Yang, Y.; Zhang, Y.; et al. ZnO nanowire and WS_2 nanotube electronics. *IEEE. Trans. Electron. Devices.* **2008**, *55*, 2988-3000. DOI
46. Wang, S.; Wang, Y.; Cai, X.; et al. A high-frequency artificial nerve based on homogeneously integrated organic electrochemical transistors. *Nat. Electron.* **2025**, *8*, 254-66. DOI
47. Xing, Y.; Zhou, M.; Si, Y.; et al. Integrated opposite charge grafting induced ionic-junction fiber. *Nat. Commun.* **2023**, *14*, 2355. DOI PubMed PMC
48. Xiong, T.; Li, C.; He, X.; et al. Neuromorphic functions with a polyelectrolyte-confined fluidic memristor. *Science* **2023**, *379*, 156-61. DOI
49. He, X.; Zhang, K.; Li, T.; Jiang, Y.; Yu, P.; Mao, L. Micrometer-scale ion current rectification at polyelectrolyte brush-modified micropipets. *J. Am. Chem. Soc.* **2017**, *139*, 1396-9. DOI
50. Helmholtz, H. Ueber einige Gesetze der Vertheilung elektrischer Ströme in körperlichen Leitern mit Anwendung auf die thierisch-elektrischen Versuche. *Ann. . Phys.* **2006**, *165*, 211-33. DOI
51. Gouy, M. Sur la constitution de la charge électrique à la surface d'un électrolyte. *J. Phys. Theor. Appl.* **1910**, *9*, 457-68. DOI
52. Chapman, D. L. A contribution to the theory of electrocapillarity. *Philos. Mag.* **1913**, *25*, 475-81. DOI
53. Grahame, D. C. The electrical double layer and the theory of electrocapillarity. *Chem. Rev.* **2002**, *41*, 441-501. DOI
54. Wang, Z. L.; Wang, A. C. On the origin of contact-electrification. *Mater. Today.* **2019**, *30*, 34-51. DOI
55. Lin, S.; Xu, L.; Chi, Wang. A.; Wang, Z. L. Quantifying electron-transfer in liquid-solid contact electrification and the formation of electric double-layer. *Nat. Commun.* **2020**, *11*, 399. DOI PubMed PMC
56. Lin, S.; Chen, X.; Wang, Z. L. Contact electrification at the liquid-solid interface. *Chem. Rev.* **2021**, *122*, 5209-32. DOI
57. Li, X.; Li, S.; Guo, X.; Shao, J.; Wang, Z. L.; Wei, D. Triboiontronics for efficient energy and information flow. *Matter* **2023**, *6*, 3912-26. DOI
58. Li, X.; Wang, Z. L.; Wei, D. Bioinspired iontronic architectures for neuromorphic intelligence. *Innovation* **2026**, *7*, 101424. DOI PubMed PMC
59. Li, X.; Wang, Z. L.; Wei, D. Redefining solid-liquid interface probing via contact electrification-driven paradigm. *Sci. Bull.* **2026**, *71*, 2659-62. DOI
60. Zhang, L.; Wang, D. Triboiontronics based on dynamic electric double layer regulation. *Matter* **2023**, *6*, 3698-9. DOI
61. Zhang, H.; Zhang, Y.; He, P.; et al. Quantifying the triboelectric series of liquid phase materials. *Adv. Mater.* **2026**, *38*, e73450. DOI
62. Liu, C.; Wang, Z.; Tong, X.; et al. Water-evaporation-induced direct current electricity generation based on stretchable hydrogel/Al_2O_3. *Matter* **2025**, *8*, 102200. DOI
63. Xia, Y.; Ye, C.; Han, R.; et al. Columnar structure solid-liquid nanogenerator based on triboiontronics. *Nano. Energy.* **2026**, *150*, 111783. DOI

64. Liang, X.; Liu, S.; Lin, S.; Yang, H.; Jiang, T.; Wang, Z. L. Liquid-solid triboelectric nanogenerator arrays based on dynamic electric-double-layer for harvesting water wave energy. *Adv. Energy. Mater.* **2023**, *13*, 2300571. DOI
65. Yin, J.; Li, X.; Yu, J.; Zhang, Z.; Zhou, J.; Guo, W. Generating electricity by moving a droplet of ionic liquid along graphene. *Nat. Nanotechnol.* **2014**, *9*, 378-83. DOI
66. Yin, J.; Zhang, Z.; Li, X.; et al. Waving potential in graphene. *Nat. Commun.* **2014**, *5*, 3582. DOI
67. Yang, S.; Su, Y.; Xu, Y.; et al. Mechanism of electric power generation from ionic droplet motion on polymer supported graphene. *J. Am. Chem. Soc.* **2018**, *140*, 13746-52. DOI
68. Kumar, S.; Sharma, A.; Gupta, V.; Tomar, M. Development of novel MoS_2 hydrovoltaic nanogenerators for electricity generation from moving NaCl droplet. *J. Alloys. Compd.* **2021**, *884*, 161058. DOI
69. Wei, Y.; Li, X.; Yang, Z.; Shao, J.; Wang, Z. L.; Wei, D. Contact electrification at the solid-liquid transition interface. *Mater. Today.* **2024**, *74*, 2-11. DOI
70. Li, R.; Li, X.; Zhang, Z.; Willatzen, M.; Wang, Z. L.; Wei, D. Triboelectric programmed droplet manipulation for plug-and-play assembly. *Adv. Funct. Mater.* **2024**, *35*, 2416457. DOI
71. Wang, K.; Wang, X.; Sun, Y.; et al. Macroscopic liquid superlubric triboelectric nanogenerator: an in-depth understanding of solid-liquid interfacial charge behavior. *Nano. Energy.* **2024**, *129*, 110038. DOI
72. Nan, Y.; Wang, X.; Xu, H.; et al. Customizing alternating and direct current dual-mode solid-liquid triboelectric nanogenerator. *Nano. Energy.* **2025**, *137*, 110812. DOI
73. Wang, M.; Liang, Y.; Zhang, L.; et al. Solid-liquid triboelectric nanogenerators as physicochemical encoders for intelligent liquid recognition. *Interdiscip. Mater.* **2026**, *5*, 573-608. DOI
74. Fan, H.; Zeng, Z.; Deng, C.; et al. High-performance solid-liquid triboelectric nanogenerator enabled by dual physicochemical modification for wearable sensing. *Nano. Energy.* **2025**, *140*, 111061. DOI
75. Zhao, X. J.; Zhu, G.; Zhao, Z. H.; Wang, Z. L.; Wang, J. High durable bio-inspired self-cleaning solid-liquid contact triboelectric nanogenerator for water wave energy harvesting. *Nano. Energy.* **2025**, *139*, 110971. DOI
76. Li, Y.; Wang, K.; Yang, H.; et al. Solid-liquid triboelectric nanogenerator based self-sensing vibration suppression device. *Nano. Energy.* **2024**, *131*, 110211. DOI
77. Ro, Y. G.; Na, S.; Kim, J.; et al. Iontronics: neuromorphic sensing and energy harvesting. *ACS. Nano.* **2025**, *19*, 24425-507. DOI
78. Mcnamee, C. E. Effect of a liquid flow on the forces between charged solid surfaces and the non-equilibrium electric double layer. *Adv. Colloid. Interface. Sci.* **2019**, *266*, 21-33. DOI PubMed
79. Zhou, S.; Panse, K. S.; Motevaselian, M. H.; Aluru, N. R.; Zhang, Y. Three-dimensional molecular mapping of ionic liquids at electrified interfaces. *ACS. Nano.* **2020**, *14*, 17515-23. DOI PubMed
80. Yu, L.; Yao, N.; Gao, Y.; et al. Probing the electric double layer structure at nitrogen-doped graphite electrodes by constant-potential molecular dynamics simulations. *J. Energy. Chem.* **2024**, *93*, 299-305. DOI
81. Zhang, C.; Calegari, Andrade. M. F.; Goldsmith, Z. K.; et al. Molecular-scale insights into the electrical double layer at oxide-electrolyte interfaces. *Nat. Commun.* **2024**, *15*, 10270. DOI PubMed PMC
82. Wang, Y.; Liang, B.; Zhu, J.; et al. Manipulating electric double layer adsorption for stable solid-electrolyte interphase in 2.3 Ah Zn-pouch cells. *Angew. Chem. Int. Ed.* **2023**, *62*, e202302583. DOI
83. Qin, S.; Zhang, J.; Xu, M.; et al. Formulating self-repairing solid electrolyte interface via dynamic electric double layer for practical zinc ion batteries. *Angew. Chem. Int. Ed.* **2024**, *63*, e202410422. DOI
84. Kim, M. M.; Choi, C. H.; Kim, H. Electric double layer charging, a new framework for optimizing electrocatalyst design and performance. *ACS. Energy. Lett.* **2026**, *11*, 2499-507. DOI
85. Li, Y.; Ping, B.; Qu, J.; et al. Constructing autoregulative electric double layer through dielectric effect toward fast charging zinc metal anode. *Adv. Energy. Mater.* **2025**, *15*, 2405804. DOI
86. Chen, L.; Zhang, H.; Li, R.; et al. Dynamic shielding of electrified interface enables high-voltage lithium batteries. *Chem* **2024**, *10*, 1196-212. DOI
87. Jing, T.; Xu, B.; Yang, Y. Liquid doping materials as micro-carrier of functional molecules for functionalization of triboelectric materials and flexible triboelectric nanogenerators for energy harvesting and gesture detection. *Nano. Energy.* **2020**, *74*, 104856. DOI
88. Wang, W.; Meng, J.; Zhang, L.; et al. Liquid jet-based triboelectric nanogenerator. *Adv. Mater.* **2025**, *38*, e07055. DOI
89. Wu, Q.; Zhang, L.; Wang, W.; et al. High-performance pneumatic solid-liquid triboelectric nanogenerator. *Nano. Energy.* **2024**, *123*, 109391. DOI
90. Qin, H.; Xu, L.; Lin, S.; et al. Underwater energy harvesting and sensing by sweeping out the charges in an electric double layer using an oil droplet. *Adv. Funct. Mater.* **2022**, *32*, 2111662. DOI
91. Bohra, D.; Chaudhry, J. H.; Burdyny, T.; Pidko, E. A.; Smith, W. A. Modeling the electrical double layer to understand the reaction environment in a CO_2 electrocatalytic system. *Energy. Environ. Sci.* **2019**, *12*, 3380-9. DOI

92. Lin, Z. H.; Cheng, G.; Lin, L.; Lee, S.; Wang, Z. L. Water-solid surface contact electrification and its use for harvesting liquid-wave energy. *Angew. Chem. Int. Ed.* **2013**, *52*, 12545-9. DOI PubMed
93. Li, X.; Wei, Y.; Gao, X.; Zhang, Z.; Wang, Z. L.; Wei, D. Harnessing triboiontronic Maxwell's demon by triboelectric-induced polarization for efficient energy-information flow. *Joule* **2025**, *9*, 101888. DOI
94. Li, X.; Wei, Y.; Ouyang, Y.; Wang, Z. L.; Cao, Y.; Di, W. Iontrovoltaic effect based on triboelectrically induced ion polarization at semiconductor-liquid interfaces. *Nat. Commun.* **2026**, 77245. DOI
95. Zachman, M. J.; Tu, Z.; Choudhury, S.; Archer, L. A.; Kourkoutis, L. F. Cryo-STEM mapping of solid-liquid interfaces and dendrites in lithium-metal batteries. *Nature* **2018**, *560*, 345-9. DOI PubMed
96. Zhang, Q.; Song, Z.; Sun, X.; et al. Atomic dynamics of electrified solid-liquid interfaces in liquid-cell TEM. *Nature* **2024**, *630*, 643-7. DOI
97. Zhang, J.; Gu, G.; Liu, Q.; Wang, Z. L. Triboelectric nanogenerator as a probe for investigating charge transfer at liquid-solid interfaces. *Chem. Rev.* **2026**, *126*, 5490-517. DOI PubMed
98. Wang, X.; Ying, Y.; Li, X.; et al. Preferred planar crystal growth and uniform solid electrolyte interfaces enabled by anion receptors for stable aqueous Zn batteries. *Energy. Environ. Sci.* **2023**, *16*, 4572-83. DOI
99. Zhang, Y.; Ni, Y.; Liang, G.; et al. Transistor-based bio-hybrid artificial afferent nerves for a mainly bio-composite reflex arc system. *SmartSys* **2026**, *2*, e70033. DOI
100. Li, N.; Bai, C.; Yang, X.; et al. Electrically driven hydrogel actuators from turgor pressure to ciliary motion. *SmartSys* **2026**, *2*, e70030. DOI
101. Wu, Q.; Mcdowell, M. T.; Qi, Y. Effect of the electric double layer (EDL) in multicomponent electrolyte reduction and solid electrolyte interphase (SEI) formation in lithium batteries. *J. Am. Chem. Soc.* **2023**, *145*, 2473-84. DOI PubMed PMC
102. Bendadesse, E.; Morozov, A. V.; Abakumov, A. M.; Perrot, H.; Tarascon, J.; Sel, O. Deciphering the double-layer structure and dynamics on a model Li_xMoO_3 interface by advanced electrogravimetric analysis. *ACS. Nano.* **2022**, *16*, 14907-17. DOI
103. Wu, C. H.; Pascal, T. A.; Baskin, A.; et al. Molecular-scale structure of electrode-electrolyte interfaces: the case of platinum in aqueous sulfuric acid. *J. Am. Chem. Soc.* **2018**, *140*, 16237-44. DOI
104. Zhang, M.; Chen, Y.; Melander, M. M.; Huang, J. Electrochemical electron transfer: key concepts, theories, and parameterization via atomistic simulations. *Chem. Rev.* **2026**, *126*, 7407-64. DOI PubMed PMC
105. Lyu, Y.; Su, Y.; Nan, K.; Zhang, Y. Bioinspiration for bioiontronics. *Iontronics* **2026**, *2*, 9. DOI
106. Luo, C.; Zhou, L.; Xu, R.; Hou, Y.; Hou, X. CNT array-based aluminum bipolar electrode iontronic memristors. *Iontronics* **2026**, *2*, 6. DOI
107. Lei, C.; He, J.; Chen, W.; Kong, X.; Wen, L. Biotic iontronics: foundations for the direct biotic-abiotic communication and modulation. *Iontronics* **2026**, *2*, 8. DOI
108. Yoo, D.; Jang, S.; Cho, S.; Choi, D.; Kim, D. S. A liquid triboelectric series. *Adv. Mater.* **2023**, *35*, 2300699. DOI PubMed
109. Kim, W.; Choi, D.; Kwon, J.; Choi, D. A self-powered triboelectric microfluidic system for liquid sensing. *J. Mater. Chem. A.* **2018**, *6*, 14069-76. DOI
110. Cai, C.; Luo, B.; Liu, Y.; et al. Advanced triboelectric materials for liquid energy harvesting and emerging application. *Mater. Today.* **2022**, *52*, 299-326. DOI
111. Zhang, R.; Lin, H.; Pan, Y.; et al. Liquid-liquid triboelectric nanogenerator for harvesting distributed energy (Adv. Funct. Mater. 51/2022). *Adv. Funct. Mater.* **2022**, *32*, 2270293. DOI
112. Wu, H.; Zhao, L.; Guo, H.; et al. Tribo-mechano transduction of solid-liquid triboelectric nanogenerators via boundary layer theory. *Renew. Energy.* **2026**, *258*, 124958. DOI
113. Li, Y.; Liu, M.; Song, G.; et al. Laser-textured superamphiphobic LF-PTFE solid-liquid hybrid triboelectric nanogenerator for stable energy harvesting and self-powered liquid sensing. *Nano. Energy.* **2026**, *155*, 112123. DOI
114. Wu, Y.; Lei, R.; Cao, J.; et al. High-sensitivity flexible self-powered pressure sensor based on solid-liquid triboelectrification. *ACS. Sens.* **2025**, *10*, 2347-57. DOI
115. Dong, Y.; Wang, N.; Yang, D.; Wang, J.; Lu, W.; Wang, D. Robust solid-liquid triboelectric nanogenerators: mechanisms, strategies and applications. *Adv. Funct. Mater.* **2023**, *33*, 2300764. DOI
116. Wang, Y.; Guo, H.; Liao, J.; Qin, Y.; Ali, A.; Li, C. Solid-liquid triboelectric nanogenerator based on curvature effect for harvesting mechanical and wave energy. *Chem. Eng. J.* **2023**, *476*, 146571. DOI
117. Luo, H.; Ni, X.; Cui, Y.; et al. High stability rotary solid-liquid triboelectric nanogenerator for ionic liquid detection. *Nano. Energy.* **2025**, *138*, 110870. DOI
118. Han, J.; Huang, R.; Shan, C.; et al. Non-electrode droplet manipulation via triboelectrification near-field energy transmission. *Research* **2026**, *9*, 1277. DOI PubMed PMC

119. Li, X.; Tao, J.; Wang, X.; Zhu, J.; Pan, C.; Wang, Z. L. Networks of high performance triboelectric nanogenerators based on liquid-solid interface contact electrification for harvesting low-frequency blue energy. *Adv. Energy. Mater.* **2018**, *8*, 1800705. DOI
120. Xu, M.; Wang, S.; Zhang, S. L.; et al. A highly-sensitive wave sensor based on liquid-solid interfacing triboelectric nanogenerator for smart marine equipment. *Nano. Energy.* **2019**, *57*, 574-80. DOI
121. Wang, B.; Zhao, H.; Jin, C.; Xu, Y.; Ding, W. Ionic-electrostatic modeling of solid-liquid triboelectric nanogenerators. *Iontronics* **2026**, *2*, 17. DOI
122. Cui, E.; Wu, P.; Wang, F.; et al. Dipole effect enhanced liquid stream-current generator. *Matter* **2026**, *9*, 102632. DOI
123. Yu, Z.; Hu, Y.; Li, K.; et al. Shape-configurable and motion-designed droplet for high performance liquid-solid triboelectric nanogenerator. *Nano. Energy.* **2026**, *149*, 111723. DOI
124. Chi, J.; Liu, C.; Che, L.; et al. Harvesting water-evaporation-induced electricity based on liquid-solid triboelectric nanogenerator. *Adv. Sci.* **2022**, *9*, 2201586. DOI PubMed PMC
125. Chen, B. D.; Tang, W.; He, C.; et al. Water wave energy harvesting and self-powered liquid-surface fluctuation sensing based on bionic-jellyfish triboelectric nanogenerator. *Mater. Today.* **2018**, *21*, 88-97. DOI
126. Zhao, X. J.; Zhu, G.; Fan, Y. J.; Li, H. Y.; Wang, Z. L. Triboelectric charging at the nanostructured solid/liquid interface for area-scalable wave energy conversion and its use in corrosion protection. *ACS. Nano.* **2015**, *9*, 7671-7. DOI PubMed
127. Zhan, F.; Wang, A. C.; Xu, L.; et al. Electron transfer as a liquid droplet contacting a polymer surface. *ACS. Nano.* **2020**, *14*, 17565-73. DOI
128. Lin, Z. H.; Cheng, G.; Lee, S.; Pradel, K. C.; Wang, Z. L. Harvesting water drop energy by a sequential contact-electrification and electrostatic-induction process. *Adv. Mater.* **2014**, *26*, 4690-6. DOI PubMed
129. Zhu, G.; Su, Y.; Bai, P.; et al. Harvesting water wave energy by asymmetric screening of electrostatic charges on a nanostructured hydrophobic thin-film surface. *ACS. Nano.* **2014**, *8*, 6031-7. DOI
130. Dong, Y.; Xu, S.; Zhang, C.; et al. Gas-liquid two-phase flow-based triboelectric nanogenerator with ultrahigh output power. *Sci. Adv.* **2022**, *8*, eadd0464. DOI PubMed PMC
131. Xu, W.; Zheng, H.; Liu, Y.; et al. A droplet-based electricity generator with high instantaneous power density. *Nature* **2020**, *578*, 392-6. DOI
132. Li, L.; Li, X.; Deng, W.; et al. Sparking potential over 1200 V by a falling water droplet. *Sci. Adv.* **2023**, *9*, eadi2993. DOI PubMed PMC
133. Chen, X.; Zhang, Y.; Huang, Y.; et al. Interfacial polarization-enhanced ultrahigh performance liquid droplet nanogenerator. *Adv. Energy. Mater.* **2025**, *15*, 2406116. DOI
134. Ye, C.; Liu, D.; Gao, Y.; et al. Electrostatic breakdown at liquid-solid-gas triple-phase interfaces owing to contact electrification. *Matter* **2025**, *8*, 102007. DOI
135. Lin, S.; Zhu, L.; Tang, Z.; Wang, Z. L. Spin-selected electron transfer in liquid-solid contact electrification. *Nat. Commun.* **2022**, *13*, 5230. DOI PubMed PMC
136. Gong, S.; Li, K.; Sun, J.; Chen, J.; Guo, H. Three-phase interfacial force regulated solid-like liquid-slider for highly efficient and robust triboelectric nanogenerator. *Adv. Mater.* **2025**, *38*, e16923. DOI
137. Li, X.; Li, R.; Li, S.; Wang, Z. L.; Wei, D. Triboiontronics with temporal control of electrical double layer formation. *Nat. Commun.* **2024**, *15*, 6182. DOI PubMed PMC
138. Liu, W.; Liang, J.; Wang, Z.; Xu, H.; Liu, Y. Oxide-based electrolyte-gated transistors: an emerging electrochemical platform for iontronic neuromorphics. *Iontronics* **2026**, *2*, 22. DOI
139. Du, Z.; Wang, Z.; Wang, S.; Liu, Z.; Li, Z.; Hou, C. Ion-conductive stretchable light-emitting devices. *Iontronics* **2026**, *2*, 15. DOI
140. Hu, Y.; Yang, W.; Ma, Y.; et al. Solid-liquid interface charge transfer for generation of H_2O_2 and energy. *Nat. Commun.* **2025**, *16*, 1692. DOI PubMed PMC
141. Peng, X.; Zhu, F.; Jiang, Y.; et al. Identification of a quasi-liquid phase at solid-liquid interface. *Nat. Commun.* **2022**, *13*, 3601. DOI PubMed PMC
142. Li, X.; Chen, C.; Niu, Q.; Li, N. W.; Yu, L.; Wang, B. Self-assembly of nanoparticles at solid-liquid interface for electrochemical capacitors. *Rare. Metals.* **2022**, *41*, 3591-611. DOI
143. Osali, S.; Ghiyasi, Y.; Esfahani, H.; Jose, R.; Ramakrishna, S. Electrospun nanomembranes at the liquid-liquid and solid-liquid interface - a review. *Mater. Today.* **2023**, *67*, 151-77. DOI
144. Lee, W. H.; Yoon, S. G.; Jin, H.; et al. Electron density-change in semiconductor by ion-adsorption at solid-liquid interface. *Adv. Mater.* **2021**, *33*, 2007581. DOI
145. Xie, L.; Lu, B.; Sima, Z.; et al. Mechanical-electric dual characteristics solid-liquid interfacing sensor for accurate liquid identification. *Nat. Commun.* **2025**, *16*, 7069. DOI PubMed PMC
146. Wu, Y.; Liu, Y.; Zhu, C.; Kong, X.; Wen, L. Olfactory-inspired nanofluidic sensor: molecular recognition and transport in confined space. *Iontronics* **2026**, *2*, 14. DOI

147. Han, Y.; Zhang, R.; Liu, D.; Luo, J. Quantum-scale friction at solid-liquid interface: simulation, detection techniques, mechanisms, and emerging applications. *Nano. Micro. Lett.* **2026**, *18*, 230. DOI PubMed PMC
148. Zhao, X. J.; Kuang, S. Y.; Wang, Z. L.; Zhu, G. Electricity-free electroluminescence excited by droplet impact driven triboelectric field on Solid-Liquid interface. *Nano. Energy.* **2020**, *75*, 104823. DOI
149. Liu, J.; Wen, Z.; Lei, H.; Gao, Z.; Sun, X. A liquid-solid interface-based triboelectric tactile sensor with ultrahigh sensitivity of 21.48 kPa^{-1}. *Nano. Micro. Lett.* **2022**, *14*, 88. DOI PubMed PMC
150. Yi, F.; Wang, X.; Niu, S.; et al. A highly shape-adaptive, stretchable design based on conductive liquid for energy harvesting and self-powered biomechanical monitoring. *Sci. Adv.* **2016**, *2*, e1501624. DOI PubMed PMC
151. Wu, Y.; Luo, Y.; Qu, J.; Daoud, W. A.; Qi, T. Liquid single-electrode triboelectric nanogenerator based on graphene oxide dispersion for wearable electronics. *Nano. Energy.* **2019**, *64*, 103948. DOI
152. Chen, X.; Xiong, J.; Parida, K.; et al. Transparent and stretchable bimodal triboelectric nanogenerators with hierarchical micro-nanostructures for mechanical and water energy harvesting. *Nano. Energy.* **2019**, *64*, 103904. DOI
153. Xia, K.; Tian, Y.; Fu, J.; et al. Transparent and stretchable high-output triboelectric nanogenerator for high-efficiency self-charging energy storage systems. *Nano. Energy.* **2021**, *87*, 106210. DOI
154. Gao, H.; Yang, Y.; Liu, Q.; Gu, G.; Zhang, J.; Wang, Z. L. Triboelectric spectroscopy for in situ detection of gas molecules in liquid. *ACS. Nano.* **2026**, *20*, 18172-80. DOI
155. Li, X.; Luo, J.; Ping, J.; Wang, Z. L. Droplet-enabled controllable manipulation of tribo-charges from liquid-solid interface. *Engineering* **2025**, *45*, 132-42. DOI
156. Zhang, J.; Wu, C.; Mo, X.; Hu, B.; Wang, Z. L. Triboelectric nanogenerators as a probe for studying charge transfer at liquid-solid interface. *MRS. Bull.* **2025**, *50*, 327-35. DOI
157. Tang, Z.; Lin, S.; Wang, Z. L. Effect of surface pre-charging and electric field on the contact electrification between liquid and solid. *J. Phys. Chem. C.* **2022**, *126*, 8897-905. DOI
158. Zhang, J.; Lin, S.; Wang, Z. L. Electrostatic charges regulate chemiluminescence by electron transfer at the liquid-solid interface. *J. Phys. Chem. B.* **2022**, *126*, 2754-60. DOI
159. Tang, Z.; Lin, S.; Wang, Z. L. Quantifying contact-electrification induced charge transfer on a liquid droplet after contacting with a liquid or solid. *Adv. Mater.* **2021**, *33*, 2102886. DOI
160. Lin, S.; Zheng, M.; Luo, J.; Wang, Z. L. Effects of surface functional groups on electron transfer at liquid-solid interfacial contact electrification. *ACS. Nano.* **2020**, *14*, 10733-41. DOI
161. Zhang, J.; Lin, S.; Zheng, M.; Wang, Z. L. Triboelectric nanogenerator as a probe for measuring the charge transfer between liquid and solid surfaces. *ACS. Nano.* **2021**, *15*, 14830-7. DOI
162. Zhang, J.; Lin, S.; Wang, Z. L. Triboelectric nanogenerator array as a probe for in situ dynamic mapping of interface charge transfer at a liquid-solid contacting. *ACS. Nano.* **2023**, *17*, 1646-52. DOI
163. Zhang, J.; Wang, X.; Wu, N.; Gu, G.; Wang, Z. L. Time-resolved mapping of interface charge transfer for real-time observation of microscopic chemical reactions. *Angew. Chem. Int. Ed.* **2026**, *65*, e1249028. DOI
164. Wei, Y.; Li, X.; Gu, Y.; et al. Probing electrical double layer via triboelectric charge transfer. *Nat. Commun.* **2025**, *17*, 402. DOI PubMed PMC
165. Li, L.; Sun, H.; Wang, J.; Guo, Z. H.; Pu, X.; Sun, F. The next chapter of human-like tactile perception: neural decoding to embodied intelligence. *SmartSys* **2026**, *2*, e70024. DOI
166. Long, Y.; Zhao, B.; Liu, M.; Hu, W.; Pu, X. Smart hydrogel tactile sensors and systems: a comprehensive review. *SmartSys* **2026**, *1*, e70015. DOI
167. Long, Y.; Zhao, B.; Niu, J.; et al. Dynamically self-adjustable liquid-liquid and self-adaptive soft-contact solid-solid triboelectric nanogenerator for wave energy harvesting. *Nano. Res.* **2025**, *18*, 94907052. DOI
168. Tang, Z.; Yang, D.; Guo, H.; Lin, S.; Wang, Z. L. Spontaneous wetting induced by contact-electrification at liquid-solid interface. *Adv. Mater.* **2024**, *36*, 2400451. DOI
169. Luo, H.; Wang, H.; Yang, L.; et al. In situ nanofluid dispersion monitoring by liquid-solid triboelectric nanogenerator based on tuning the structure of the electric double layer. *Adv. Funct. Mater.* **2022**, *32*, 2200862. DOI
170. Wei, X.; Wang, B.; Cao, X.; Zhou, H.; Wu, Z.; Wang, Z. L. Dual-sensory fusion self-powered triboelectric taste-sensing system towards effective and low-cost liquid identification. *Nat. Food.* **2023**, *4*, 721-32. DOI
171. Feng, M.; Kong, X.; Feng, Y.; et al. A new reversible thermosensitive liquid-solid TENG based on a P(NIPAM-MMA) copolymer for triboelectricity regulation and temperature monitoring. *Small* **2022**, *18*, 2201442. DOI
172. Kaswan, K.; Khan, A.; Chatterjee, S.; et al. Glassy metallic nanotube arrays-based solid-liquid triboelectric nanosensor for wastewater contaminants sensing and its treatment by thermocatalysts. *Adv. Funct. Mater.* **2025**, *36*, e26347. DOI

173. Li, X.; Weng, M.; Liu, T.; et al. Bioinspired heterogeneous wettability triboelectric sensors for sweat collection and monitoring. *Adv. Mater.* **2025**, *38*, e09920. DOI
174. Zhao, H.; Xu, M.; Shu, M.; et al. Underwater wireless communication via TENG-generated Maxwell's displacement current. *Nat. Commun.* **2022**, *13*, 3325. DOI PubMed PMC
175. Han, S. H.; Kwon, S.; Baek, S.; Chung, T. Ionic circuits powered by reverse electrodialysis for an ultimate iontronic system. *Sci. Rep.* **2017**, *7*, 14068. DOI PubMed PMC
176. Li, T.; Qu, Z.; Si, J.; Lee, Y.; Bandari, V. K.; Schmidt, O. G. Monolithically integrated solid-state vertical organic electrochemical transistors switching between neuromorphic and logic functions. *Sci. Adv.* **2025**, *11*, eadt5186. DOI PubMed PMC
177. Jiang, F.; Poh, W. C.; Chen, J.; et al. Ion rectification based on gel polymer electrolyte ionic diode. *Nat. Commun.* **2022**, *13*, 6669. DOI PubMed PMC
178. Ling, Y.; Yu, L.; Guo, Z.; et al. Single-pore nanofluidic logic memristor with reconfigurable synaptic functions and designable combinations. *J. Am. Chem. Soc.* **2024**, *146*, 14558-65. DOI
179. Liu, W.; Mei, T.; Cao, Z.; et al. Bioinspired carbon nanotube-based nanofluidic ionic transistor with ultrahigh switching capabilities for logic circuits. *Sci. Adv.* **2024**, *10*, eadj7867. DOI PubMed PMC
180. Li, Z.; Myers, S. K.; Xiao, J.; et al. Neuromorphic ionic computing in droplet interface synapses. *Sci. Adv.* **2025**, *11*, eadv6603. DOI PubMed PMC
181. Zhang, Y.; Tan, C. M. J.; Toepfer, C. N.; Lu, X.; Bayley, H. Microscale droplet assembly enables biocompatible multifunctional modular iontronics. *Science* **2024**, *386*, 1024-30. DOI PubMed
182. Kim, Y.; Kim, K. J.; Kim, S. H.; Choi, J. Unveiling ion dynamics in the electric-double layer under piezoionic actuation of chemo-mechanical energy harvesters. *Adv. Energy. Mater.* **2024**, *14*, 2402216. DOI
183. Liu, J.; Li, C.; Lv, Q.; et al. Reconstruction of electric double layer on the anode interface by localized electronic structure engineering for aqueous Zn ion batteries. *Adv. Energy. Mater.* **2024**, *14*, 2401118. DOI
184. Vallem, V.; Roosa, E.; Ledinh, T.; et al. A soft variable-area electrical-double-layer energy harvester. *Adv. Mater.* **2021**, *33*, 2103142. DOI
185. Gao, G.; Yu, J.; Yang, X.; et al. Triboiontronic transistor of MoS_2. *Adv. Mater.* **2018**, *31*, 1806905. DOI
186. Kim, J.; Kang, M.; Lee, S.; So, C.; Chung, D. S. Interfacial electrostatic-interaction-enhanced photomultiplication for ultrahigh external quantum efficiency of organic photodiodes. *Adv. Mater.* **2021**, *33*, 2104689. DOI
187. Dai, X.; Liang, Q.; Wu, Y.; et al. Ultrathin and highly conformal self-powered sensors by liquid-phase transferring. *Research* **2025**, *8*, 0785. DOI PubMed PMC
188. Song, Y.; Melik, R.; Rabie, A. N.; et al. Electrochemical activation and inhibition of neuromuscular systems through modulation of ion concentrations with ion-selective membranes. *Nat. Mater.* **2011**, *10*, 980-6. DOI PubMed PMC
189. Hook MJ, Nawy S, Thoreson WB. Voltage- and calcium-gated ion channels of neurons in the vertebrate retina. *Prog. Retin. Eye. Res.* **2019**, *72*, 100760. DOI PubMed PMC
190. Pressey, J. C.; De, Saint-rome. M.; Raveendran, V. A.; Woodin, M. A. Chloride transporters controlling neuronal excitability. *Physiol. Rev.* **2023**, *103*, 1095-135. DOI PubMed
191. Wu, R.; Benzenberg, L. R.; Svingou, D.; Zenobi, R. The structure of cyclic neuropeptide somatostatin and octapeptide octreotide in the presence of copper ions: insights from transition metal ion FRET and native ion mobility-mass spectrometry. *J. Am. Chem. Soc.* **2023**, *145*, 10542-7. DOI PubMed
192. Tibbs, G. R.; Posson, D. J.; Goldstein, P. A. Voltage-gated ion channels in the PNS: novel therapies for neuropathic pain? *Trends. Pharmacol. Sci.* **2016**, *37*, 522-42. DOI PubMed
193. Didier, M. E. P.; Tarun, O. B.; Jourdain, P.; Magistretti, P.; Roke, S. Membrane water for probing neuronal membrane potentials and ionic fluxes at the single cell level. *Nat. Commun.* **2018**, *9*, 5287. DOI PubMed PMC
194. Devine, M. J.; Kittler, J. T. Mitochondria at the neuronal presynapse in health and disease. *Nat. Rev. Neurosci.* **2018**, *19*, 63-80. DOI PubMed
195. Luo, F.; Sclip, A.; Merrill, S.; Südhof, T. C. Neurexins regulate presynaptic GABAB-receptors at central synapses. *Nat. Commun.* **2021**, *12*, 2380. DOI PubMed PMC
196. Zimmerman, A. L.; Kovatsis, E. M.; Pozsgai, R. Y.; Tasnim, A.; Zhang, Q.; Ginty, D. D. Distinct modes of presynaptic inhibition of cutaneous afferents and their functions in behavior. *Neuron* **2019**, *102*, 420-34.e8. DOI PubMed PMC
197. Yin, J.; Jia, P.; Ren, Z.; et al. Recent advances in self-powered sensors based on ionic hydrogels. *Research* **2025**, *8*, 0571. DOI PubMed PMC
198. Kells, P. A.; Gautam, S. H.; Fakhraei, L.; Li, J.; Shew, W. L. Strong neuron-to-body coupling implies weak neuron-to-neuron coupling in motor cortex. *Nat. Commun.* **2019**, *10*, 1575. DOI PubMed PMC

199. Stürner, T.; Brooks, P.; Serratosa, Capdevila. L.; et al. Comparative connectomics of Drosophila descending and ascending neurons. *Nature* **2025**, *643*, 158-72. DOI PubMed PMC
200. Midya, R.; Pawar, A. S.; Pattnaik, D. P.; et al. Artificial transneurons emulate neuronal activity in different areas of brain cortex. *Nat. Commun.* **2025**, *16*, 7289. DOI PubMed PMC
201. Kuijpers, M.; Haucke, V. Neuronal autophagy controls the axonal endoplasmic reticulum to regulate neurotransmission in healthy neurons. *Autophagy* **2021**, *17*, 1049-51. DOI PubMed PMC
202. Vandael, D.; Okamoto, Y.; Jonas, P. Transsynaptic modulation of presynaptic short-term plasticity in hippocampal mossy fiber synapses. *Nat. Commun.* **2021**, *12*, 2912. DOI PubMed PMC
203. Shepherd, J. D. Deconstructing the synapse. *Nat. Neurosci.* **2018**, *21*, 1294-5. DOI PubMed PMC
204. Li, S.; Sheng, Z. Energy matters: presynaptic metabolism and the maintenance of synaptic transmission. *Nat. Rev. Neurosci.* **2021**, *23*, 4-22. DOI
205. Mojumder, M. R. H.; Kim, S.; Yu, C. Soft artificial synapse electronics. *Research* **2025**, *8*, 0582. DOI PubMed PMC
206. Li, X.; Kvarnström, C.; Ivaska, A.; Wei, D. Triboiontronic logic control via dynamic regulation of electrical double layers. *Iontronics* **2026**, *2*, 28. DOI